Lithology and Source Rock Generative Potential of the Eggerding Formation

(Lower Oligocene, Molasse Basin)

Thesis submitted for the degree of

Master of Science

Birgit Leitner

October, 2008

Presented in the

Department of Applied Geosciences and Geophysics

Chair in Petroleum Geology

University of Leoben

Supervisor:

Univ. Prof. Dr. Reinhard F. Sachsenhofer

I declare in lieu of oath, that I wrote this thesis and performed the associated research myself, using only literature cited in this volume.

Birgit Leitner, October 2008

Acknowledgement

I thank Rohöl Aufsuchungs AG (RAG, Vienna), especially Dr. H.-G. Linzer, for providing core material, well logs, seismic data and valuable geologic information. I acknowledge financial support from RAG.

Special thanks go to Dr. R.F. Sachsenhofer for his outstanding scientific management, explanations, long discussions and linguistic corrections.

The help of Dr. R. Gratzer in the biomarker analysis and data interpretation, Dr. S. Coric in the investigation of the nannoflora and the patience of Dr. G. Rantisch with the Leco and with me is highly appreciated.

Last but not least I want to thank Dipl.-Ing. D. Reischenbacher for help whenever I needed it.

Abstract

The Lower Oligocene succession in the Molasse basin is divided from bottom to top into Schöneck Formation (formerly fish shale), Dynow Formation (bright marlestone), Eggerding Formation (banded marl) and Zupfing Formation (Rupelian shale-marlstone).

The Schöneck Formation (TOC: 2-12 %) is considered as main source rock of oil and thermal gas in the Austrian part of the Molasse basin. Apart from the Schöneck Formation, also the Dynow (TOC: 0.5-3%) and the Eggerding formations show some source potential (Schmidt & Erdogan, 1996; Sachsenhofer & Schulz, 2006).

In this study the facies and source rock generative potential of the Eggerding Formation are investigated. The study is mainly based on samples from drill cores (Eggerding 2, Oberschauersberg 1, Puchkirchen 3, Voitsdorf 1) and well logs.
The Eggerding Formation reaches typically a thickness of 40 meter. The lower part of the Eggerding Formation consists of organic-rich (2-6 % TOC) shaly marlstone with calcite contents up to 18 %. White bands from which the former name “banded marl” is derived are rich in coccolithoporides. Some samples include coccolithoporides characteristic for reduced salinity and deposition during nannoplankton zone NP23. The upper part of the Eggerding Formation consists of a homogenous sequence of marly shale, with low carbonate content (~10 %).
The Zupfing Formation has an average calcite content of about 30 %. TOC content (<1 %) and HI (average: 150 mgHC g^{-1}TOC) are lower than in the Eggerding Formation. Only near the base of the Zupfing Formation TOC contents are about 1.5 %. Nannoplankton blooms indicative for NP24 are detected near the base of the Zupfing Formation.

Despite of the E-W extension of the study area of about 100 km, variances in the log pattern of the Eggerding Formation are minor. Consequently, laterally uniform depositional environments can be presumed. The continuity allows determining minor deviations from the typical pattern and consequently locating and dating submarine erosion events during and after deposition of the Eggerding Formation.

The lower part of the Eggerding Formation has a very good source rock potential (TOC: 3.2%; HI: 436 mgHC/gTOC), whereas its upper part holds a good potential (TOC: 1.65%; HI: 300 mgHC/gTOC). Because of its higher thickness, the source potential index (SPI; 0.58 tHC/m^2) of the Eggerding Formation exceeds that one in the Schöneck Formation (0.35 tHC/m^2). This and biomarker data suggest that the contribution of the Eggerding Formation to the Molasse oil has been underestimated until now.

Zusammenfassung

Das Unteroligozän des Molasse Beckens wird vom Liegenden ins Hangende in Schöneck-Formation (früher: Fischschiefer), Dynow-Formation (Heller Mergelkalk), Eggerding-Formation (Bändermergel) und Zupfing-Formation (Rupel Tonmergel) eingeteilt.

Die Schöneck-Formation (TOC: 2-12 %) wird als wichtigstes Muttergestein für Öl und thermisches Gas erachtet. Daneben weisen auch die Dynow-Formation (TOC: 0.5-3%) und die Eggerding-Formation ein gewisses Muttergesteinspotential auf(Schmidt & Erdogan, 1996; Sachsenhofer & Schulz, 2006).

In dieser Diplomarbeit werden Fazies und Muttergesteinspotential der Eggerding-Formation untersucht. Die Studie basiert hauptsächlich auf Kernproben der Bohrungen Eggerding 2, Oberschauersberg 1, Puchkirchen 3 und Voitsdorf 1 und geophysikalischen Bohrlochmessungen.

Die Eggerding-Formation, durchschnittlich 40 m mächtig, besteht im liegenden Teil aus organisch-reichem (2-6 % TOC) Mergelton mit Kalzitgehalten bis zu 18 %. Weiße Bänder sind namensgebend für die alte Bezeichnung „Bändermergel“. Sie sind reich an Coccolithophoriden. Einige Proben beinhalten Vergesellschaftungen, die indikativ für reduzierte Salinität und Ablagerung während der Nannoplankton Zone NP23 sind. Der obere Teil der Eggerding-Formation besteht aus einem homogenen mergeligen Ton mit einem Kalzitgehalt um 10 %.

Die Zupfing-Formation besitzt einen durchschnittlichen Kalzitgehalt von 30 %. Der TOC Gehalt (<1%) und der HI (durchschnittlich 150 mgHC g-1TOC) sind geringer als in der Eggerding-Formation. Höhere TOC Gehalte (1.5%) und Nannoplankton Blüten, bezeichnend für NP24, sind auf die Basis der Zupfing-Formation beschränkt.

Trotz einer E-W Erstreckung von circa 100 km, bleiben Variationen in den Log-Mustern der Eggerding-Formation gering. Dies deutet auf ein lateral gleichförmiges Ablagerungsmilieu hin. Wegen der Kontinuität können auch geringe Abweichungen vom typischen Log-Muster erkannt werden, wodurch die Lokalisierung und Datierung submariner Erosionsereignisse während und nach Ablagerung der Eggerding-Formation ermöglicht wird.

Der untere Teil der Eggerding-Formation besitzt ein sehr gutes Muttergesteinspotential (TOC: 3.2%; HI: 436 mgHC/gTOC), der obere Teil weist ein gutes Potential (TOC: 1.65%; HI: 300 mgHC/gTOC) auf. Aufgrund der höheren Mächtigkeit übersteigt der Muttergestein-Potential-Index (SPI) der Eggerding-Formation (0.58 tHC/m^2) jenen der Schöneck-Formation (0.35 tHC/m^2). Dies und Biomarkerdaten lassen vermuten, dass der Beitrag der Eggerding-Formation zum Molasse Öl bislang unterschätzt wurde.

INHALTSVERZEICHNIS

1. Introduction

The Oligocene Schöneck Formation (formerly fish shale) is regarded as the main source rock for oil and thermogenic gas in the Molasse basin (Fig. 1).

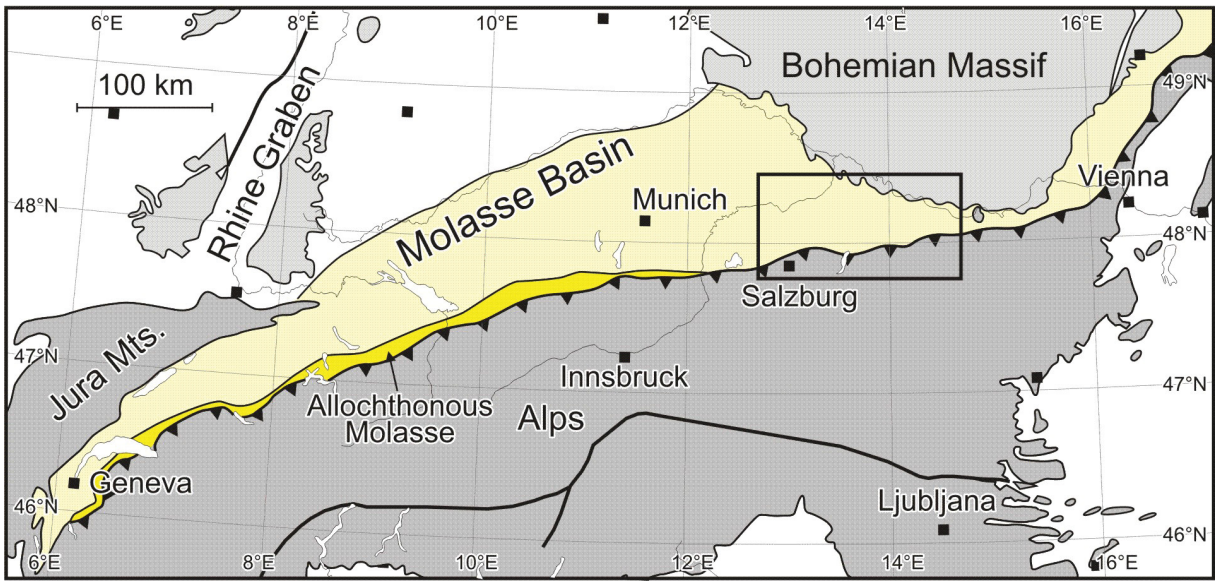

Fig. 1: Sketch map of the Molasse basin extending from Geneva to Vienna (Sachsenhofer & Schulz, 2006). The black rectangle marks the study area.

Schmidt and Erdogan (1996) recognized that beside the Schöneck Formation, the Eggerding Formation has some additional, but subordinate source rock potential. Sachsenhofer and Schulz (2003) made the observation that the total organic carbon (TOC) content is very high in the Schöneck Formation, drops at the boundary to the overlying Dynow Formation, increases upwards within the Dynow Formation and reaches relatively high values at the base of the Eggerding Formation. Therefore, they speculate that the source potential of the Eggerding Formation could be underestimated.

The aim of the present study is to investigate the source potential of the Eggerding Formation more closely. The investigation is based on core material and log data kindly provided by Rohöl - Aufsuchungs AG (RAG; Austria). Because the Eggerding Formation has never been a target horizon, the choice of cores was restricted:
Cores from well Oberschauersberg 1 have been used to investigate the lower Eggerding Formation in continuation of the study of Sachsenhofer and Schulz (2003). For the study of the upper part of the Eggerding Formation and the lower part of the Zupfing Formation, cores from wells Puchkirchen 3 and Voitsdorf 1 were available. The well Eggerding 2 is the type locality of the Eggerding Formation and provides information on Eggerding Formation deposited in a near shore environment. Therefore, and because cores representing the whole Eggerding Formation are available, this well was included in the investigation.

At first, bulk geochemical properties, such as TOC and TIC (total inorganic carbon) contents, sulfur content, Hydrogen index and genetic potential were determined in order to estimate

the source rock potential.
Biomarker molecules in rock extracts were analysed to allow statements on depositional environment, maturity and to enable oil-source rock correlations.
Log correlations across the Molasse basin provide information on lateral variations of depositional environments and on post depositional processes. The latter were checked using seismic sections.

The integration of all data shall give a more detailed idea of the source rock potential of the Eggerding Formation and its contribution to the Molasse oil.

2. Geological Settings

The Molasse Basin extends along the northern margin of the Alps from France to the eastern border of Austria. In its present day configuration, the basin is about 900 km long and up to 120 km wide in the German sector. The Molasse Basin is a Cenozoic Foreland Basin. It developed by subduction of the European plate under the Adriatic plate (Ziegler 1987). It is delineated to the north by the outcropping basement of the Bohemian Massif. The southern part of the basin is overthrust by the Alpine nappes.
Within the Alpine Foreland, the sedimentary history was characterised by three stages separated by unconformities: Permo-Carboniferous graben sedimentation; Mesozoic mixed carbonate-siliciclastic shelf sedimentation; and Cenozoic molasse sedimentation (Wagner 1998).

Overlying crystalline basement or Mesozoic rocks, the oldest sediments marking the initial evolution of the Molasse Basin are of Late Eocene age (Fig. 2) and were deposited in an area structured by troughs and highs along Mesozoic faults.
The upper Eocene sedimentary sequence is characterised by highly variable facies associations. During the Priabonian shallow marine sediments onlapped northward onto fluvial and limnic deposits. During this period the NW–SE trending Central Swell Zone (Boigk, 1981; Kollmann 1977) separated a shallow lagoon from the open sea. Algal (Lithothamnium) reefs on top of the paleo-swell shed debris to the north (lagoon) and to the south (open marine shelf edge; Wagner, 1980).
During the early Oligocene, the Molasse Basin deepened and widened abruptly (Sissingh, 1997). Additionally, the initial separation of Paratethys and Mediterranean Sea, coincident with a worldwide climate cooling (Bruch, 1998; Prothero, 1994) caused major changes in sedimentary facies and marine fauna. Within the study area, the main Eocene carbonate platform with algal reefs was drowned (Bachmann et al., 1987) and replaced by organic-rich rocks of the Schöneck Formation:

- The Schöneck Formation (formerly Lattorf Fischschiefer) is a succession of two organic rich marlstone units and an upper shale unit. The formation from the upper slope has a typical thickness of 10 to 20 meter. The water depth during deposition of the Schöneck Formation increased from 400 to 600 m (Schulz et al., 2002, Sachsenhofer and Schulz, 2006).

During the early Kiscellian (nannoplankton zone NP 22) fresh water incursions led to a progressive break-down of the water stratification. Oligotrophic surface water conditions were established and carbonate-rich, organic-lean rocks were deposited (Dynow Formation; formerly “Heller Mergelkalk”). They reflect cyclic patterns triggered by initially massive blooms of coccolithophorides, but constant organic carbon input:

- A sharp boundary separates the *Dynow Formation* from the underlying Schöneck Formation. The Dynow Formation develops in a 2 cm broad interval, in which the carbonate content rises fast to a white-gray mudstone (classification after Dunham,

1962). The overlying Dynow Formation, about 5 m thick, consists of interbedded strata of laminated to undulated, white to dark gray, silty marlstone. Schulz (2003) describes a cyclic structure of the interbedded layers mentioned above. The cyclicity can also be followed by differences in organic carbon and calcite contents. He recognizes four cycles. The bright marlstone layer at the end of the fourth cycle, which lithostratigraphically is considered as part of the Dynow Formation, leads to the sedimentation process of the Eggerding Formation.

Photic zone anoxia was established. Cyclicity was caused by periodic decreases in fresh water ingressions during each cycle and led to bottom currents. These oceanographic conditions stabilized and were coupled to marine ingressions at the end of the NP 23. This prevailing oceanographic setting is referred to a Black Sea-like scenario with formation of organic-rich sediments, Eggerding Formation (Schulz, 2003):

- The *Eggerding Formation* (formerly “Banded Marl”) is composed of dark gray laminated pelites with thin layers of nannoplankton. The thickness of the Eggerding Formation varies typically in the range of 35 to 50 m (Sachsenhofer and Schulz, 2006).

In the later Kiscellian gradually open marine conditions were restored ("Tonmergelstufe" = Zupfing-Formation; Wagner, 1998):

- The *Zupfing Formation* (formerly “Rupelian Marl”) can reach a thickness up to 450 m. It consists mainly of dark gray hemipelagites and distal turbidities from the south. They intercalate with slumps, slides and turbidities derived from the northern slope. Limestone layers with nannofossils occur in the lower part of the section (Wagner, 1998).

The Alpine thrust system moved to the north and with it also the axis of the deep part of the Molasse basin. Consequently intensive erosion occurred on the Zupfing Formation. The developed lows were filled with the sediments of the *Puchkirchen Formation* (Egerian to Early Eggenburgian), which are composed of more than 80% of slided and contorted slump material from both sides of the basin (Wagner 1998). The intense internal and submarine erosions are typical for all basins and slope deposits in the Upper Austrian Molasse.
After the most prominent submarine erosion across the Molasse Basin, a new fauna from the Indian Ocean immigrated in the *Hall Group* (Steininger and Rögl, 1979; Rögl and Steininger, 1983). The oldest sediments, *Lukasedt Formation*, are restricted to the SW of Upper Austria (Salzburg) and consist of micaceous, calcareous sandstones, siltstones, sandy pelites and darker muddy conglomerates with plant fragments (Wagner, 1998). The *Lukasedt Formation* was deposited on top of the Molasse imbrications in a narrow erosional channel. The northwards moving imbricates and the consequently shifted submarine erosion formed new channels in which the *Lindach Formation* (similar to the *Lukasedt Formation*) took place. Afterwards the whole Molasse basin was filled with micaceous, sandy pelites of the “Hall Schlier”.

Within the Ottnangian *Innviertel Group* each formation begins and ends with major submarine erosion. Because of erosion, Karpatian deposits are missing in the Upper Austrian Molasse basin. From Badenian to Pannonian times, freshwater sediments with coal seams were deposited. The uppermost formation is the Hausruck gravel (Fig. 2).

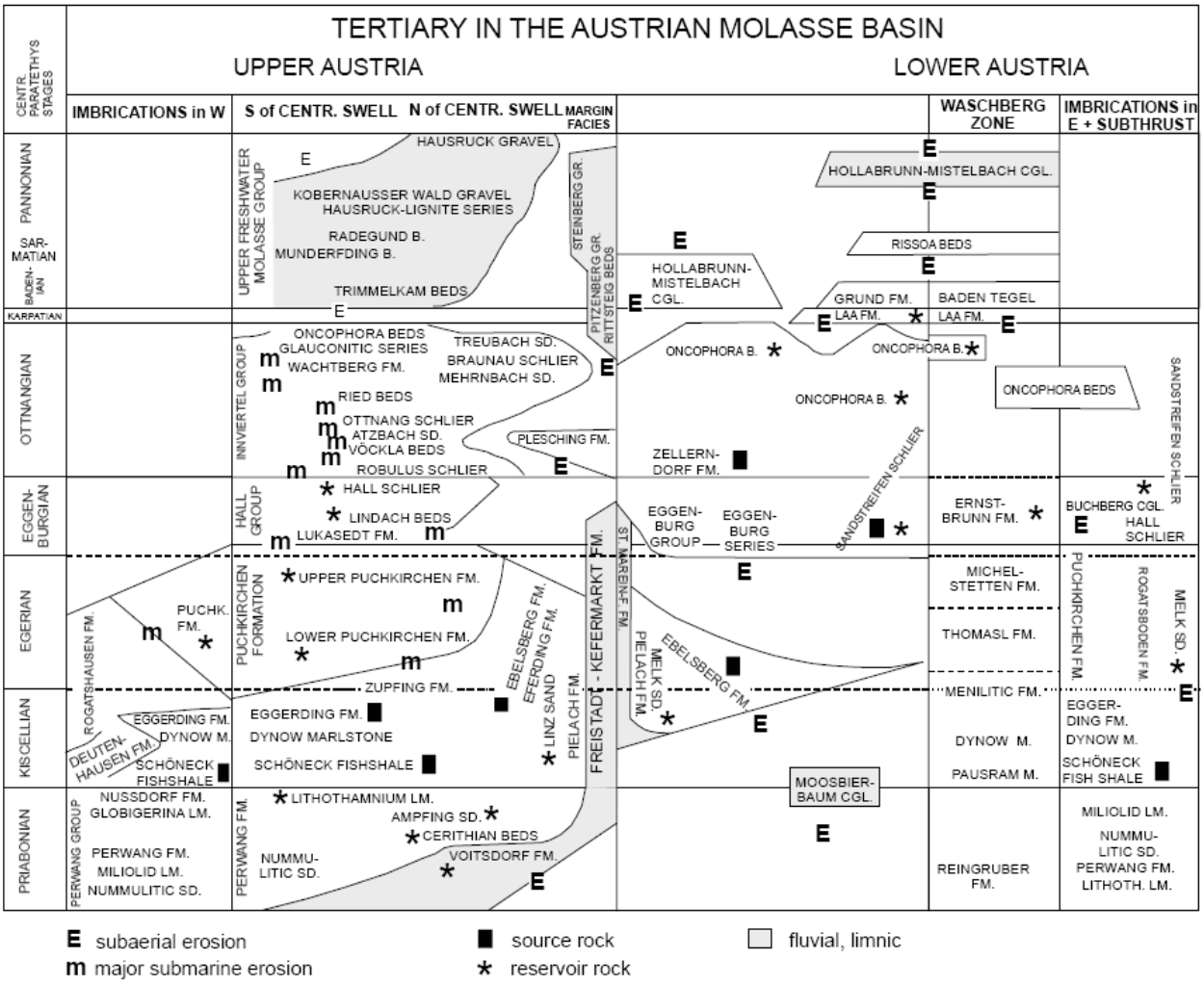

Fig. 2: Stratigraphic Chart of the Austrian Molasse Basin (Wagner 1998).

According to sequence stratigraphic analysis, shallow-marine Eocene sediments and deeper marine Lower Oligocene deposits (Schöneck, Dynow and Eggerding formations) form a transgressiv systems tract (Jin et al.1995; Zweigel 1998), whereas the Zupfing Formation represents very distal, basinal high stand deposits (Zweigel, 1998). A major sea level fall (200 m) occurred at the boundary between Lower and Upper Oligocene (e.g. Haq et al. 1987). Its consequence for the development of the Molasse Basin is not fully understood (Zweigl 1998).

Whereas deep marine conditions with water depth exceeding 1000 m persisted during late Oligocene to Early Miocene times east of the river Inn, a prograding–retrograding delta complex filled the western part of the basin.

The Cenozoic sediments are divided structurally into the Autochthonous Molasse and the Allochthonous Molasse. The Autochthonous Molasse rests relatively undisturbed on the European basement. The Allochthonous Molasse, including the Imbricated Molasse, is composed of Molasse sediments, which are included in the Alpine thrusts and which are moved tectonically into and across the southern Autochthonous Molasse.

The fault pattern in the Molasse Basin is dominated by NW- and NE-trending fault systems, which already existed in Paleozoic times and which were reactivated in Early Jurassic, Early Cretaceous and Early Tertiary times. Through these periods of tectonic activity, the crystalline basement and its cover were pulled apart using the old fault planes. During the latest Eocene and earliest Oligocene a dense network of W-E-trending antithetic and synthetic extensional faults developed. During the Tertiary and Quaternary the pre-Tertiary and Early Tertiary extensional fault system became reactivated by a dextral and sinistral transpression with shear, strike-slip and overthrust structures (Wagner 1998).

3. Samples and Database

The location of studied wells is shown in Fig. 3; geophysical logs of the Eggerding Formation are show in Fig. 4.

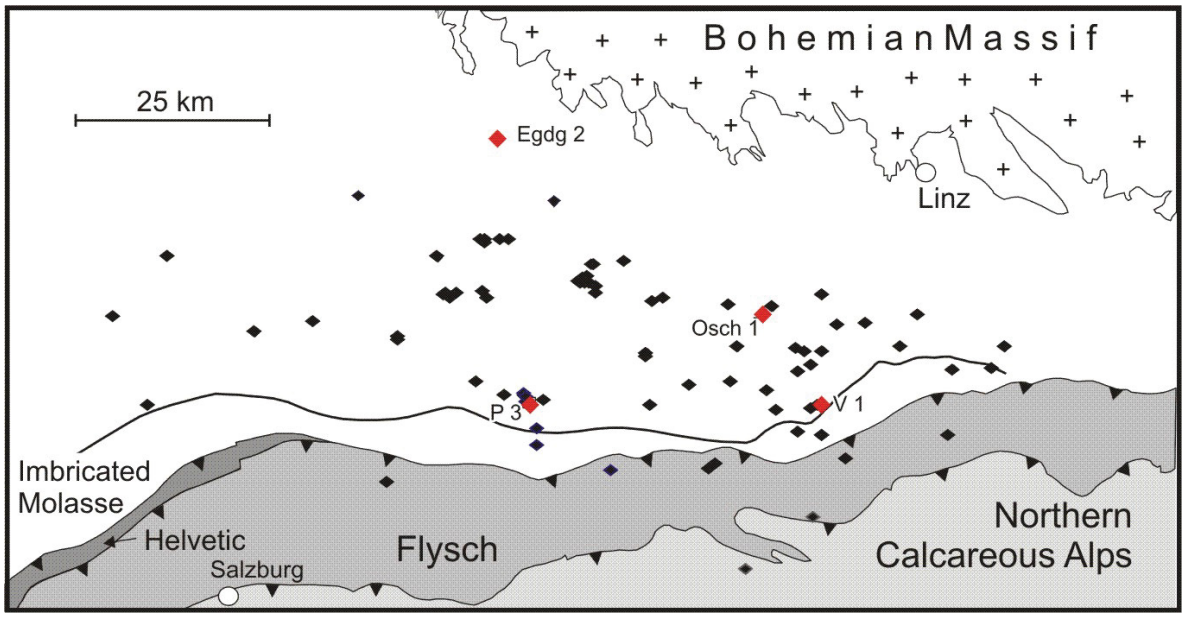

Fig. 3: Map of study area; investigated wells are highlighted in red: Egdg 2 – Eggerding 2, P 3 – Puchkirchen 3, Osch 1 - Oberschauersberg 1, V 1 – Voitsdorf 1.

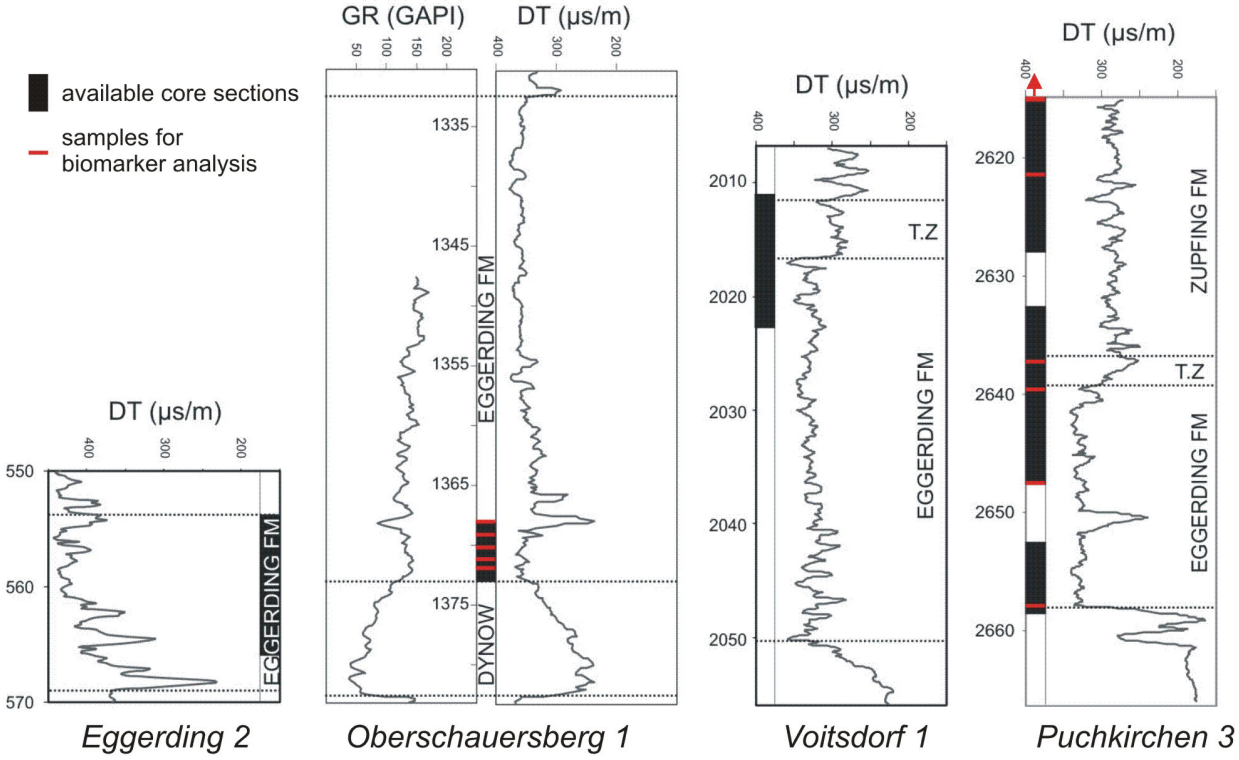

Fig. 4: Logs of investigated wells; black bars show position of analyzed cores; red bars show position of samples used for biomarker analysis. GR – Gamma Ray, GAPI – American Petroleum Institute gamma units; DT – Sonic log; T.Z. – Transition Zone.

Cores with Eggerding Formation from the following wells have been selected for the study:

- Eggerding 2. This well is located in the shallow, northern part of the Molasse Basin. The cores represent the entire Eggerding Formation in a marginal, land-near facies.
- Oberschauersberg 1. Cores are available only from the lowermost 5 m of the Eggerding Formation and include the transition to the underlying Dynow Formation.
- Voitsdorf 1. Cores from well Voitsdorf 1 represent the transition between the Eggerding and Zupfing formations.
- Puchkirchen 3. Cores represent a large portion of the Eggerding Formation, but its lowermost part is probably missing.

In total 87 core samples have been taken in the core shed of Rohöl - Aufsuchungs AG (RAG, Austria) at Pettenbach. The distance between two samples is typically about 1 m. Only the Oberschauersberg core has been sampled using a higher resolution approach (0.24 - 0.5 m). Whereas most samples are from the Eggerding Formation, samples from the lower part of the Zupfing Formation have been analysed as well. A single sample from well Puchkirchen 2 represents Lithothamnium limestone. A sample list can be found in the appendix.
Twelve samples have been selected for biomarker analysis. Five of them are from the Eggerding Formation of well Oberschauerberg 1, the rest is from well Puchkirchen 3. In the latter well, four samples represent the Eggerding Formation, one the “transition zone” and two the Zupfing Formation (Fig. 4).
About 92 wells were correlation based on wireline logs were provided by RAG. The correlations are mainly based on sonic log (DT) and gamma-ray log (GR).

4. Methods

4.1 Determination of total inorganic carbon, organic carbon (TOC) and sulphur contents

Powdered samples were analysed for total sulphur (TS), total carbon (TC), and total organic carbon contents (TOC, after acidification of samples to remove carbonate) using a Leco CS-300 analyser. The difference between TC and TOC is the total inorganic carbon content (TIC). TIC contents were used to calculate calcite equivalent percentages (=8.34 * TIC).

4.2 Rock - Eval pyrolysis

Pyrolysis was carried out using a Delsi Rock-Eval instrument Version RE II.
The samples were initially heated up to 300°C. During that time the mobile, free and adsorptive bounded hydrocarbons were released from the pore space and were detected as S1 peak (mgHC g^{-1}rock). Afterwards the sample was heated to 550°C and the organic matter became pyrolized. Thereby released hydrocarbons were recorded by a flame ionization detector as S2 peak (mgHC g^{-1}rock). The amount of hydrocarbons (mgHC g^{-1}rock) released from kerogen during gradual heating is normalised to total organic carbon (TOC) to give the Hydrogen Index (HI) defined as S2/TOC (Espitalié et al., 1977). The sum of S1 and S2 gives the genetic potential of a rock (mgHC/g rock). The temperature of maximum hydrocarbon generation (Tmax), is a pyrolysis maturation indicator.

4.3 Biomarker analysis

For geochemical analyses, representative portions of the core material were crushed in a steel mortar and extracted for approximately 1 h using dichloromethane in a Dionex ASE 200 accelerated solvent extractor at 75 °C and 50 bar.
After evaporation of the solvent to 0.5 ml total solution in a Zymark TurboVap 500 closed cell concentrator, asphaltenes were precipitated from a hexane–dichloromethane solution (80:1) and separated by centrifugation. The fractions of the hexane–soluble organic matter were separated into NSO compounds, saturated hydrocarbons, and aromatic hydrocarbons by medium-pressure liquid chromatography using a Köhnen–Willsch MPLC instrument (Radke et al., 1980).
The saturated and aromatic hydrocarbon fractions were analyzed by a gas chromatograph equipped with a 25-m DB-1 fused silica capillary column (i.d. 0.25 mm) and coupled to a Finnigan MAT GCQ ion trap mass spectrometer. The oven temperature was programmed from 70 to 300 8C at a rate of 4 8C/min followed by an isothermal period of 15 min. Helium was used as a carrier gas. The mass spectrometer was operated in the electron impact (EI) mode and a scan range from 50 to 650 Da (0.7 s total scan time). Data were processed with

a Finnigan data system. Identification of individual compounds was accomplished by retention time in the total ion current (TIC) chromatogram and by comparison of the mass spectra with published data (Philp, 1985, and references therein). Relative percentages of different compound groups in the saturated and aromatic hydrocarbon fractions were calculated using peak areas from the gas chromatograms (Bechtel et al., 2007).

4.4 Well Log measurements

In this study well log information was used for correlation of formation sections across the study area in the Molasse basin.

4.4.1 Gamma ray log

The gamma-ray log measures naturally occurring gamma radiation to characterize rocks or sediments. Three elements and their decay chains are responsible for the radiation emitted by rock: potassium, thorium and uranium.
Shale emits a lot of natural gamma-rays, because potassium is a part of its clay content and because it has the tendency to absorb uranium and thorium as well.
The difference in radioactivity between shales and sandstones/carbonate rocks allows the gamma tool to distinguish between shales and non-shales. A traditional gamma-ray log records the total radiation, and cannot distinguish between the radioactive elements.

4.4.2 Sonic log

Depending on its density and elasticity, every rock has a specific acoustic velocity. The sonic log displays the travel time of P-waves versus depth. Therefore the transmitter of a sonic log emits sound waves into the formation and measures the time taken to detect at a receiver of known distance from the transmitter. The first arrival is the compressional or 'p' wave, which is used to calculate the transit time DT (μs/m). The distance between transmitter and receiver defines the resolution of the log, which means the lowest thickness of rock strata of which specific velocity is still measurable (Rider, 1996).
The DT velocities are inversely proportional to the amount of calcite in a formation (see Schulz et al., 2004). In this study they were therefore also used for correlation of core material with log patterns (core to log shift).

rocks	sonic traveltime in μs/m
mudstone	197 - 558
sandstone	174 - 328
limestone	156 - 174
dolomite	126 - 148
rock salt	219 - 220
anhydrite	164
gypsum	171 - 174
polyhalite	189 - 190
sylvinite	243

Fig. 5: Average sonic velocities for different lithologies (after Rider, 1996).

4.5 Determination of nannoflora

Samples from the Eggerding Formation, the “Transition Zone” and the Zupfing Formation were investigated for calcerous nannoplankton by Stepan Coric (Geological Survey of Austria). Standard smear slides were analysed using a light microscope (1000 x magnification) at normal and crossed nicols. Abbundance and preservation of nannoplankton assemblages, as well as abundance of detected taxa are described semi quantitatively.

5. Results

5.1 Lithology

5.1.1 Lower Eggerding Formation

The lower part of the Eggerding Formation has been investigated in well Oberschauersberg 1. Here, the dark grey laminated shaly marlstone shows white bands (Fig. 6a, c) made up of calcareous nannoplankton. Because of these bands the Eggerding Formation was formerly termed “banded marl” (Bändermergel). There are no signs of bioturbation.

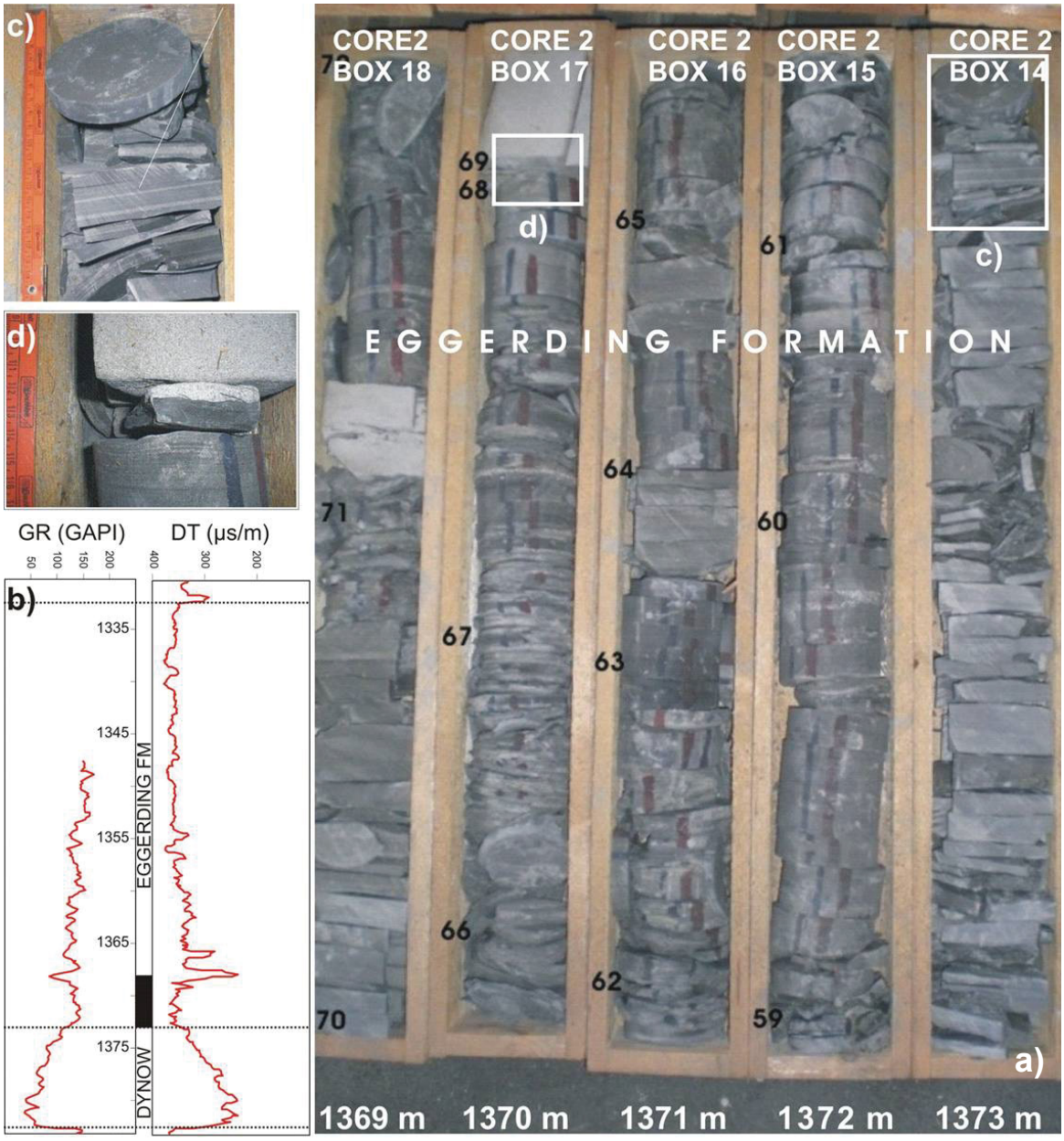

Fig.6: a) Section of drill core 2 from well Oberschauersberg 1. Labels on the side of the core boxes denote sample numbers; b) Sonic (DT) and gamma-ray (GR) logs, location of core section shown in a) is shown by a black bar; c) detail of banded marl; d) base of turbiditic sandstone.

The coccolithophorides Braarudosphaera bigelowii (found in the samples Osch 64 and Osch 68) is characteristic for reduced salinity. Apart from redeposited Cretaceous to Eocene coccolithophoridae, the following Oligocene taxa were detected by S. Coric in the lower part of the Eggerding Formation (f – frequent, c – common, r – rare):
Coccolithus pelagicus, Cyclicargolithus floridanus, Discoaster sp., Reticulofenestra bisecta, R. lockerii, R. stavensis, Sph. cf. capricornutus, Braarudosphaera bigelowii small f/c, Reticulofenestra sp. r, R. small, Thoracosphaera heimii r.

Some turbiditic sandstone layers exist in the lower part of the Eggerding Formation of well Oberschauersberg 1 (Fig. 6d). The calcite content of the fine-grained rocks fluctuates between 1.3% and 17.0% (average 9.6%).

5.1.2 Upper Eggerding Formation and Lower Zupfing Formation

The upper part of the Eggerding Formation (Fig. 7) consists of a homogenous sequence of marly shale (calcite contents: 3 - 12 %). In contrast to the lower part, it does not show the typical white bands from which the “banded marl” derived its name and does not include any calcareous nannoplankton.
The boundary between the Eggerding Formation and Zupfing Formation is sharp. Cores of the Zupfing Formation are more compact than cores from the Eggerding Formation. This is a consequence of a higher calcite content of the clay marl in the lower part of the Zupfing Formation (20 - 37 %). The upper Eggerding Formation and the lower Zupfing Formation is investigated in the wells Voitsdorf 1 and Puchkirchen 3.

Apart from redeposited Cretaceous to Eocene coccolithophorides, the following Oligocene taxa were detected by S. Coric in the lower part of the Zupfing Formation from the well Puchkirchen 3 (“transition zone”; f – frequent, c – common, r – rare):
Coccolithus pelagicus f, Cyclicargolithus abisectus r, Cy. floridanus c, Pontosphaera multipora r, Reticulofenestra bisecta r, R. lockerii f, R. small r, R. cf. tokodoensis r, Sphenolithus moriformis r, Thoracosphaera saxea r, Zygrhablithus bijugatus r.

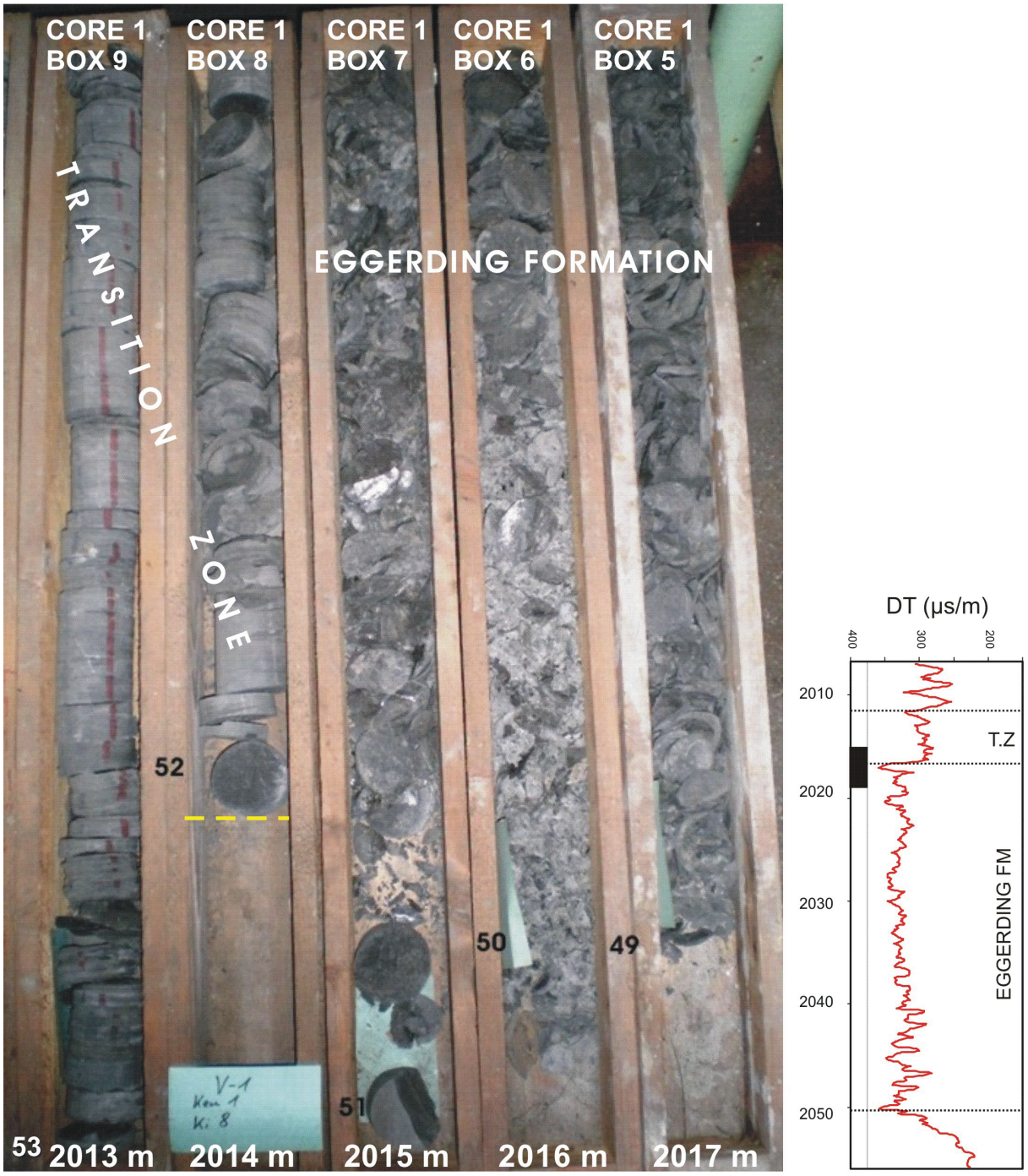

Fig.7: Section of the drill core 1 from the well Voitsdorf 1. Inset shows DT (Sonic) log, location of the core section is shown by a black bar. Labels on the side of the core boxes denote sample numbers.

5.1.3 Near-shore facies

Eggerding Formation, deposited in a land near position, has been drilled in well Eggerding 2 (Fig. 8). This well has been selected as a type locality for the Eggerding Formation. Characteristic for the near-shore facies are abundant sandstone layers and the frequent occurrence of land plants (Fig. 8b).

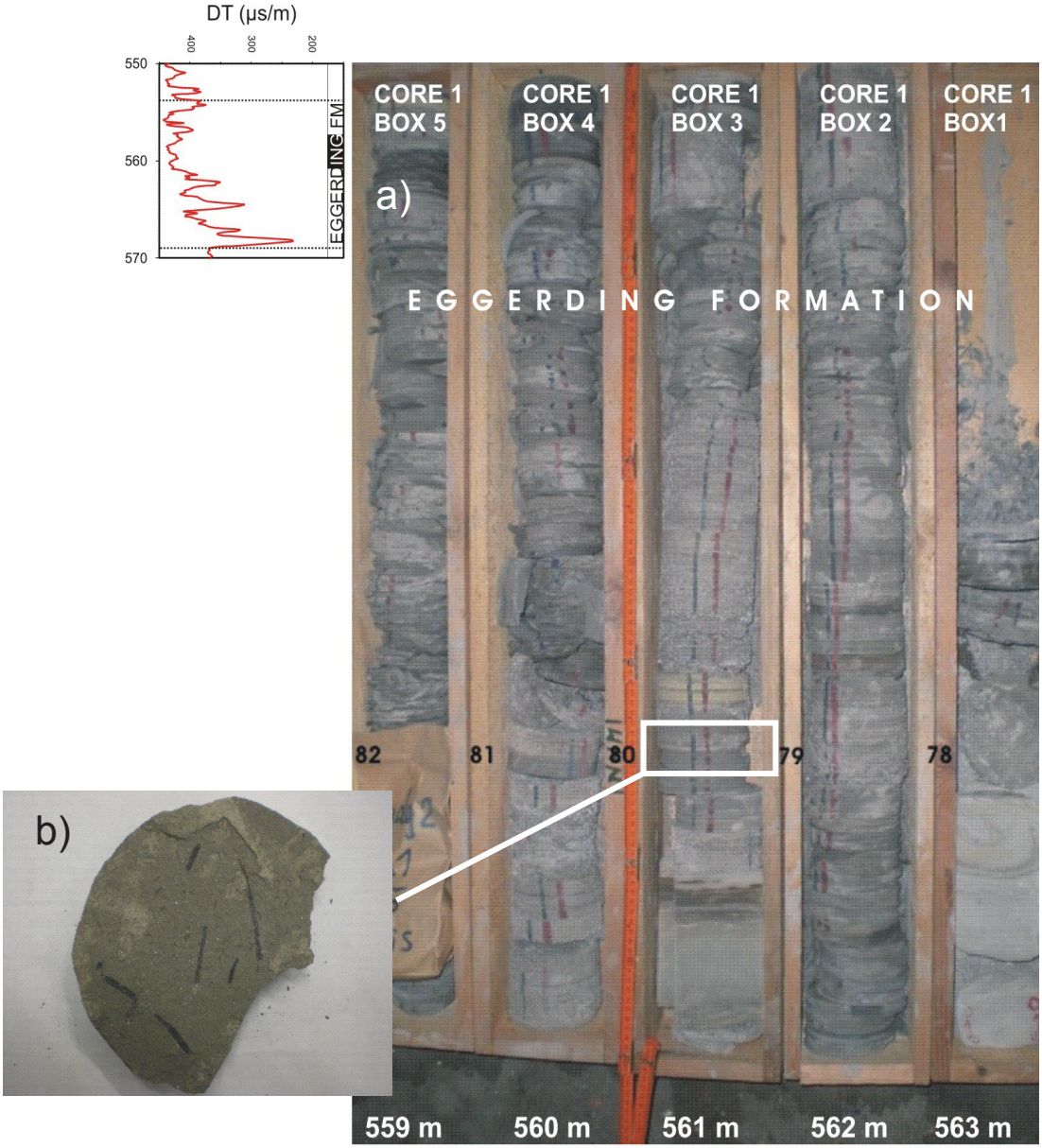

Fig. 8: a) Section of drill core 1 from the near shore well Eggerding 2; inset shows DT (Sonic) log; location of the core section is shown by a black bar; b) land plants.

5.2 Organic geochemistry

5.2.1 Bulk organic geochemistry

In this chapter basic geochemical proxies for the wells Eggerding 2, Puchkirchen 3, Oberschauersberg 1 and Voitsdorf 1 are shown together with their sonic logs.

5.2.1.1 Bulk organic parameters of well Eggerding 2

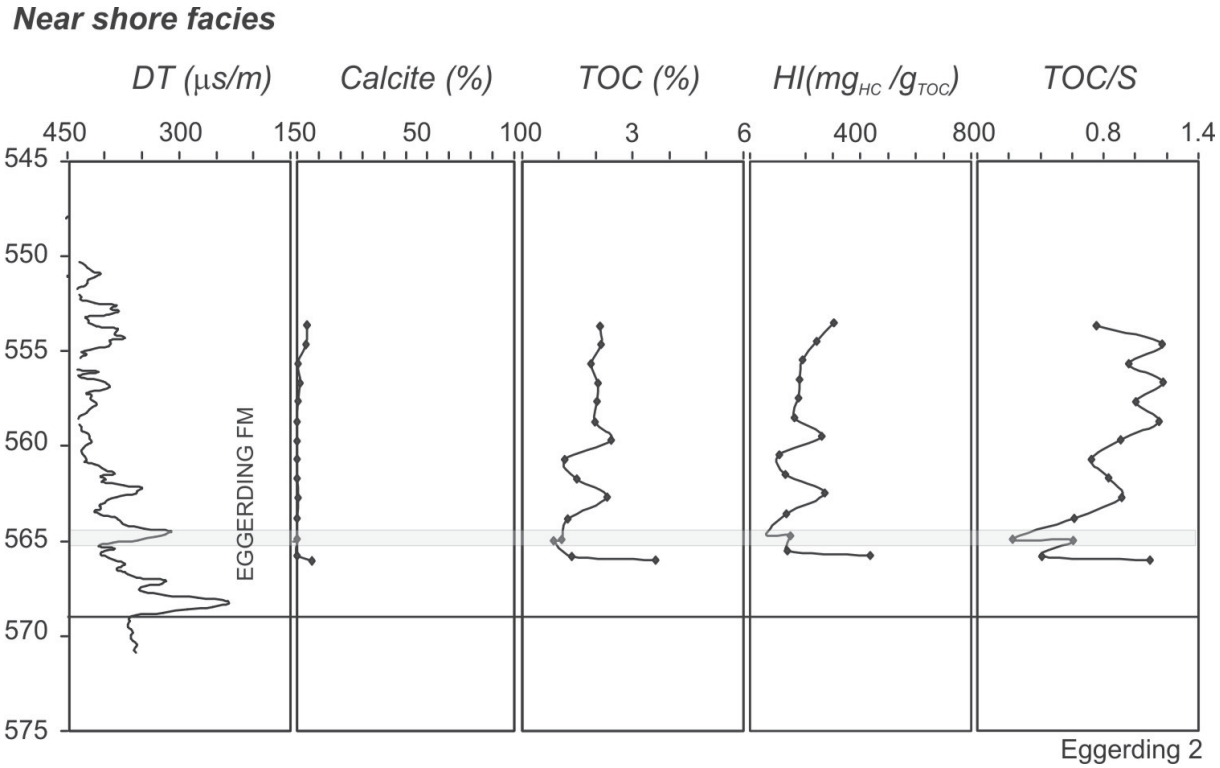

Fig. 9: Sonic log (DT) and source-rock data from well Eggerding 2.

15 samples (553.65 m - 566.02 m measured depth (MD)) from well Eggerding 2 (Fig. 9) show total organic carbon contents (TOC) between 0.84% and 3.62%. Hydrogen index (HI) values range from 60 mgHC g^{-1}TOC to 436 mgHC g^{-1}TOC (type III – II kerogen). Although sandy layers have not been analyzed, the partly small TOC contents may result from dilution by detrital material. Low HI values reflect the near shore depositional environment and the input of terrestrial plants. The TOC/S ratios range from 0.2 to 1.2.

5.2.1.2 Bulk organic parameters of well Oberschauersberg 1

The cores of the Schöneck Formation, Dynow Formation and one meter of Eggerding Formation in well Oberschauerberg 1 were investigated by Schulz et al. (2002, 2004). A part

from them is shown in Fig. 10. The remaining 13 samples of the Eggerding Formation were analyzed within the frame of this study. They cover only the lowermost part of the Eggerding Formation.

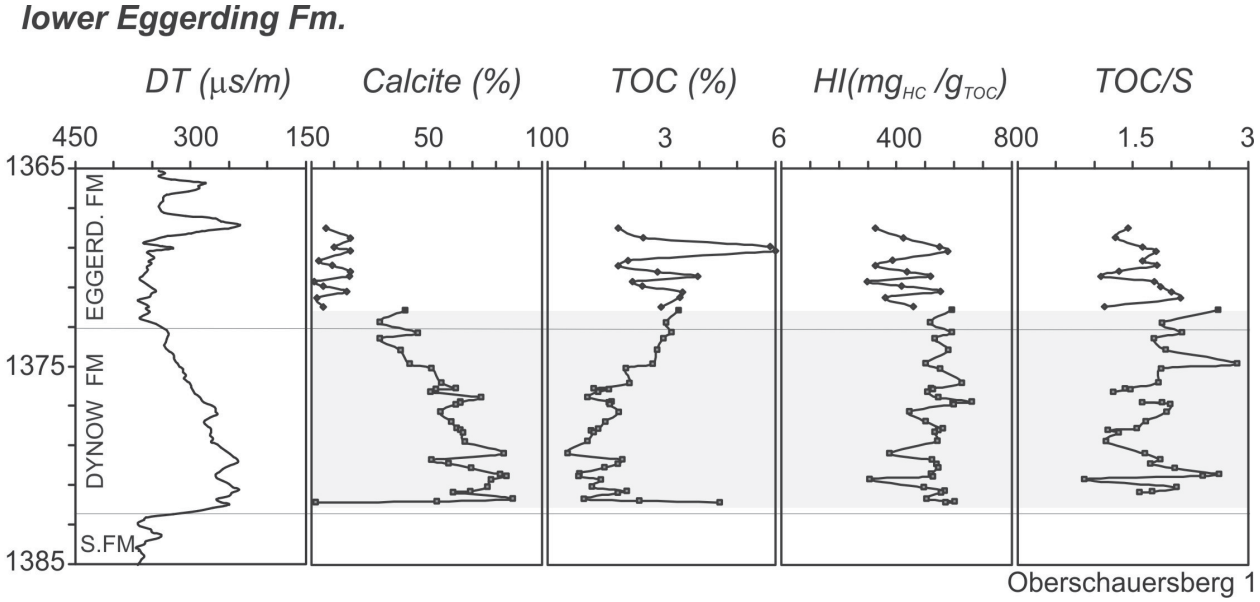

Fig. 10: Sonic log (DT) and source-rock data from the well Oberschauersberg 1. Data from Schulz et al. (2004) are highlighted by grey shading.

In the Schöneck Formation the TOC content is high (average ~ 5%), whereas the calcite equivalent content is low. Towards the Dynow Formation the calcite content increases abruptly to nearly 90%, while the TOC content decreases simultaneously to 0.5%. Within the Dynow Formation, calcite contents decrease and TOC contents increase upwards.
Within the lower Eggerding Formation TOC contents range from 1.9% to 6.0% (average: 3.2%). The HI varies between 300 mgHC g^{-1}TOC and 590 mgHC g^{-1}TOC (type II kerogen). The TOC/S ratio is higher than in the upper Eggerding Formation drilled in wells Voitsdorf 1 and Puchkirchen 3 (1.1 -2.6).

5.2.1.3 Bulk organic parameters of well Voitsdorf 1

The 14 samples from well Voitsdorf 1 (2008 m – 2021 m (MD)) belong to the lower part of the Zupfing Formation and the upper part of the Eggerding Formation.
In Fig. 11 the position of the samples is illustrated according to the original depth labels from the core boxes. The calcite equivalent curve and the sonic log usually match very well. Therefore, a misfit between calcite and DT trends suggests that core data have to be shifted downwards (Fig. 12).
The TOC content of the upper Eggerding Formation ranges from 1.3% to 2.4% (1.8%). The HI varies between 230 mgHC g^{-1}TOC and 380 mgHC g^{-1}TOC (type III/II– II kerogen).

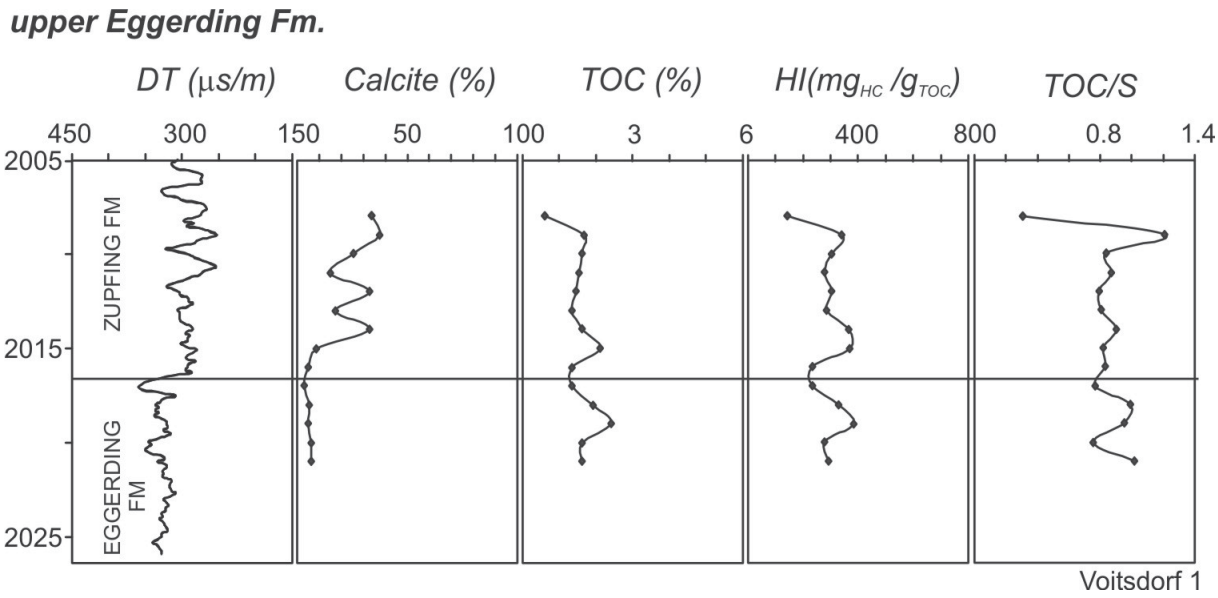

Fig. 11: Sonic log (DT) and source-rock from well Voitsdorf 1.

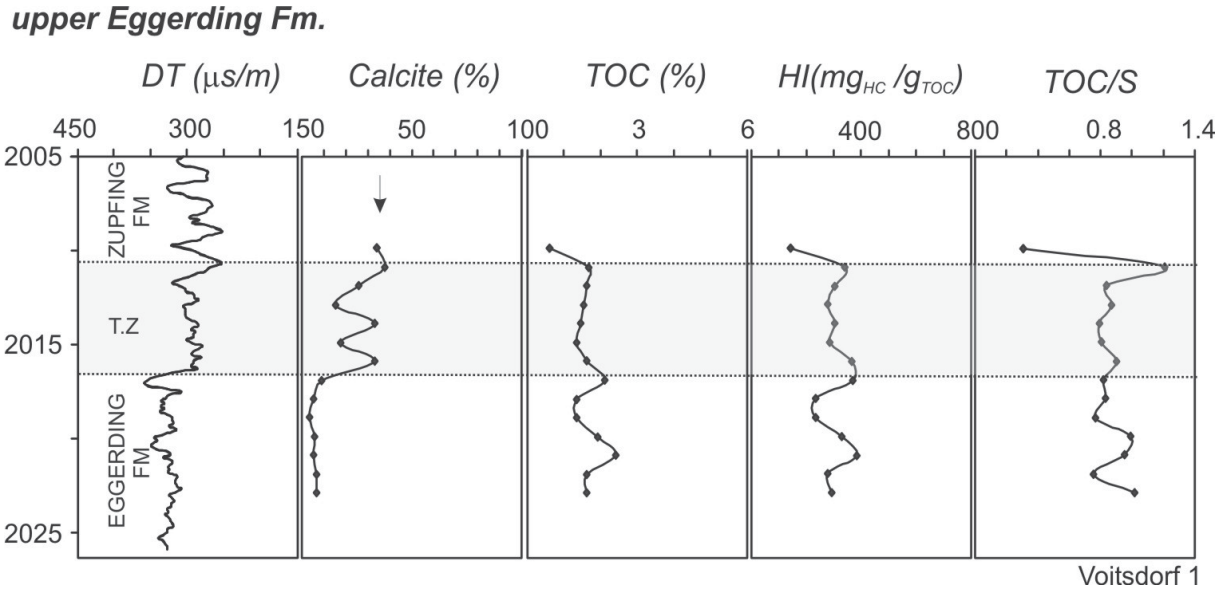

Fig. 12: Sonic log (DT) and source-rock data from well Voitsdorf 1. Source-rock data are vertically shifted in order to account for the difference between log and core depth.

As expected, the samples from the Zupfing Formation show higher calcite equivalent percentages (about 30%). Surprisingly the TOC content of the lowermost six samples is nearly as high as in the Eggerding Formation and drops only in the uppermost sample. A new informal term is introduced for this interval: “Transition zone”. Because of the high calcite content, the Transition zone should form part of the Zupfing Formation on geophysical

logs. The average TOC content of the Transition zone is 1.5%. This value is only slightly lower than the average TOC content in the upper Eggerding Formation. A similar behaviour can be detected by the HI value: 312 mgHC g^{-1}TOC.
The remaining sample of the “normal” Zupfing Formation has a TOC content of only 0.6% and a HI of140 mgHC g^{-1}TOC (type III kerogen).

5.2.1.4 Bulk organic parameters of well Puchkirchen 3

The 44 samples from the Puchkirchen 3 well (core 1: 2610 m– 2628.5m (MD); core 2: 2628.5 m – 2647.0 m (MD); core 3: 2647 m – 2655.5 m (MD)) belong to three different formations. One sample derives from the Lithothamnium limestone. 14 samples belong to the Eggerding Formation. Three samples are from the “Transition zone”. The remaining 25 samples represent the Zupfing Formation.

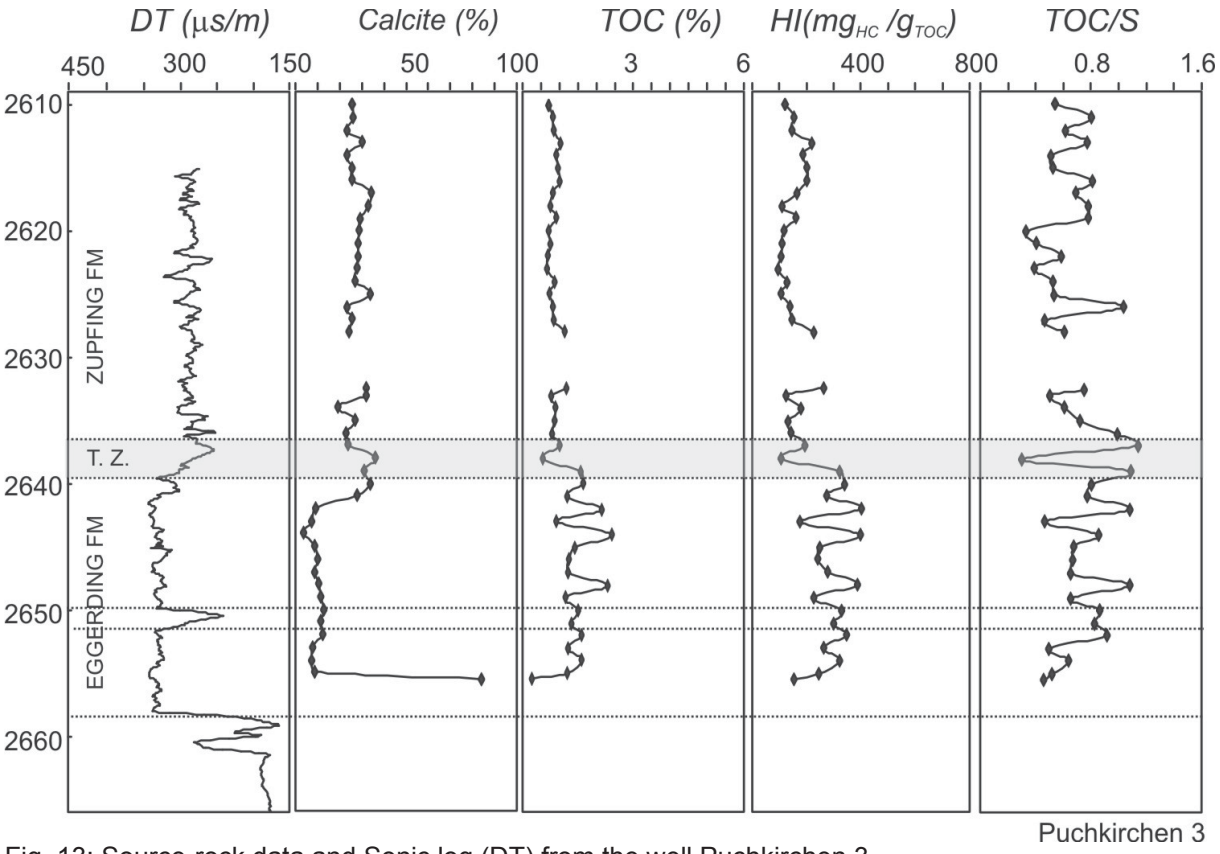

Fig. 13: Source-rock data and Sonic log (DT) from the well Puchkirchen 3.

In Fig. 13 the samples are illustrated according to the original depth labels from the core boxes. Fig. 14 shows the shifted curves, so that a good fit between measured calcite equivalent contents and DT log response has been achieved. Note the significant loss of core material in core 1 and core 2.

The TOC content of the Lithothamnium limestone sample is 0.26%, the HI value is 155 mgHC g^{-1}TOC (type III kerogen). TOC contents in the Eggerding Formation range from 1.0 to 2.4% (1.5%), their HI varies from 177 mgHC g^{-1}TOC to 401 mgHC g^{-1}TOC (type III – II kerogen). In the "Transition zone" the TOC (1.2 – 1.5%) and the calcite equivalent value (28 - 34%) reach relatively high contents. The HI ranges from 275 mgHC g^{-1}TOC to 340 mgHC g^{-1}TOC (type II/III – II kerogen). In the Zupfing Formation the TOC content lies between 0.5 - 1.2% (0.8%). The HI ranges from about 100 mgHC g^{-1}TOC to 260 mgHC g^{-1}TOC (type III – III/II kerogen).

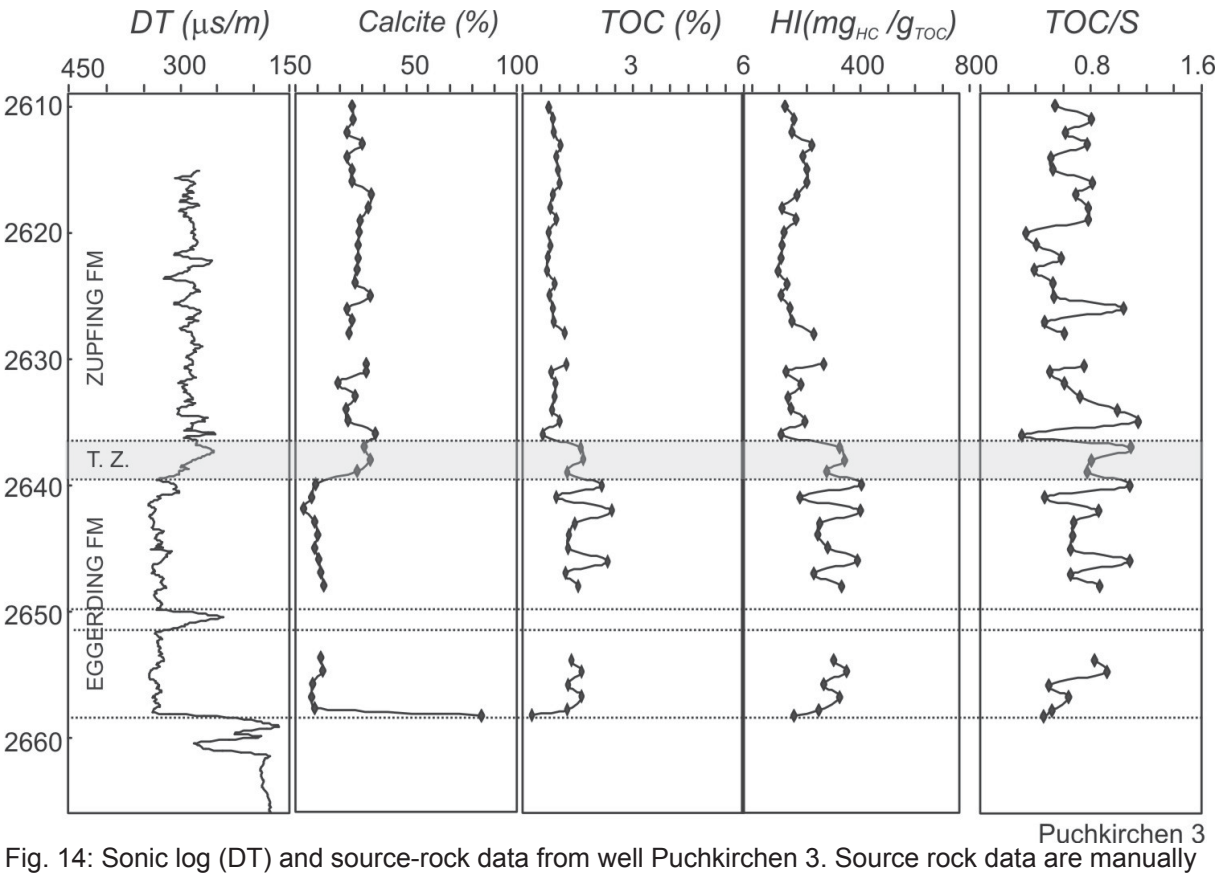

Fig. 14: Sonic log (DT) and source-rock data from well Puchkirchen 3. Source rock data are manually adapted on the Sonic – log.

5.2.1.5 Bulk organic parameters of well Hiersdorf 5 (from Sachsenhofer et al., 2008)

Apart from the Eggerding 2 well (which drilled Eggerding Formation in a near shore facies), there are no continuous cores representing the entire Eggerding Formation. Therefore, the complete lower Oligocene succession was investigated using cuttings samples from well Hiersdorf 5 by Sachsenhofer et al. (2008). To allow a high-resolution approach, cuttings samples were taken every meter.

According to this report, the measured bulk organic parameters change depending on the applied washing procedure. The results from well Hiersdorf 5, therefore, might be (slightly) influenced by drilling mud and were not used for calculations of total average values. Nevertheless, they provide important information on general trends.

The Schöneck Formation exhibits a subdivision into a marly lower part with moderate TOC contents (“units a, b” according to Schulz et al., 2002) and a shaly upper part with very high TOC contents (“unit c”). In contrast, the Dynow Formation is characterised by high carbonate and relatively low TOC contents.

Cutting samples

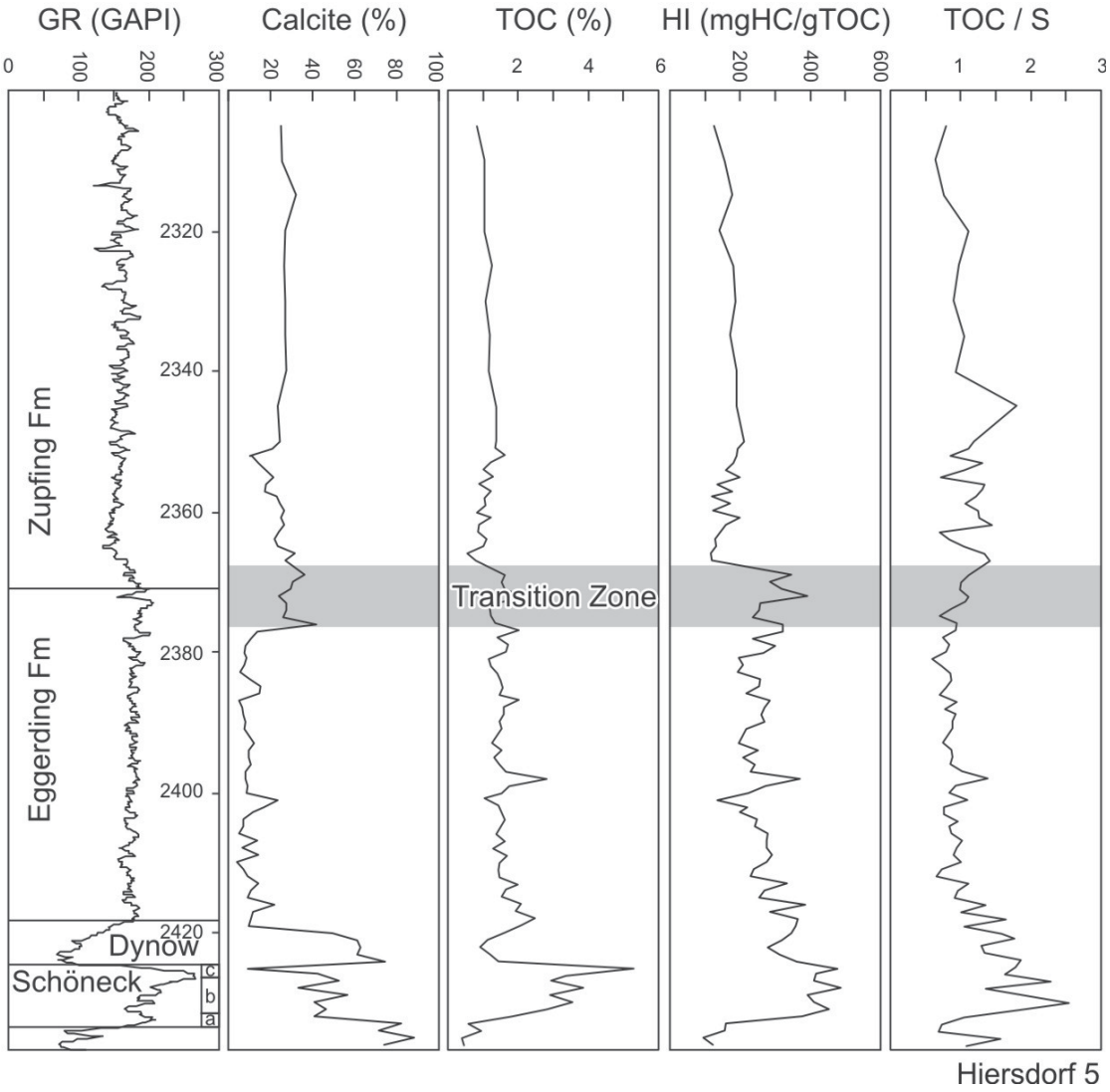

Fig. 15: Gamma-ray log (GR) and source-rock data from well Hiersdorf 5.

The Eggerding Formation in well Hiersdorf 5 is characterised by carbonate contents around 10% and TOC contents around 1.6%. In contrast, the average carbonate and TOC contents in the Zupfing Formation are 25% and 1.1%, respectively. Thereby, the lower Eggerding Formation exhibits a TOC content of 2.2% and the upper Eggerding Formation a content of 1.6%. The “Transition zone” is about 8 m thick and is characterized by both, high carbonate (30%) and TOC contents (1.5%).

Measured HI values for the entire succession from the Schöneck Formation to the transition zone are typically between 200 and 450 mgHC g^{-1}TOC.

5.2.2 Biomarker

5.2.2.1 Extract amount

The average extract yield of samples from the Zupfing Formation is 325 ppm. The extract yield of the upper and lower Eggerding Formation ranges from 1100 ppm to 2450 ppm and from 1010 ppm to 3700 ppm, respectively. The TOC-normalized bitumen contents are 34.5 mg g^{-1}TOC for the Zupfing Formation and range between 52 and 107 mg g^{-1}TOC for the upper and from 45 and 62 mg g^{-1}TOC for the lower Eggerding Formation. The results from the sample of the Transition zone are concordant with the upper Eggerding Formation. In Fig. 16 the results are illustrated in a TOC (%) – extract yield (ppm) diagram.

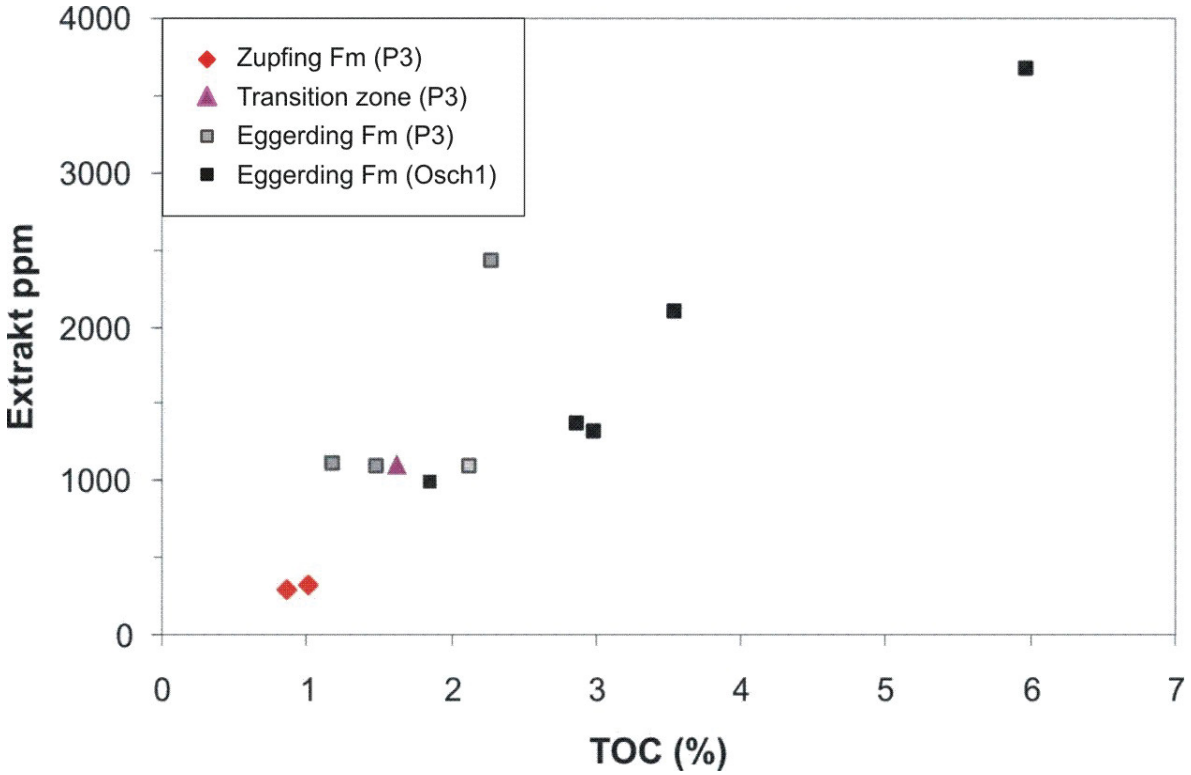

Fig.16: Extract amount in ppm versus TOC in %.

As expected, TOC contents and extract yield correlate positively. At a given TOC content, samples from the upper Eggerding Formation in well Puchkirchen 3 tend to higher extract yields. This is most likely a consequence of slightly higher thermal maturity (see below) due to the deeper position of the Eggerding Formation in the Puchkirchen 3 well.
In comparison to the other samples an extract loss of the P15 sample can not be excluded.

5.2.2.2 Hydrocarbon fractions

For the biomarker analyses the extracts where fractionated initially into asphaltenes and maltenes. Thereafter, the maltenes were divided into saturated hydrocarbons, aromatic hydrocarbons and NSO compounds. Percentages of different fractions in different samples are displayed in Fig. 17. Because of analytical problems, there are no data for saturated hydrocarbons in sample Osch 65.

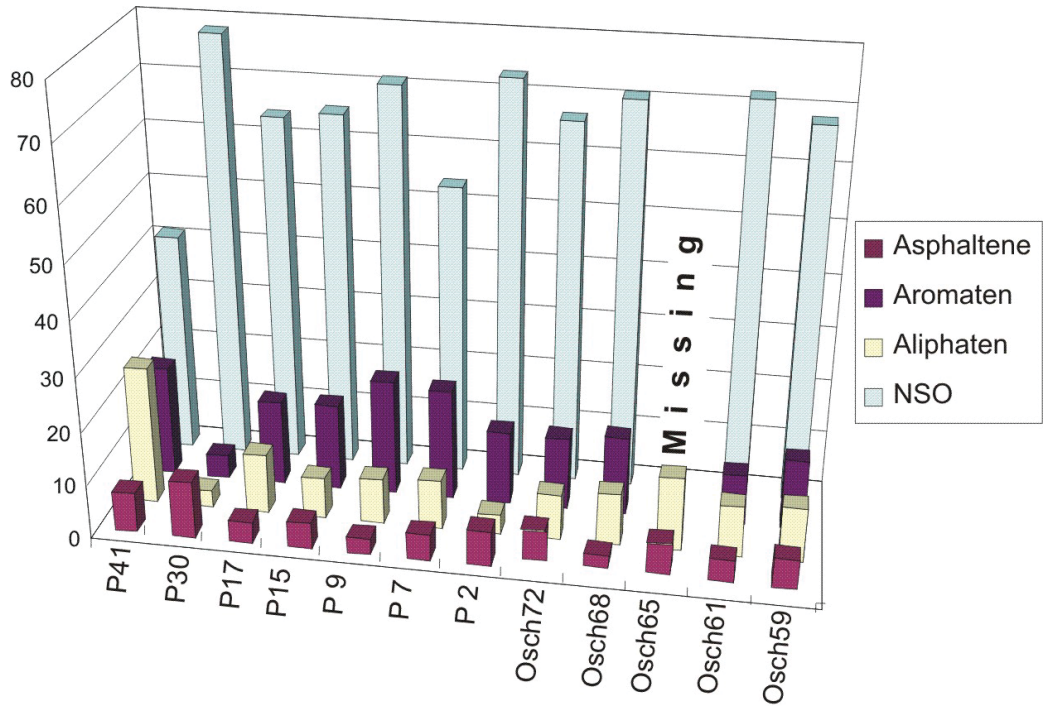

Fig.17: Hydrocarbon fractions of different samples from wells Puchkirchen 3 and Oberschauersberg 1.

5.2.2.3 Saturated Hydrocarbons

5.2.2.3.1 Acyclic Hydrocarbons

a) n-C_{27-31} and n-C_{15-19}

In Fig. 18 the samples are plotted in the diagram *n*-C_{15-19}/*n*-alkanes versus n-C_{27-31}/*n*-alkanes. An increased concentration of short-chain *n*-alkanes (*n*-C_{15}, *n*-C_{17}, *n*-C_{19}) indicates generally a biological origin from lacustrine or marine algal material. In contrast, long-chain *n*-alkanes (*n*-C_{27}, *n*-C_{29}, *n*-C_{31}) support an origin from higher terrestrial plants.
The samples show more or less a negative correlation.

Formation	Sample	MD	*n*-C_{15-19}/ *n*-Alkanes	*n*-C_{21-25}/ *n*-Alkanes	*n*-C_{27-31}/ *n*-Alkanes
Zupfing	P41	2613	0.21	0.32	0.34
Zupfing	P30	2624	0.12	0.31	0.43
Transition	P17	2640	0.19	0.34	0.34
upper Eggerding	P15	2642	0.21	0.30	0.38
upper Eggerding	P 9	2648	0.10	0.47	0.27
upper Eggerding	P 7	2650	0.15	0.35	0.37
upper Eggerding	P 2	2655	0.12	0.33	0.41
lower Eggerding	Osch72	1368	0.16	0.31	0.43
lower Eggerding	Osch68	1369.17	0.19	0.34	0.33
lower Eggerding	Osch65	1370.2	0.10	0.35	0.43
lower Eggerding	Osch61	1371.22	0.19	0.28	0.38
lower Eggerding	Osch59	1371.98	0.13	0.25	0.53

Tab.1: Relative proportions of *n*-alkanes with different number of carbon atoms in samples from the Eggerding and Zupfing formations. MD = measured depth.

There are two outliers, one from the lower Eggerding Formation (Osch 59) and one from the upper part of the Eggerding Formation (P9). Osch 59 shows a higher concentration of *n*-C_{27-31}; P9 shows a lower concentration in both *n*-C_{27-31} and *n*-C_{15-19} and consequently a high concentration in mid-chain *n*-alkanes (*n*-C_{21-25}).

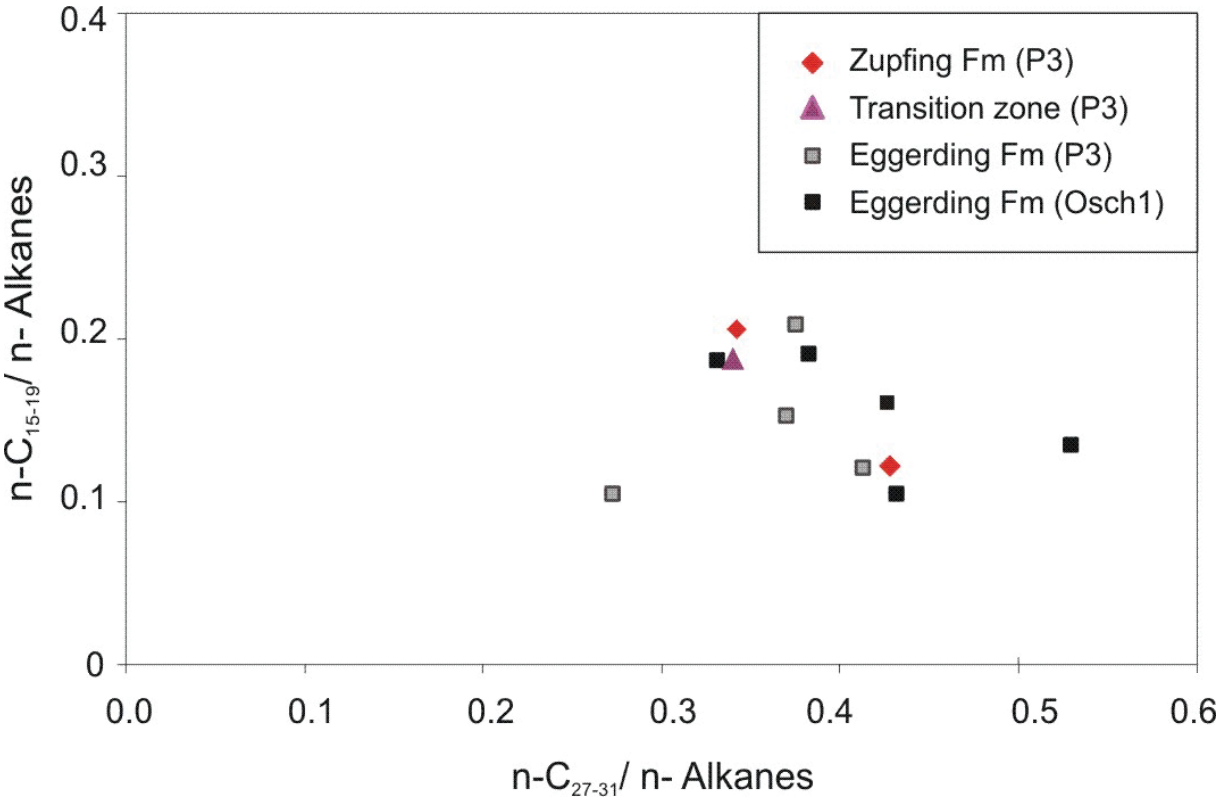

Fig.18: Crossplot of *n*-C_{15-19}/*n*-Alkanes versus n-C_{27-31}/*n*-Alkanes.

b) The Carbon – Preference – Index (CPI)

The Carbon – Preference – Index (CPI) is calculated according to the following formula (Bray & Evans, 1961)

$$\frac{\frac{C_{25}+C_{27}+C_{29}+C_{31}+C_{33}}{C_{24}+C_{26}+C_{28}+C_{30}+C_{32}}+\frac{C_{25}+C_{27}+C_{29}+C_{31}+C_{33}}{C_{26}+C_{28}+C_{30}+C_{32}+C_{34}}}{2}$$

It provides information on maturation and composition of the organic material. Higher plants are typically characterized by long-chain, odd-numbered hydrocarbons. Therefore, these hydrocarbons are abundant in samples with a high input of terrestrial plants. Maturation results in a decrease in CPI to a value close to 1.

The upper Eggerding Formation in the relatively deep Puchkirchen 3 well shows lower CPI values than the lower Eggerding Formation in the shallow Oberschauersberg 1 well. This suggests a higher maturity in the Puchkirchen area.
Sample Osch 61 has a very low CPI. Sample Osch 59, characterized by a high amout of long-chain *n*-alkanes (Fig. 18) is characterized by the the highest CPI index (Tab. 2). This suggests a high contribution of land plants to the organic matter.

Formation	Sample	MD	CPI
Zupfing	P41	2613	1.32
Zupfing	P30	2624	1.07
Transition	P17	2640	1.14
upper Eggerding	P15	2642	1.13
upper Eggerding	P 9	2648	1.19
upper Eggerding	P 7	2650	1.18
upper Eggerding	P 2	2655	0.78
lower Eggerding	Osch72	1368	2.00
lower Eggerding	Osch68	1369.17	1.20
lower Eggerding	Osch65	1370.2	1.87
lower Eggerding	Osch61	1371.22	0.59
lower Eggerding	Osch59	1371.98	2.41

Tab. 2: Carbon preference index of samples from the Puchkirchen (P) and Oberschauersberg (Osch) wells.

c) Pristane and Phytane

Fig. 19 shows the distribution of the samples in a pristane (Pr)/ *n*-C_{17} versus phytane (Ph)/ *n*-C_{18} diagram. This diagram has proven valuable in oil-oil and oil-source rock correlations, because general information on biodegradation, maturity and depositional environment are provided (Connan & Cassou, 1980; Peters et al., 1999). Generally, high pristane/phytane

ratios Pr/ *n*-C_{17} indicate oxic conditions during organic matter deposition. Maturation results in a shift of Pr/ *n*-C_{17} and Ph/ *n*-C_{18} ratios towards lower values. On the other hand an increase in Pr/ *n*-C_{17} and Ph/ *n*-C_{18} ratios could imply biodegradation, because bacteria preferably attack *n*-alkanes.

Most samples plot into the mixed kerogen II-III field. Two samples from the lower Eggerding Formation (Osch 59, Osch 72) and one sample from the Zupfing Formation (P41) show enhanced terrestrial input.
One sample from the lower Eggerding Formation plots near the border towards marine algal material.

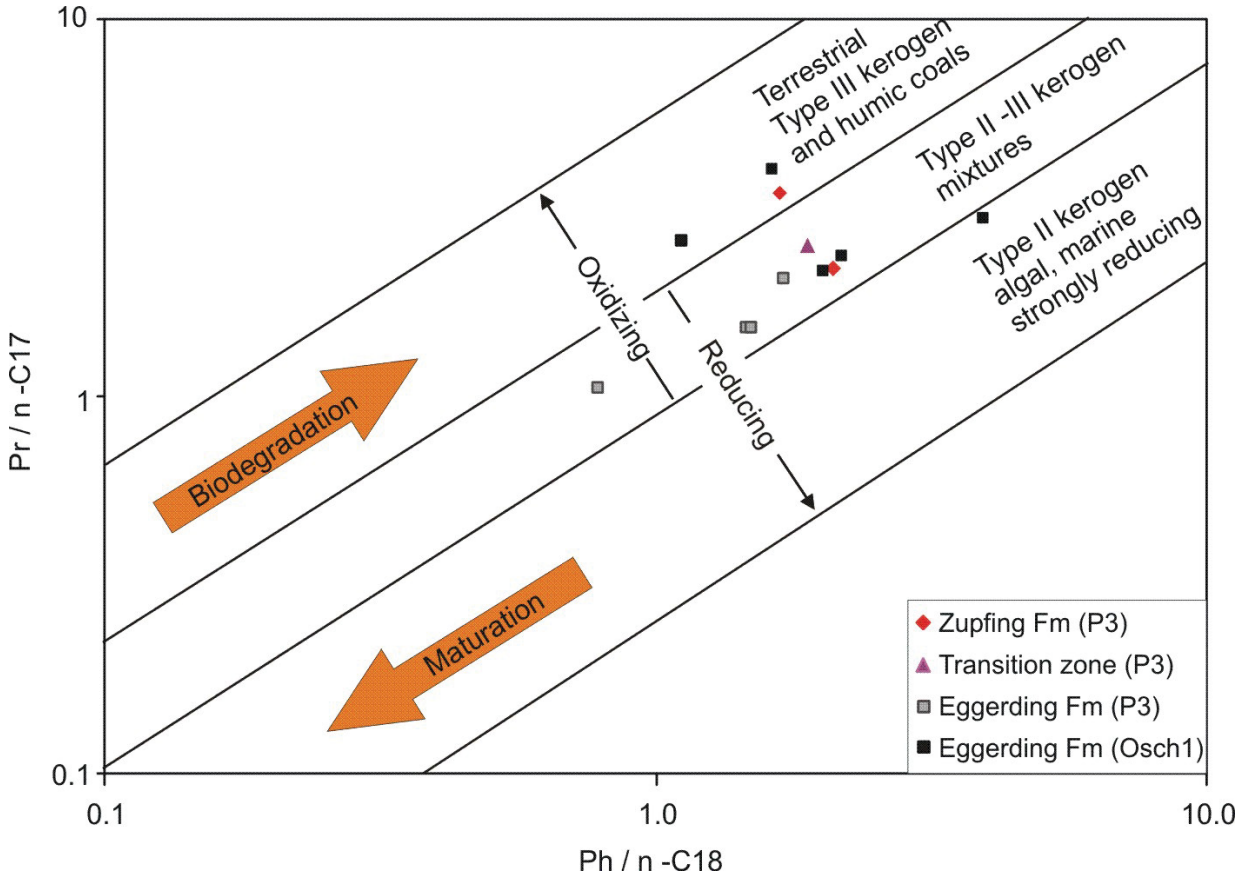

Fig. 19: Crossplot of Pr/ *n*-C_{17} versus Ph/ *n*-C_{18}.

Formation	Sample	MD	Pr / *n*-C_{17}	Ph / *n*-C_{18}	Pr / Ph
Zupfing	P41	2613	3.59	1.67	1.38
Zupfing	P30	2624	2.29	2.09	0.86
Transition	P17	2640	2.65	1.88	1.10
upper Eggerding	P15	2642	2.10	1.71	1.26
upper Eggerding	P 9	2648	1.54	1.49	0.96
upper Eggerding	P 7	2650	1.54	1.47	1.08
upper Eggerding	P 2	2655	1.07	0.79	0.88
lower Eggerding	Osch72	1368	2.63	1.11	1.25
lower Eggerding	Osch68	1369.17	3.03	3.95	0.61
lower Eggerding	Osch65	1370.2	2.41	2.18	0.89
lower Eggerding	Osch61	1371.22	2.18	2.02	1.19
lower Eggerding	Osch59	1371.98	4.11	1.63	2.32

Tab. 3: Pristane and Phytane ratios of samples from the Puchkirchen (P) and Oberschauersberg (Osch) wells.

5.2.2.3.2 Cyclic Hydrocarbons

a) Pentacyclic Terpenoids (Hopane)

Formation	Sample	MD	Ts / Tm	Hopane/ Moretane	22S/(22S+22R) C_{31}-Hopanes
Zupfing	P41	2613	0.55	5.80	0.57
Zupfing	P30	2624	0.35	2.60	0.56
Transition	P17	2640	0.57	5.95	0.55
upper Eggerding	P15	2642	0.71	6.06	0.57
upper Eggerding	P 9	2648	0.59	7.67	0.57
upper Eggerding	P 7	2650	0.57	5.96	0.56
upper Eggerding	P 2	2655	0.42	4.79	0.57
lower Eggerding	Osch72	1368	0.58	6.18	0.31
lower Eggerding	Osch68	1369.17	0.56	5.39	0.38
lower Eggerding	Osch65	1370.2			
lower Eggerding	Osch61	1371.22	0.61	7.09	0.32
lower Eggerding	Osch59	1371.98	0.52	3.84	0.34

Tab. 4: Various ratios of the pentacyclic terpanoids of samples from the Puchkirchen (P) and Oberschauersberg (Osch) wells.

There is only one known biological precursor of the hopane, bakteriohopanteriol, a C_{35} hopanoid, part of the cell membrane of prokaryots (Ourisson et al., 1979). In living organism exist some lipids; these change into saturated hydrocarbons. These hydrated hopanes are normally present in their 17β(H),21β(H)-configuration, which is thermodynamically not stable. With increasing maturation they change into 17α(H),21β(H)–hopanes and 17β(H),21α(H)–moretanes. Hopanes are more stable than moretanes. The ratio of hopane and moretane should increase with maturation.
The ratios of the studied samples do not follow a clear trend.

Hopanes which exceed the number of 31 carbon atoms have an additional chiral center on position of C_{22}. It allows a 22R and 22S configuration. With maturation the R configuration becomes instable and changes to the S-configuration. At the onset of the oil window (corresponding to a vitrinite reflectance of 0.5% Rr), the equilibrium of about 60% 22S and 40% 22R is reached. With increasing maturation there are no additional changes in the epimer ratio. Thus, the 22S/ (22S+22R) ratio rises from 0 to about 0.6 (Seifert and Moldowan, 1986) during maturation. Samples showing a ratio in the range 0.5 to 0.54 are marginally mature, while ratios in the range of 0.57 to 0.62 indicate that the main phase of oil generation has been reached or surpassed (Peters and Moldowan, 1993).
The ratios in table 4 show a clear differentiation between samples from the well Puchkirchen 3 and the well Oberschauersberg 1. The Puchkirchen samples are from about 2650 m depth and achieve nearly the equilibrium (average 0.56). In contrast, shallow samples from the well Oberschauersberg 1 (~1370 m) are characterized by an average value of only 0.34 (see also Fig. 25).
With increasing maturation Tm (C_{27} 17α(H)-trisnorhopane) has a lower stability than Ts (C_{27} 18α(H)-Trisnorneohopane and therefore the concentration of the latter one increases. The ratio also depends on the organic input: it reacts sensible to the changes of redox-condition in the sedimentation area (Moldowan et al., 1986). Tm should increase under oxic conditions. The Ts/Tm ratio in table 4 does not show a clear trend.

b) Sterane distribution

Biological precursors of steranes are C_{27}-C_{30} steroles in the cell membranes of eukaryotic organisms. Besides regular steranes, diagenetically modified steranes, so-called diasteranes, exist. They have additional methyl-groups on the C_5 and the C_{14} atom and H-atoms on the position C_{10} and C_{13}.
C_{27}, C_{28} and C_{29} steranes are often used in ternary diagrams to identify depositional environments (see Fig. 20) and for correlation purposes (see section 6.4). High amounts of C_{29} are indicative for terrestrial organic matter, whereas C_{27} steranes are often related to algal material. An increase in C_{28} steranes through geological time has been related to an increased diversification of phytoplankton assemblages including diatoms, coccolithophorides and dinoflagellates (Grantham & Wakefield, 1988). Relatively high percentages of C_{28} steranes in the lower Eggerding Formation, therefore, might be related to the presence of layers with coccolithophorides.

Formation	Sample	MD	C_{27}-Sterane / Steranes	C_{28}-Sterane / Steranes	C_{29} -Sterane / Steranes	20S/(20S+20R) $\alpha\alpha$ C_{29}- Steranes	C_{27} Diasterane / C_{27} Sterane
Zupfing	P41	2613	0.35	0.31	0.34	0.19	0.32
Zupfing	P30	2624	0.35	0.31	0.33	0.16	0.45
Transition	P17	2640	0.35	0.34	0.31	0.22	0.30
upper Eggerding	P15	2642	0.33	0.35	0.32	0.21	0.32
upper Eggerding	P 9	2648	0.38	0.32	0.30	0.26	0.17
upper Eggerding	P 7	2650	0.28	0.39	0.32	0.20	0.27
upper Eggerding	P 2	2655	0.38	0.29	0.33	0.30	0.46
lower Eggerding	Osch72	1368	0.30	0.39	0.31	0.06	0.35
lower Eggerding	Osch68	1369.17	0.20	0.42	0.38	0.04	0.30
lower Eggerding	Osch65	1370.2	0.23	0.47	0.30		
lower Eggerding	Osch61	1371.22	0.22	0.47	0.30	0.00	0.66
lower Eggerding	Osch59	1371.98	0.28	0.37	0.35	0.07	0.32

Tab. 5: Various steranes ratios of samples from the Puchkirchen (P) and Oberschauersberg (Osch) wells.

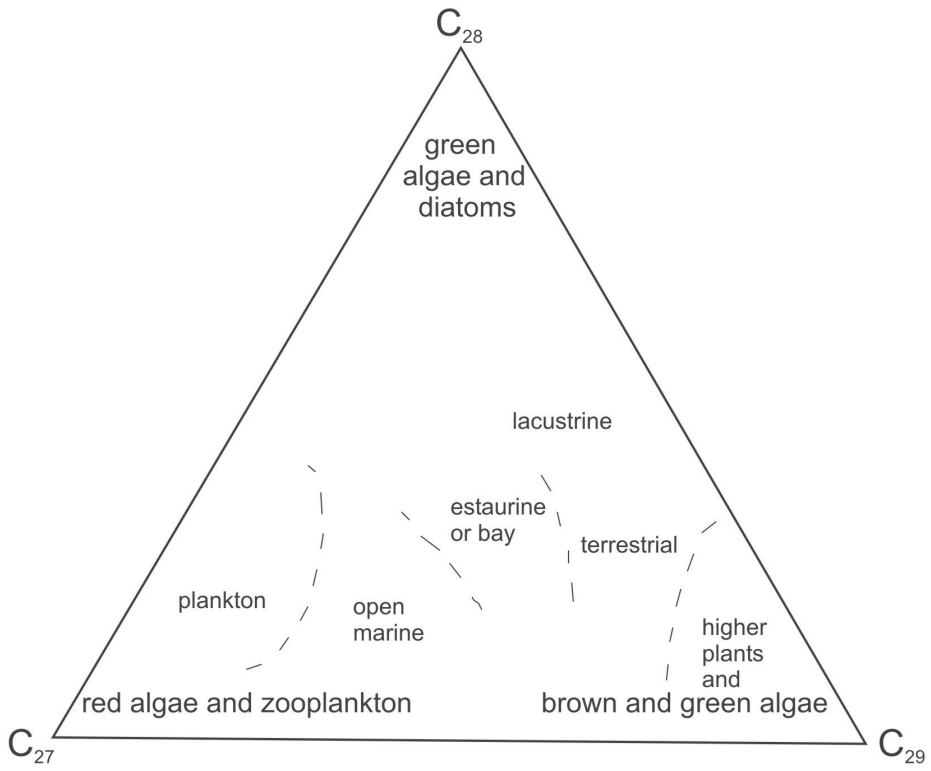

Fig. 20: Ternary diagram of C_{27}, C_{28} and C_{29} steranes (Hunt, 1995).

In the ternary diagram of C_{27}, C_{28} and C_{29} steranes all samples plot near the center of the diagram. There is little variation in the relative amount of C_{29} steranes. Based on C_{27} and C_{28} steranes, the samples are split into two groups:

1. samples from the lower Eggerding Formation and one sample from the upper Eggerding Formation are characterized by a dominance of C_{28} steranes, whereas
2. samples from the upper Eggerding Formation, the Transition zone and the Zupfing Formation include a higher proportion of C_{27} steranes (Fig. 21).

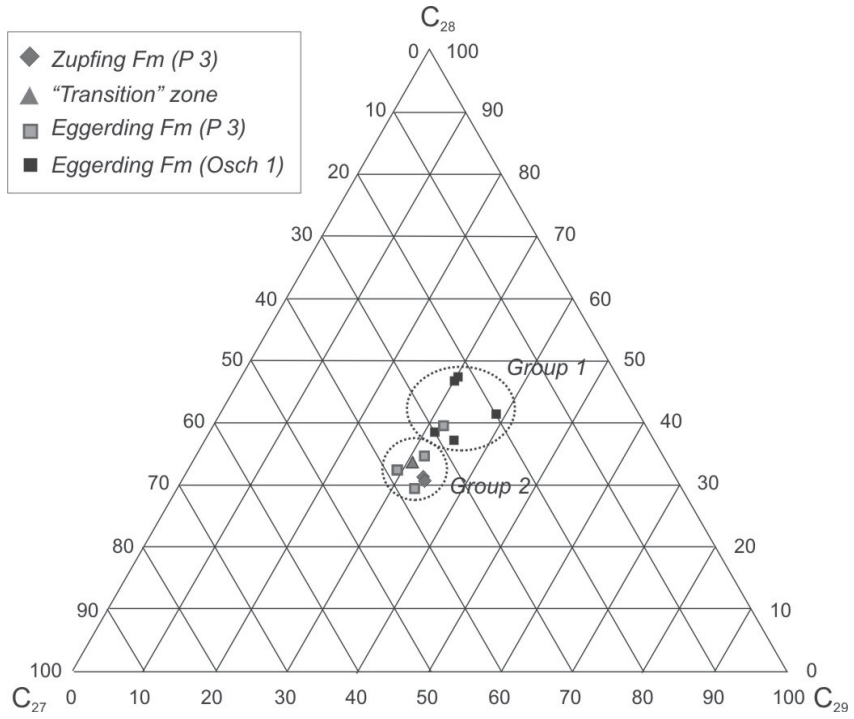

Fig. 21: Ternary diagram of C_{27}, C_{28} and C_{29} steranes.

Steranes/diasteranes ratios were often used to differentiate between clastic or carbonate dominated source rocks. Ratios below 0.3 generally suggest anoxic conditions and/or a carbonate-rich environment with a low clay amount. Ratios above 0.3 suggest clay-rich source rocks.
Thus, steranes/diasteranes ratios should be correlated negatively with calcite percentages. However, data in Fig. 22 show no clear trend.

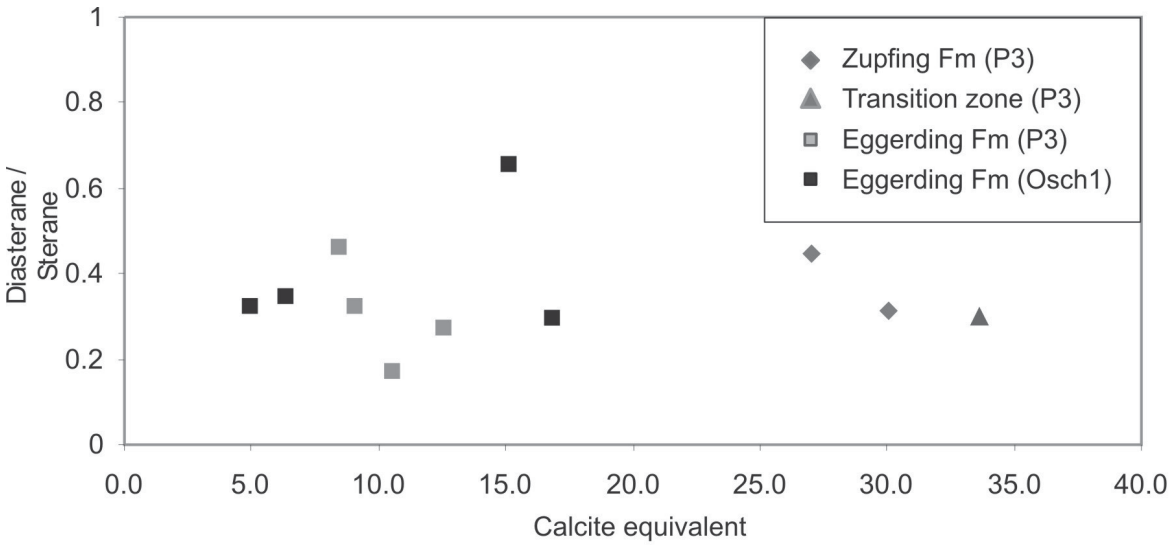

Fig. 22: Crossplot of diasteranes/dteranes ratios versus calcite equivalent percentages.

The 20S/(20S+20R) isomer ratios of the 5α(H),14α(H),17α(H)-C_{29} steranes is a maturation parameter. 20S is the more stable configuration. The 20S/(20S+20R) ratio increases from 0.0 to about 0.5 (0.52 to 0.55 = equilibrium; Seifert and Moldowan, 1986) with increasing maturity. Peters and Moldowan (1993) do not recommend the usage of the 20S/(20S+20R) ethylcolestane (C_{29}) ratio as indicator of the onset of petroleum generation unless it is calibrated for each basin and source rock.
The samples from the deep Puchkirchen 3 well show higher ratios than those from the well Oberschauersberg 1 (table 5). Fig. 23 shows a cross-plot of hopane and sterane isomerization ratios emphasizing the higher maturity of Puchkirchen samples.
Although the vertical distance between the samples in the Puchkirchen 3 well is small, a downward increasing trend in sterane isomerization is visible (see Fig. 24).

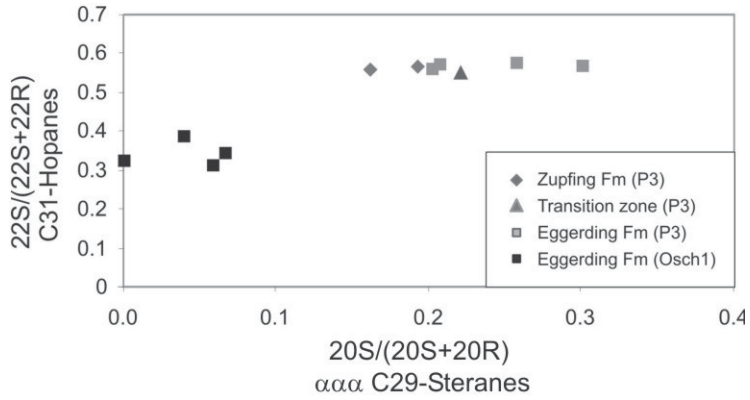

Fig. 23: Crossplot of hopane versus sterane isomerization.

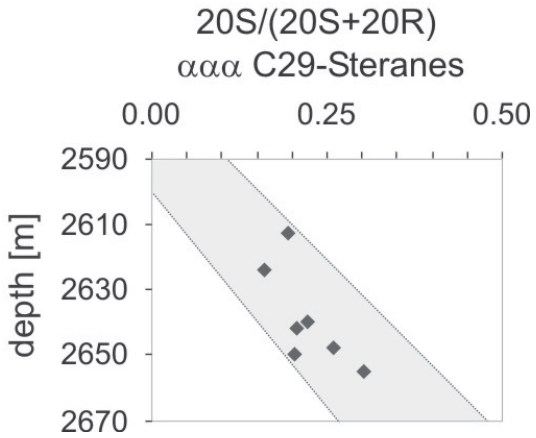

Fig. 24: Vertical variation of the 20S/(20S+20R) isomer ratio of 5α(H),14α(H),17α(H)-C_{29} steranes in the lower Oligocene succession in well Puchkirchen 3.

In Fig. 25 the steranes/hopanes ratio is plotted against the TOC/S ratio. According to Moldowan et al. (1985) high steranes/hopanes ratios (≥ 1) seem to typify marine organic matter with major contributions from planktonic and/or benthic algae. Lower sterane/hopane ratios are more indicative for terrigenous and/or microbially reworked organic matter (Tissot and Welte, 1984).

TOC/S ratios (see. also chapter 6.1.2) around 2.8 (±0.8) are typical for normal marine conditions. Values above or below characterize freshwater and euxinic conditions, respectively.
Both parameters are positively correlated. This suggests both, a higher proportion of bacterially reworked organic matter in the upper Eggerding and the Zupfing formations (P) and a strictly anoxic depositional environment.

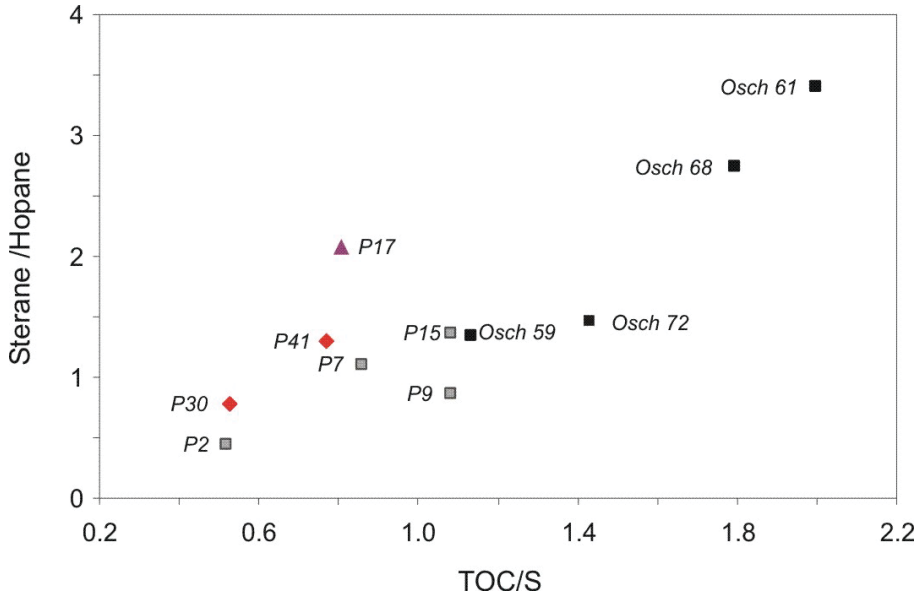

Fig. 25: Crossplot of steranes/hopanes ratio versus TOC/S ratio.

In Fig. 26 the steranes/hopanes ratio is plotted against the ration of C_{27}/C_{28} steranes. It suggests that low steranes/hopanes ratios are found in samples with high contents in C_{28} steranes implying a relative high contribution of coccolithophorides, dinoflagellates and/or diatoms.

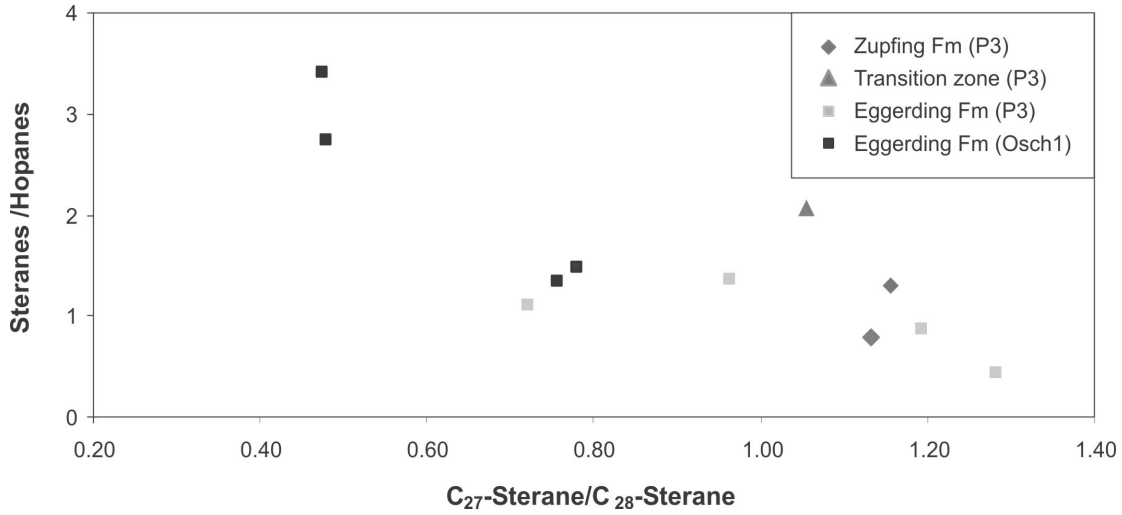

Fig. 26: Crossplot of steranes/hopanes ratio versus C_{27}/C_{28} Sterane.

5.2.2.3 Aromatic Hydrocarbons

5.2.2.3.1 Aromatic Steroids

The aromatization of C-ring monoaromatic (MA) steroid to triaromatic steroids (TA) involves a loss of a methyl group. The ratio TA/(MA+TA) increases from 0 to 100 percent during thermal maturation (Mackenzie, 1984).
Fig. 27 shows again the higher maturity of the Puchkirchen samples.

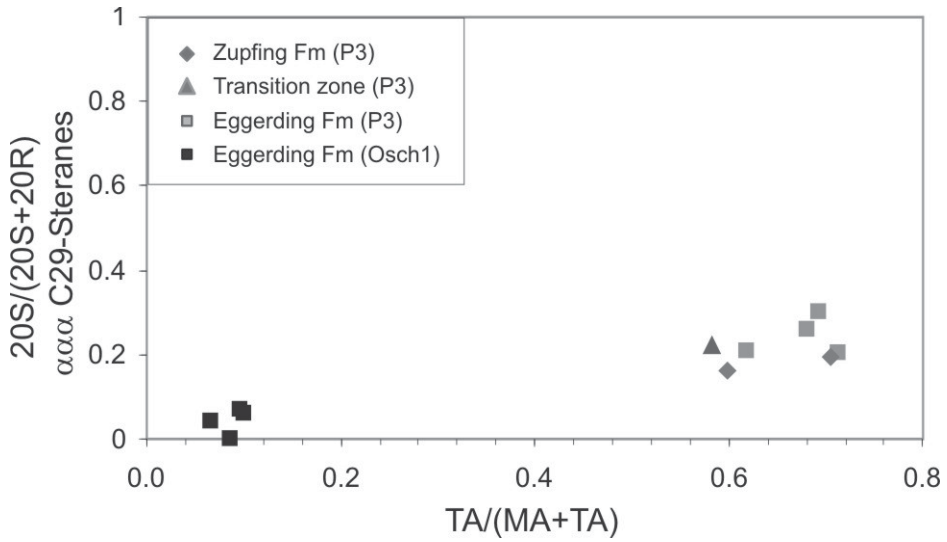

Fig. 27: Crossplot of 20S/20S+20R ratio from 5α(H),14α(H),17α(H)-C_{29} steranes versus TA/(MA+TA).

5.2.2.3.1 di- / tri- MTTC

The methylated 2-methyl-2-(trimethyltridecyl) chromans (MTTCs) occur in significant amounts only in the lower Eggerding Formation of the well Oberschauersberg 1. These data are shown in Fig. 28 together with values from the underlying Dynow and Schöneck formations of well Oberschauersberg 1 (Schulz et al.; 2005). The 2,5,7,8-tetramethyl-2-(4',8',12'-trimethyltridecyl) chroman (tri-MTTC) predominates in all samples over the 2,5,8-trimethyl-2-(4',8',12'-trimethyltridecyl) chroman (di-MTTC).
The origin of methylated MTTCs is not yet understood (Sinninghe Damsté et al., 1993). Whereas Barakat and Rullkötter (1997) suggested that chromans may be formed by cyclisation of alkylated phenols, Li et al. (1995) raised the possibility that they may be derived from condensation of alkyl phenols and chlorophyll.
Regardless of their potential biological precursor, methylated MTTCs have been widely used for palaeosalinity reconstruction (Sinninghe Damsté et al., 1993; Barakat and Rullkötter, 1997). The di-/tri-MTTC ratio is proportional to the salinity.
Fig. 28 shows the di-/tri-MTTC ratio and the pristane/phytane ratio versus depth together with the Sonic log (DT). The di-/tri-MTTC ratio increases from unit a towards unit b and unit c of

the Schöneck Formation (Sachsenhofer and Schulz, 2006). In the upper part of unit c the ratio decreases abruptly and remains low within the Dynow Formation. Towards the Eggerding Formation the di-/tri-MTTC ratio rises again and reaches the highest values of the investigated samples, before it drops to values similar to those in the Dynow Formation. The pristane/phytane ratio is rather inversely proportional to the di-/tri-MTTC ratio, except for the lower part of the Eggerding Formation; here the pristane/phytane ratio does not follow the major fluctuations of the di-/tri-MTTC ratio.

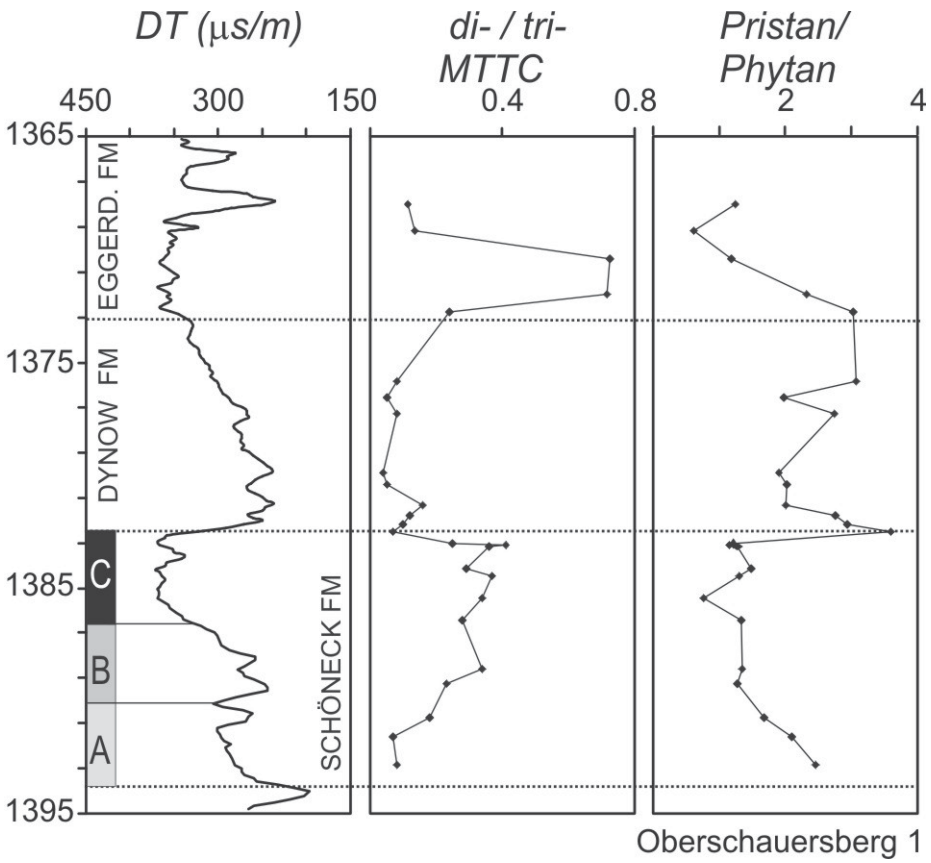

Fig. 28: Sonic log (DT) data, di-/tri- MTTC data and pristane/phytane data from the well Oberschauersberg 1 versus depth. Data from the Schöneck Formation, the Dynow Formation and the lowest sample of the Eggerding Formation are from Schulz et al. (2005).

5.3 Log correlation

Gamma Ray (GR) and Sonic (DT) logs are routinely used as correlation tools. In the case of the Lower Oligocene succession in the Molasse Basin, the DT log proved to be the better correlation tool (Schulz et al., 2004; Sachsenhofer and Schulz, 2006). This is because the DT log reacts very sensitive to variations in carbonate contents and because the GR log is influenced by small amounts of glauconite within the Schöneck Formation.
Consequently the present study is mainly based on the DT log.

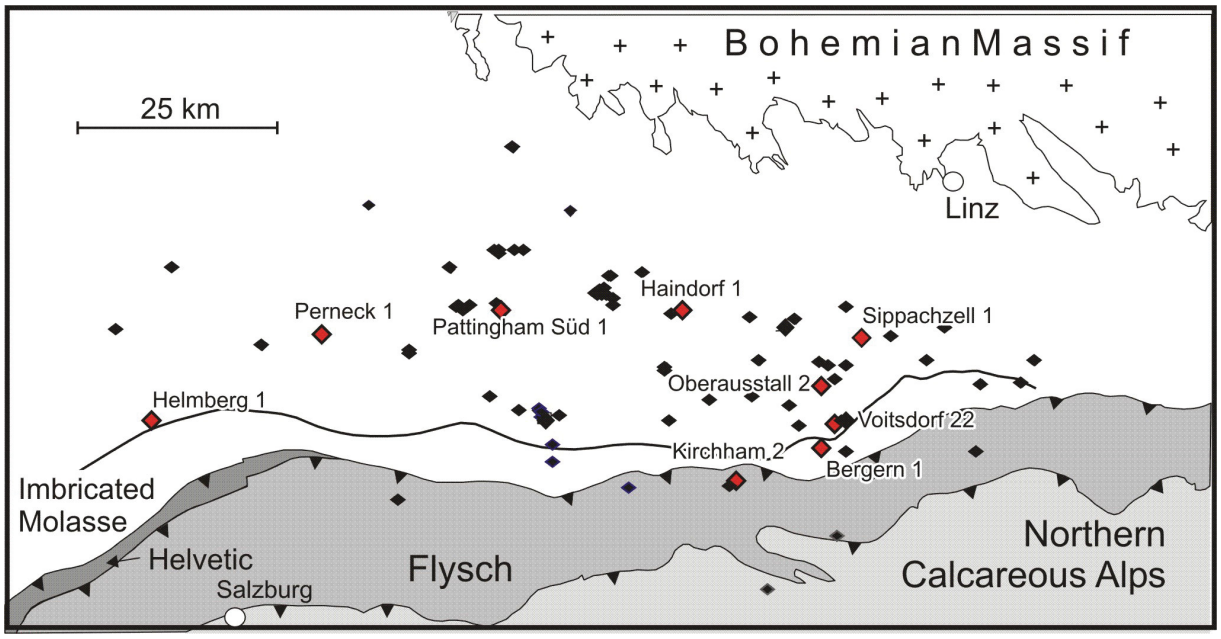

Fig. 29: Position of key wells (highlighted in red) in the study area: From west to east Helmberg 1, Perneck 1, Pattigham Süd 1, Haindorf 1, Kirchham 2, Bergern 1, Oberaustall 2, Voitsdorf 22, Sipbachzell 1.

In chapter 5.3.1, key wells (marked by rectangles in Fig. 29) located in different parts of the study area are presented in order to show typical log patterns of the Eggerding Formation and to investigate large-scale lateral facies variations. In chapter 5.3.2 detailed correlations for single areas, partly on a field basis, are presented.

5.3.1 Key wells

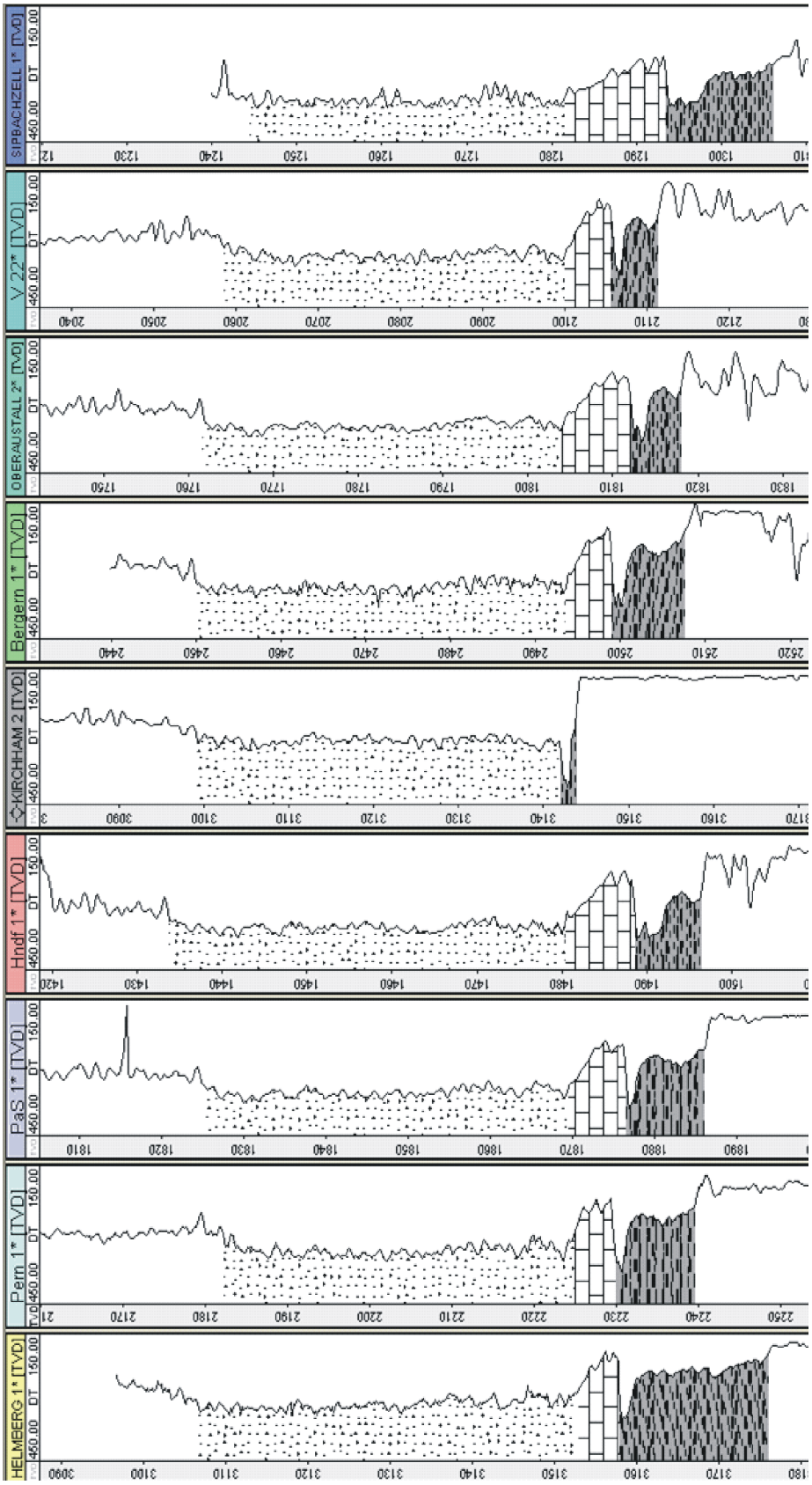

Fig. 30: DT logs from „key wells“. See Fig. 29 for position of wells.

Only boreholes with a more or less complete Eggerding Formation were selected as key wells (i.e. wells with erosion were neglected). DT logs of the chosen key wells (Helmberg 1, Perneck 1, Pattigham Süd 1, Haindorf 1, Kirchham 2, Bergern 1, Oberaustall 2, Voitsdorf 22, Sipbachzell 1) are illustrated in Fig. 30 using the base of the Eggerding Formation as datum. The Eggerding Formation is about 40 to 50 m thick in all key wells. In comparison to both, the underlying Dynow Formation and the overlying Zupfing Formation, it is characterized by low sonic velocities (high DT). Within the Eggerding Formation the log pattern is relatively smooth, although some low amplitude variations and a few prominent log peaks are visible.

In order to study similarities and differences between log patterns from different areas, the DT log of each key well is compared to that from well Pattigham Süd 1, located in the central part of the study area. In order to facilitate the comparison the logs are displayed together with the “ghost” of Pattigham Süd 1 in Fig. 31.

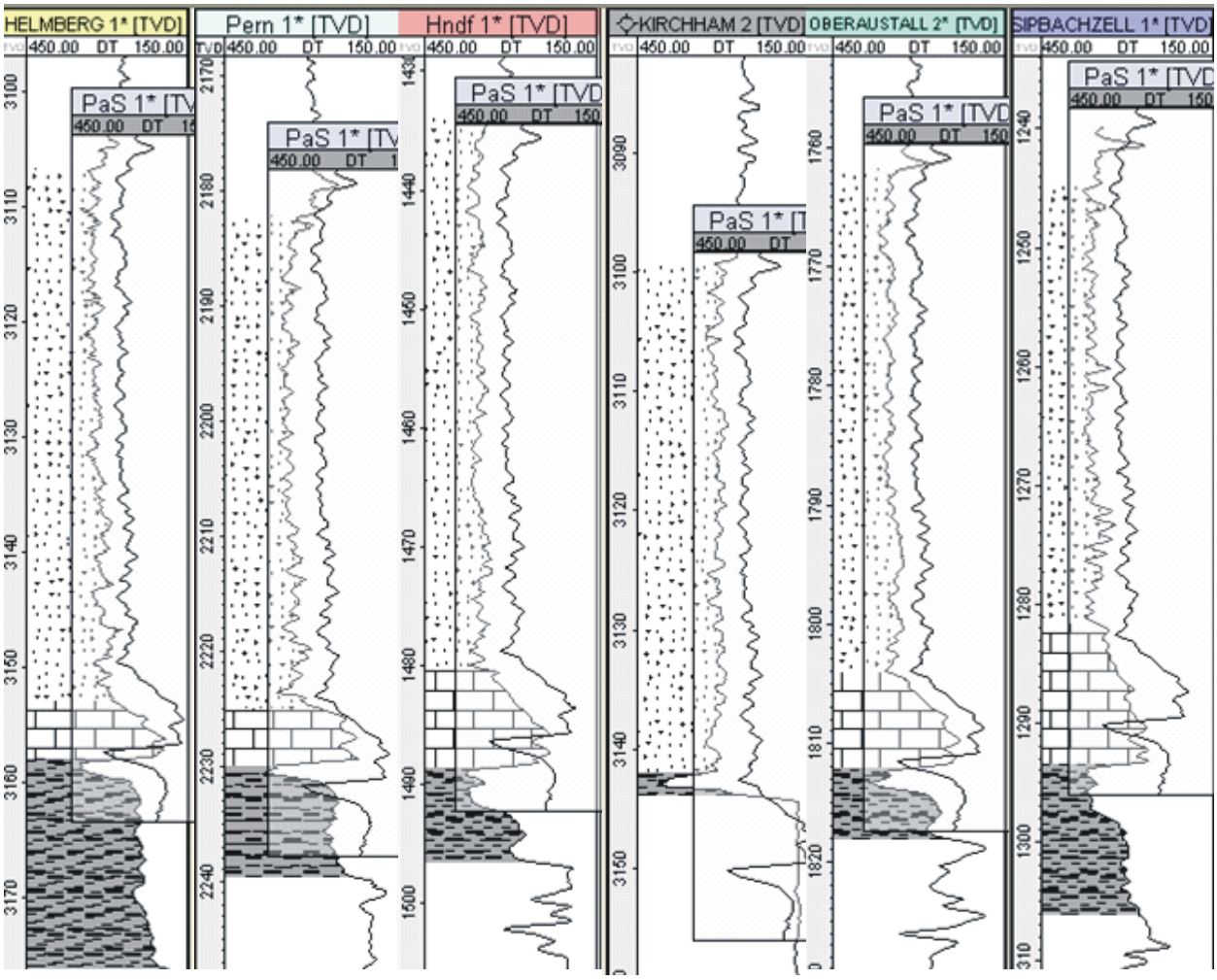

Fig. 31: DT logs from „key wells“. The “ghost” of PaS 1 (Pattigham Süd 1) is shown together with each well for a detailed comparison.

Helmberg 1: At Helmberg the lower Oligocene formations occur in more than 3.1 km depth. Although Helmberg 1 is located about 50 km southwest of Pattigham, the correlation with the shallow Pattigham Süd 1 well shows an excellent match. Only the vertical

distance between some peaks varies slightly.

Perneck 1: The Eggerding Formation of Perneck 1 matches excellently with the more eastern located one of Pattigham Süd1

Haindorf 1: The fit between logs in wells Haindorf 1 and Pattigham Süd 1is excellent in the upper part, but moderate in the rest of the section.

Kirchham 2 shows a typical log pattern in the deep southern part of the central sector of the study area. Considering the distance between the Kirchham and Pattigham wells, they show a perfect match, especially in the upper part of the section. The lower part of the section in the Kirchham area might be affected by erosion, because the whole Dynow Formation is missing.

Oberaustall 2: Despite the significant distance between wells Oberaustall 2 and Pattigham Süd 1, the logs of both wells correlate perfectly on a peak to peak base.

Sippachzell 1: The correlation between Pattigham Süd 1 and Sippachzell 1 is not as good as that with other wells. This is especially true for the upper part of the Eggerding Formation. Perhaps the (moderate) misfit results from the paleogeographic position of Sippbachzell 1 close to the former coastline.

Voitsdorf 22: A detailed comparison of well Voitsdorf 22 with Pattigham Süd 1 shows an excellent match for both, the upper and lower part of the Eggerding Formation (Fig. 32). However, an interval about 12 m thick present in the Pattigham Süd 1 well is missing in the Voitsdorf 22 well at a depth of about 2084 m. At the moment it is impossible to decide whether this is due to faulting, non-deposition or erosion.

Bergern 1: The log of Bergern 1 is very serrated. Nevertheless, the match with the Pattigham Süd 1 well is excellent.

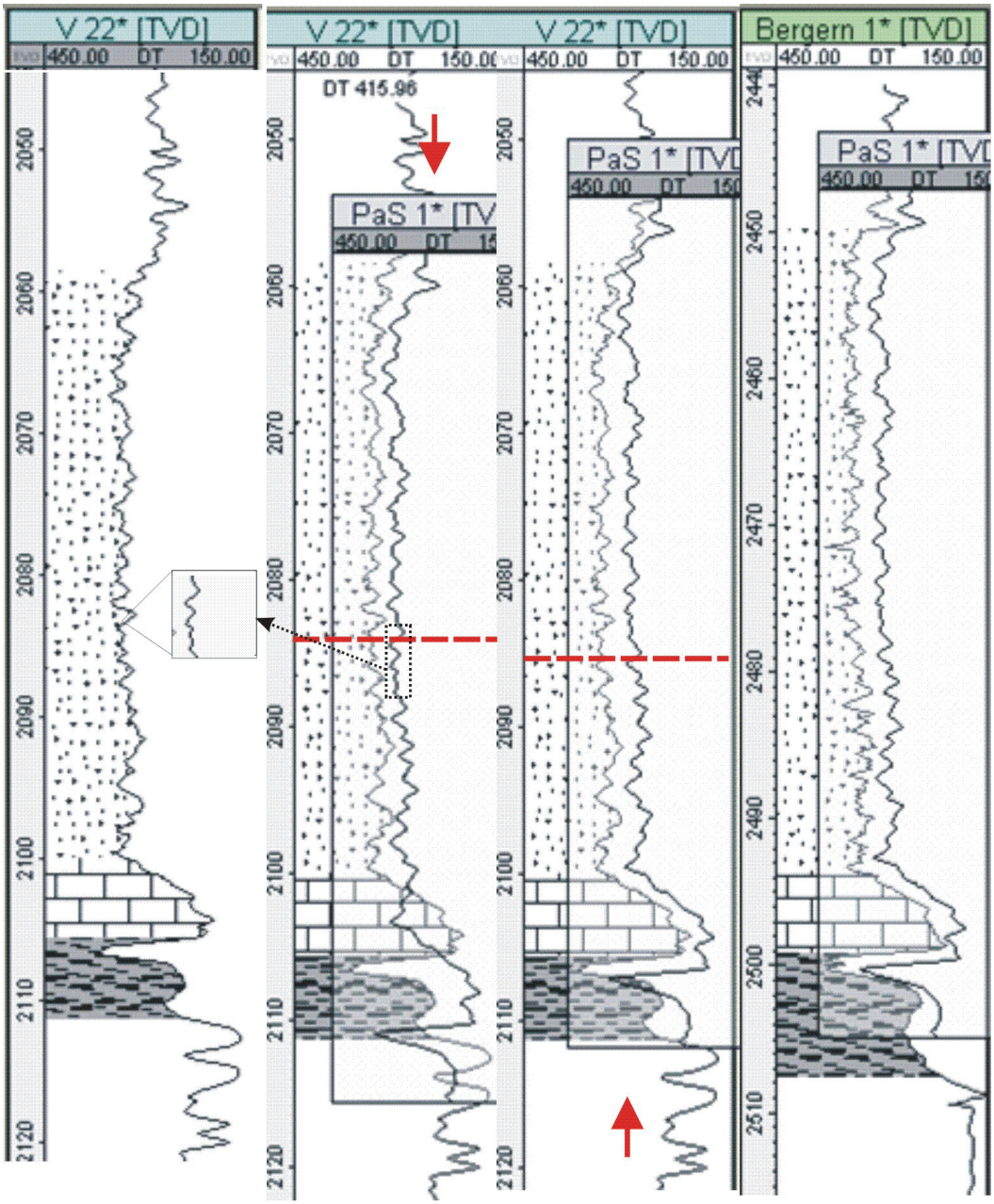

Fig. 32: DT logs from „key wells“ Voitsdorf 22 and Bergern 1. The “ghost” of PaS 1 (Pattigham Süd 1) is shown together with each well for a detailed comparison. Broken red line in the second and third column represents the stratigraphic level down/up to which a good fit is realized. A stratigraphic interval about 12 m thick, which is present in PaS 1, is missing in Voitsdorf 22.

5.3.2 Detailed correlation

5.3.2.1 West

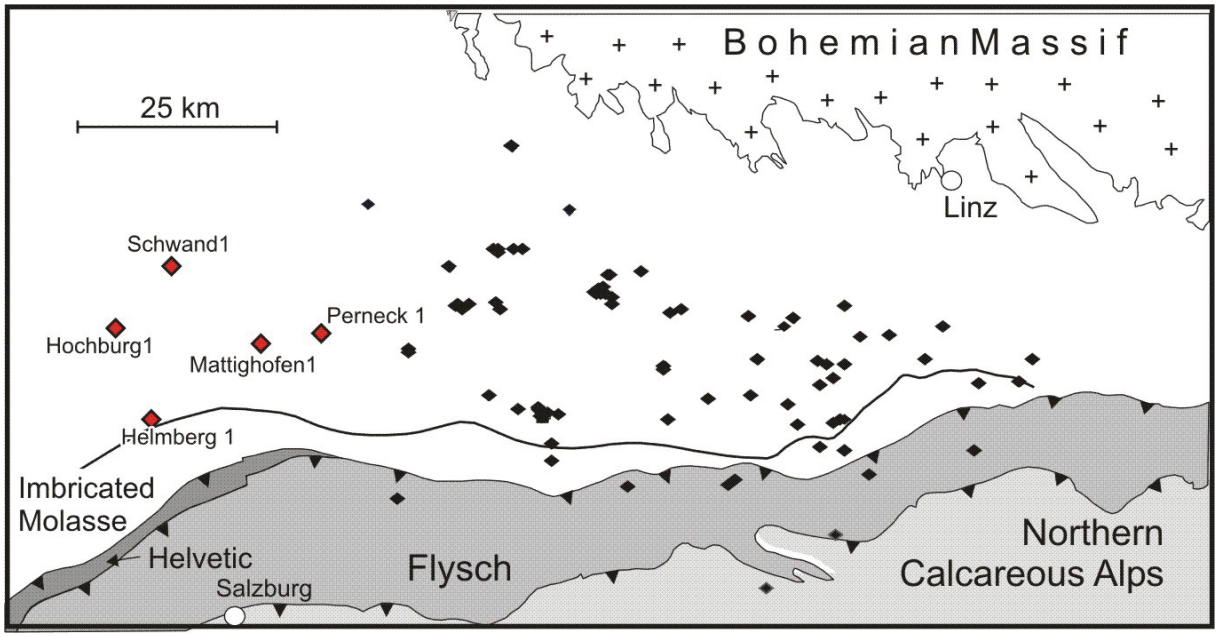

Fig. 33: Index map showing position of the study area “West”.

Fig. 34 shows from W to E the logs of the western part of the study area (Fig. 33). The Schöneck Formation is present in all five wells, but not uniform in thickness. Thickness variations are probably due to a paleo-relief after deposition of the Lithothamnium Limestone (Sachsenhofer and Schulz, 2006). The Schöneck Formation of the Helmberg log is very thick, but this is caused probably by its deeper position on the paleo-slope. Helmberg is therefore also included in the section on the “southern wells”.

The Dynow Formation is about 5 m thick in all wells and shows similar log patterns.

The Eggerding Formation in wells Hochburg (Hobg) 1 and Perneck (Pern) 1 shows typical log patterns. A comparison of the Mattighofen 1 and the key well Perneck 1 shows that in Mattighofen 1 an interval, about 4 m thick, is missing in the lower middle part of the Eggerding Formation (see red line in Fig. 34). This is caused either by a small normal fault or local erosion.

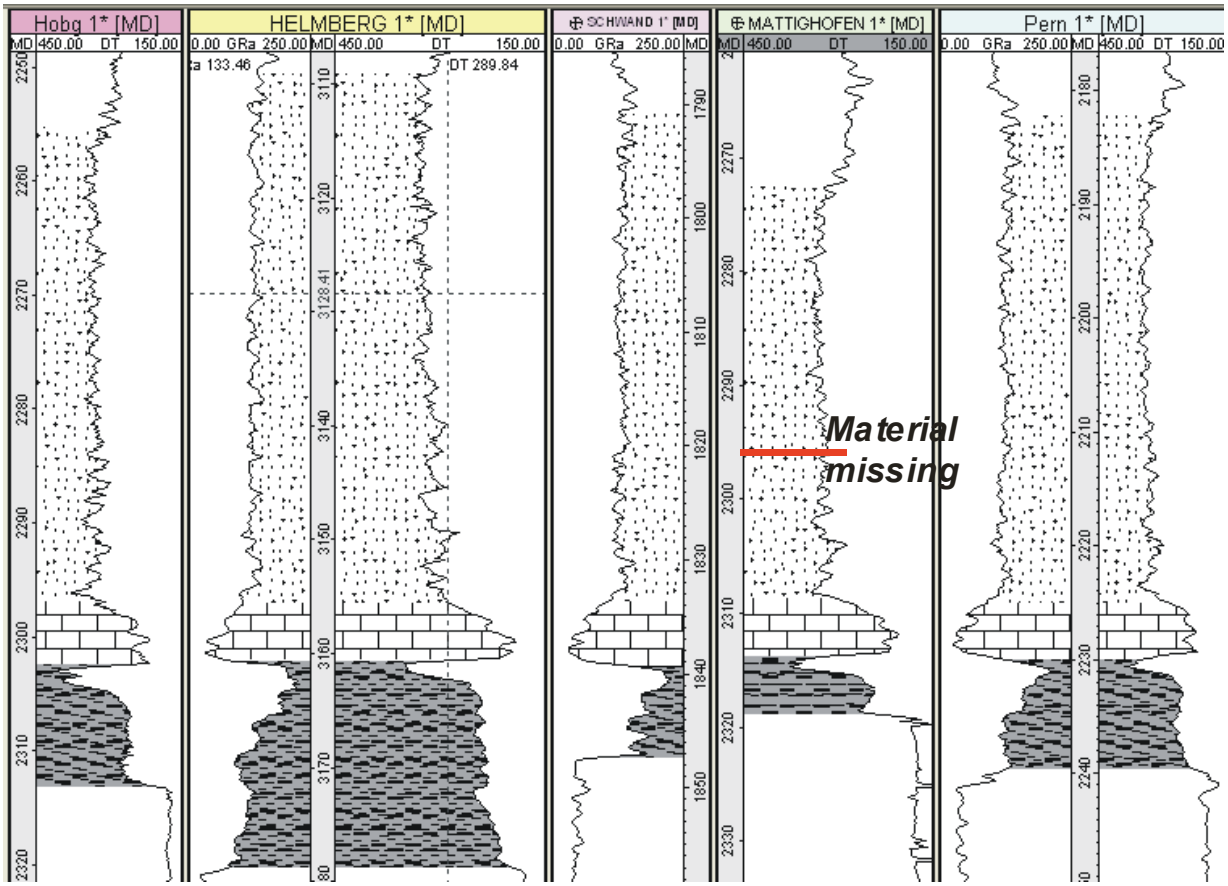

Fig. 34: Logs from the study area “West”. See Fig. 33 for position of “West” within the Molasse basin. Red line shows position of the missing material.

5.3.2.2 Ried

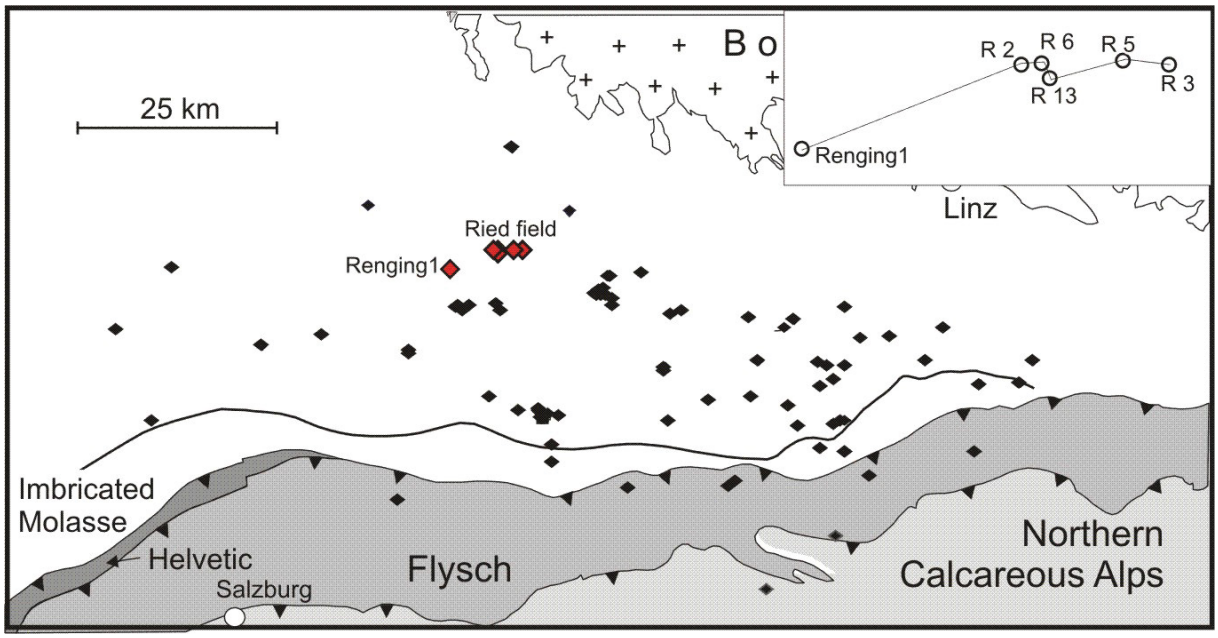

Fig. 35: Index map showing position of the Ried field. Inset shows position of the wells Renging 1, Ried (R) 2, 6, 13, 5 and 3.

The Ried field is located in the central, northern part of the study area (Fig. 35). Complete Schöneck and Dynow formations are present between wells Renging 1, located west of the Ried field, and Ried 3. Thickness and log pattern of the Eggerding Formation are more or less uniform between wells Renging 1 and Ried 13, whereas only the lower part of the Eggerding Formation is preserved in the eastern wells (Ried 5, Ried 3).

Therefore an erosion event after deposition of the Eggerding Formation must have taken place. In the eastern part of the Ried field erosion even removed Schöneck and Dynow formations (Sachsenhofer and Schulz, 2006). Note that wells from the eastern part of the Ried field are not shown in Fig. 36.

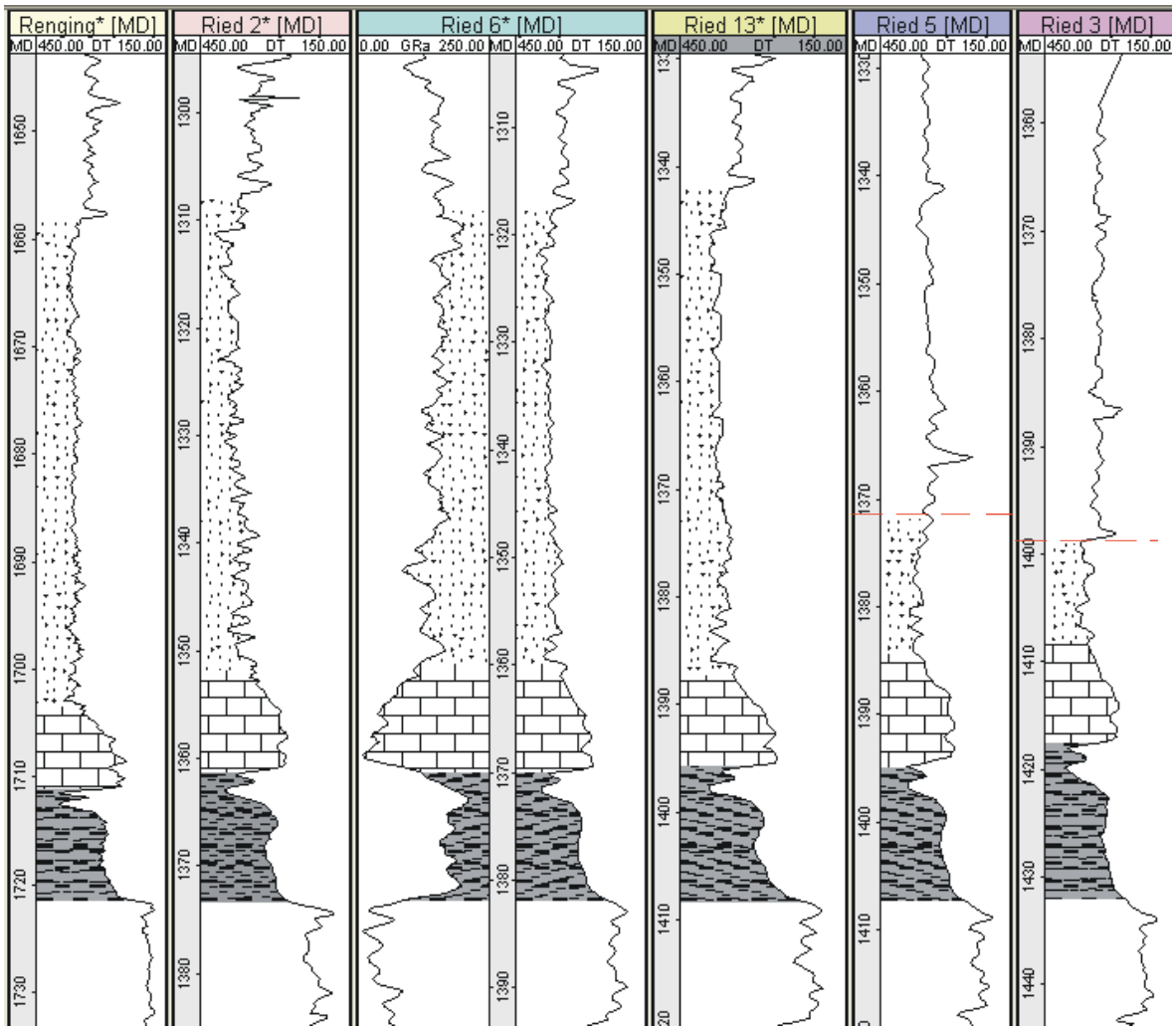

Fig. 36: Logs from well Renging 1 and wells in the Ried field. Red lines show the position of missing material.

5.3.2.3 Trattnach - Aistersheim

The Trattnach field is located southeast of the Ried field (Fig 37).

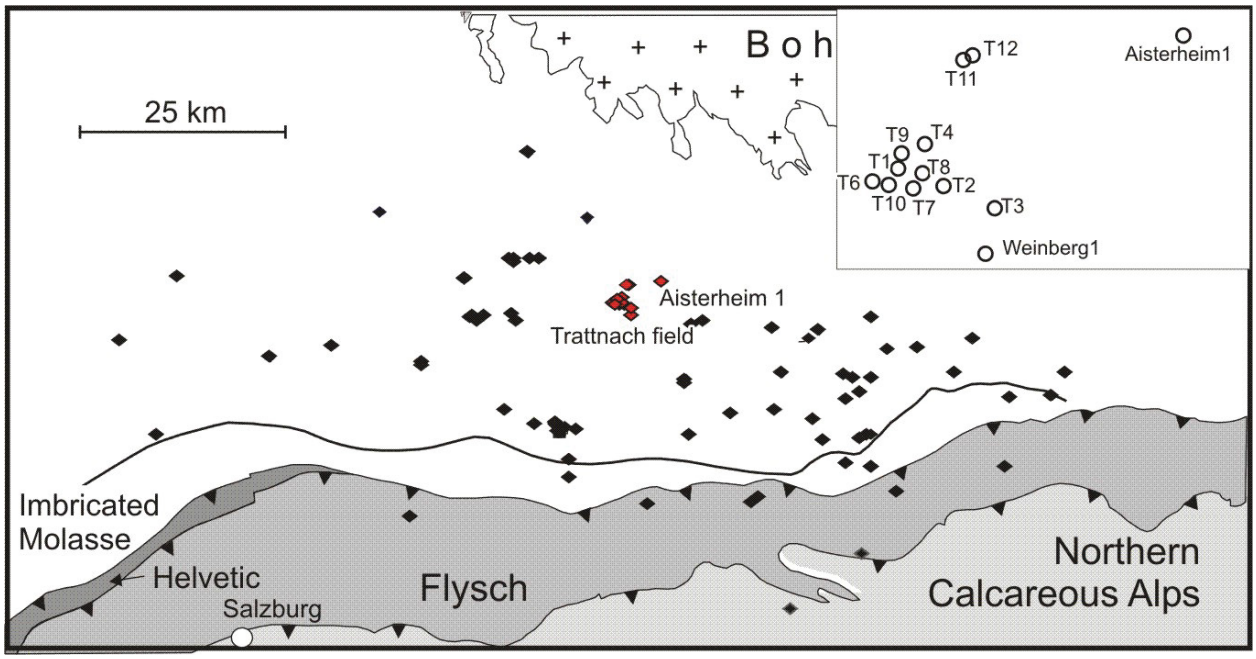

Fig. 37: Index map showing position of the “Trattnach – Aistersheim” area. Inset shows position of wells within the Trattnach – Aistersheim area.

The wells shown in Fig. 38 are flattened to the bottom of the Lithothamnium Limestone. They show that there has been at least one major erosion event. This event removed the lower part of the Eggerding Formation, the Dynow Formation, the Schöneck Formation and parts of the Lithothamnium Limestone. Therefore, the upper part of the Eggerding Formation is laying directly on erosional remnants of the Lithothamnium limestone (e.g. Trattnach 6, 10, 1). Erosion must have taken place during deposition of the Eggerding Formation.
In the wells Trattnach 7 and 8 erosion removed parts of the Eggerding Formation, but did not cut deeply into the Dynow Formation. Differences in thickness of the preserved part of the Eggerding Formation might indicate that erosion occurred earlier in wells Trattnach 1 and Trattnach 4. Alternatively, the higher thickness of Eggerding Formation in these wells could be due to re-deposited material, which filled the deeper parts of the erosional channels.

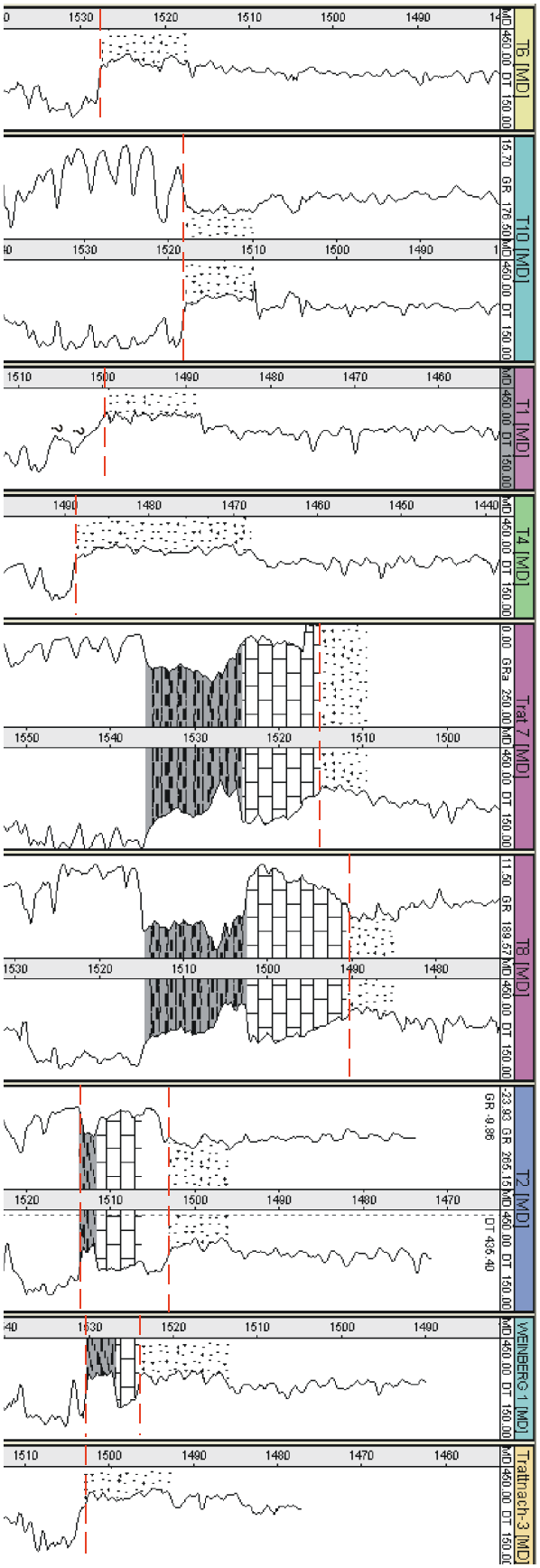

Fig. 38: Logs from the “Trattnach - Aisterheim area”. Red lines show erosion horizons.

The correlation of the wells from the eastern part of the Trattnach area (Trattnach 2, Weinberg 1, Trattnach 3) suggest the presence of two erosion events (see two red lines in Fig. 38):

a) An early erosion phase took place during deposition of the Schöneck Formation and cut at least 5 m into the Lithothamnium Limestone;

b) A second erosion event occurred during deposition of the (upper part of the) Eggerding Formation and removed the lower part of the Eggerding Formation and parts of the Dynow Formation. In Trattnach 3 the second event even cut into the Lithothamnium Limestone.

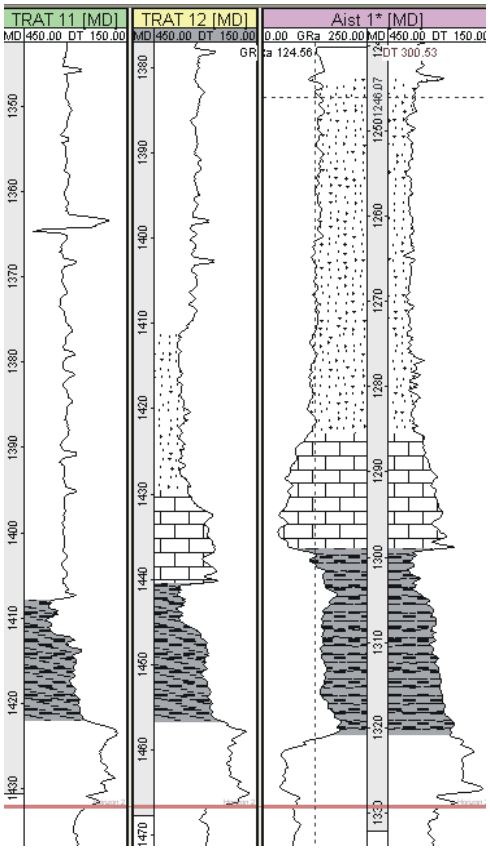

Fig. 39: Logs from “Trattnach Nord - Aistersheim” area.

In the Trattnach Nord field (Fig. 39), the wells Trattnach 11 and 12 have a complete Schöneck Formation. In Trattnach 11 this formation is overlain directly by Zupfing Formation. In contrast, Trattnach 12 has a complete Dynow Formation and lower part of Eggerding Formation.

It is often difficult to separate between the effects of normal faulting and erosion. This is also true in the present case:

a) “erosional” explanation: erosion after deposition of Eggerding Formation removed the entire Eggerding Formation and the Dynow Formation in Trattnach 11, but erosion removed only the upper Eggerding Formation in Trattnach 12.

b) However, about 40 m of the lowermost Zupfing Formation are missing in Trattnach 12. Thus, it seems probable that both wells drilled the same normal fault, which dips in into a south western direction (Fig. 40).

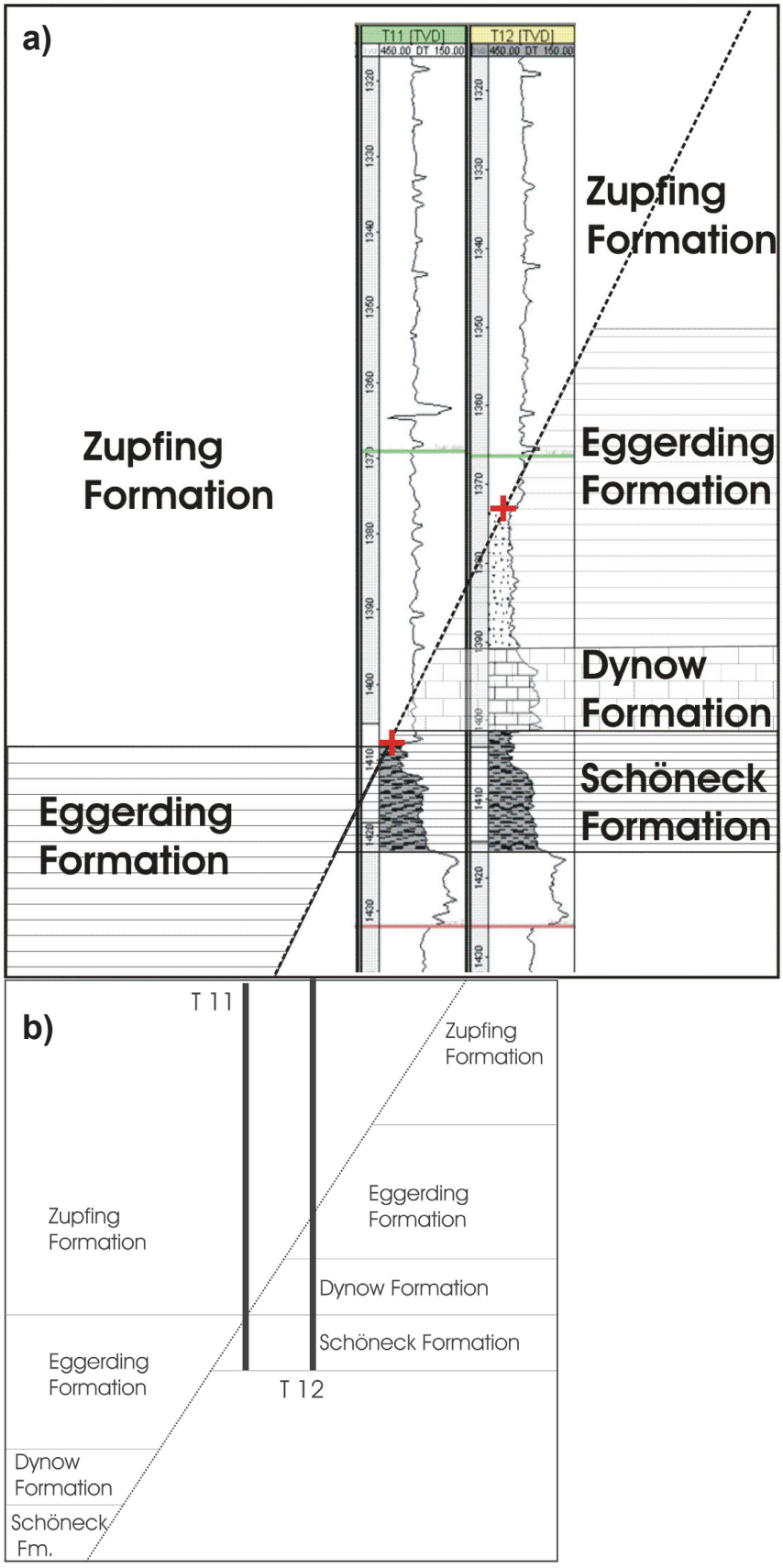

Fig. 40: a) Trattnach 11 and Trattnach 12 cut by a normal fault. Red crosses show the intercept points between logs and normal fault. b) Schematic sketch of a).

5.3.2.4 Kemating

The Kemating field (Fig. 41) is located west of the Trattnach field and southwest from the Ried field and north eastern from the Puchkirchen field.

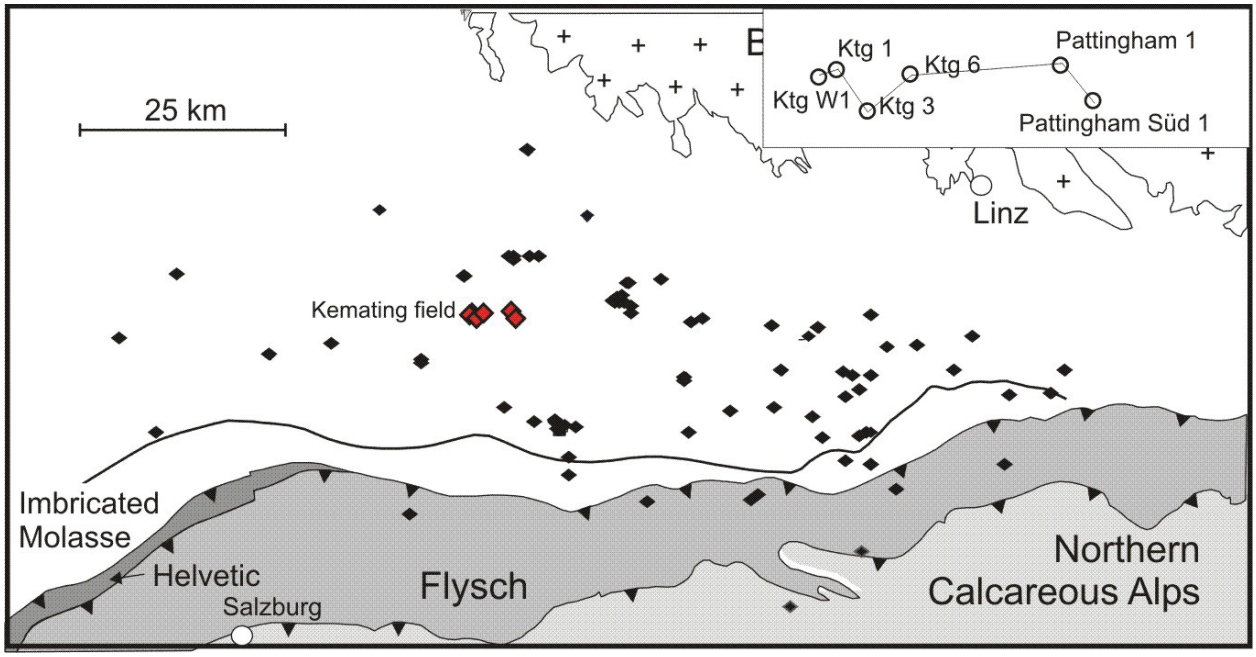

Fig. 41: Index map showing position of the Kemating field. Inset shows position of Kemating (Ktg) and Pattigham (Pa) wells.

The Kemating wells show from west to east an interesting development of their Oligocene formations. In Kemating W1 the Lithothamnium Limestone is directly overlain by 22 m of the middle part of Eggerding Formation.

All other wells show Schöneck and Dynow formations. Differences in thickness of the Schöneck Formation (especially its lower part; “unit a” according to Sachsenhofer and Schulz, 2006) are due to a paleo-relief existing before the deposition of the Schöneck Formation.

The thickness of the Eggerding Formation increases from west to east. A peak-to-peak correlation suggests that this is because the uppermost part of the Eggerding Formation is missing due to erosion in the western wells. Note that the difference in thickness between the Pattigham 1 and Pattigham Süd 1 wells is due to different sedimentation rates.

In contrast to the Trattnach Nord field, the lowermost Zupfing Formation is complete in all five wells.

From the correlation results it is obvious that the missing top of the Eggerding Formation has been eroded before deposition of the Zupfing Formation. Depending on the position, Eggerding Formation more or less thick has been eroded; the maximum erosion of the illustrated wells is in Kemating 1.

For the missing Dynow and Schöneck formations in Kemating W1, an additional, earlier erosion event (after deposition of the lower Eggerding Formation), or normal faulting has to be assumed.

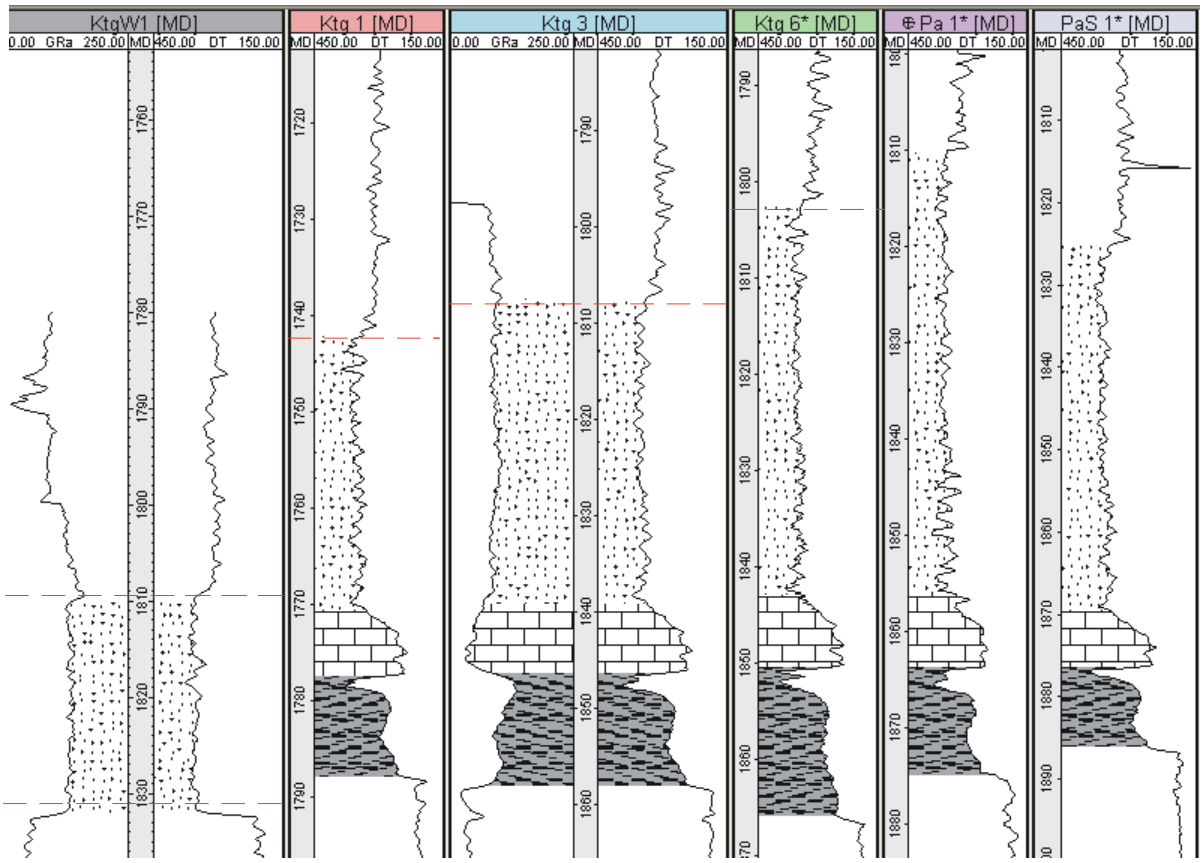

Fig. 42: Logs from “Kemating” area. Red lines show the erosion horizons.

5.3.2.5 Kohleck- Wolfersberg

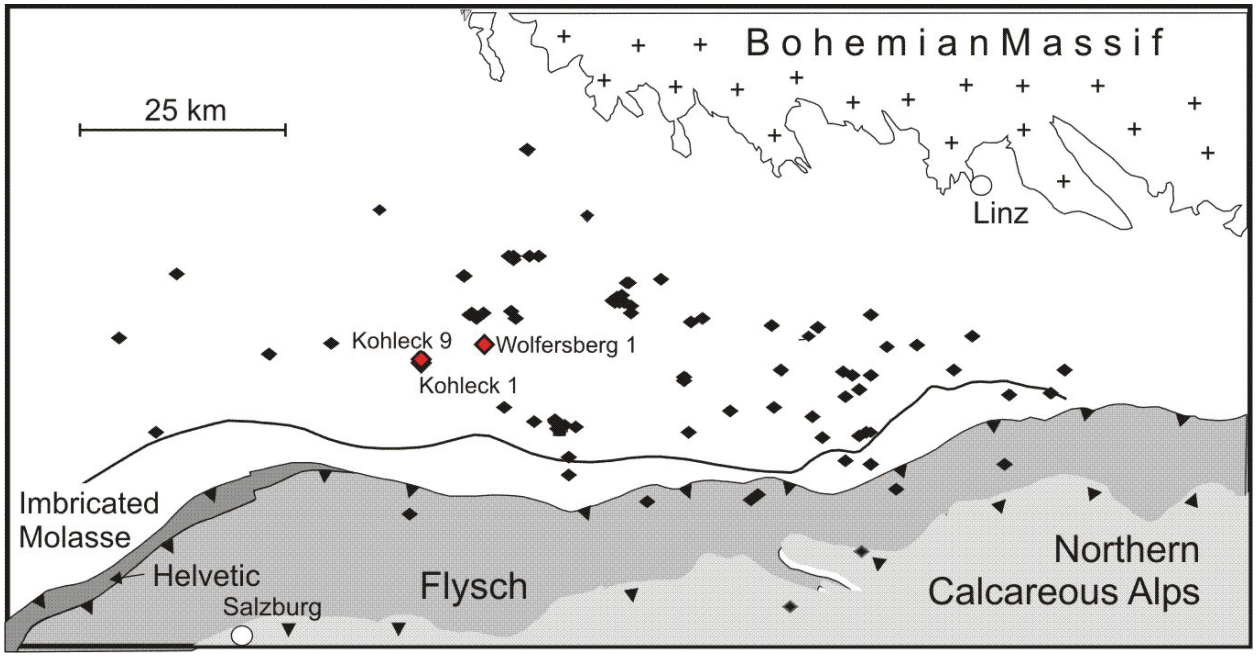

Fig. 43: Index map showing position of the Kohleck – Wolfersberg wells. Inset shows position of the wells.

Wells Kohleck 1 and 9, and Wolfersberg 1 are situated southwest of the Kemating and northwest of Puchkirchen (Fig. 43). Logs from the wells are shown in Fig. 44. Logs from key well Perneck 1, located west of Kohleck, are used for comparison.

The lower part of Schöneck Formation in both Kohleck wells is thin, whereas the Dynow Formation has a normal thickness. The comparison with the Perneck 1 well shows that in both Kohleck wells the upper part of the Eggerding Formation is missing.
The GR log of the Lower Oligocene succession in well Wolfersberg 1 is abnormal. Therefore, the formation boundaries are poorly defined. Probably the upper part of the Schöneck Formation (“unit c”) and the Dynow Formation are missing. Moreover, the Eggerding Formation is only about 14 m thick.
It is clear that an erosion event occurred in the Kohleck area after deposition of the Eggerding Formation. Perhaps the abnormal log in the Wolfersberg well results from re-deposited material.

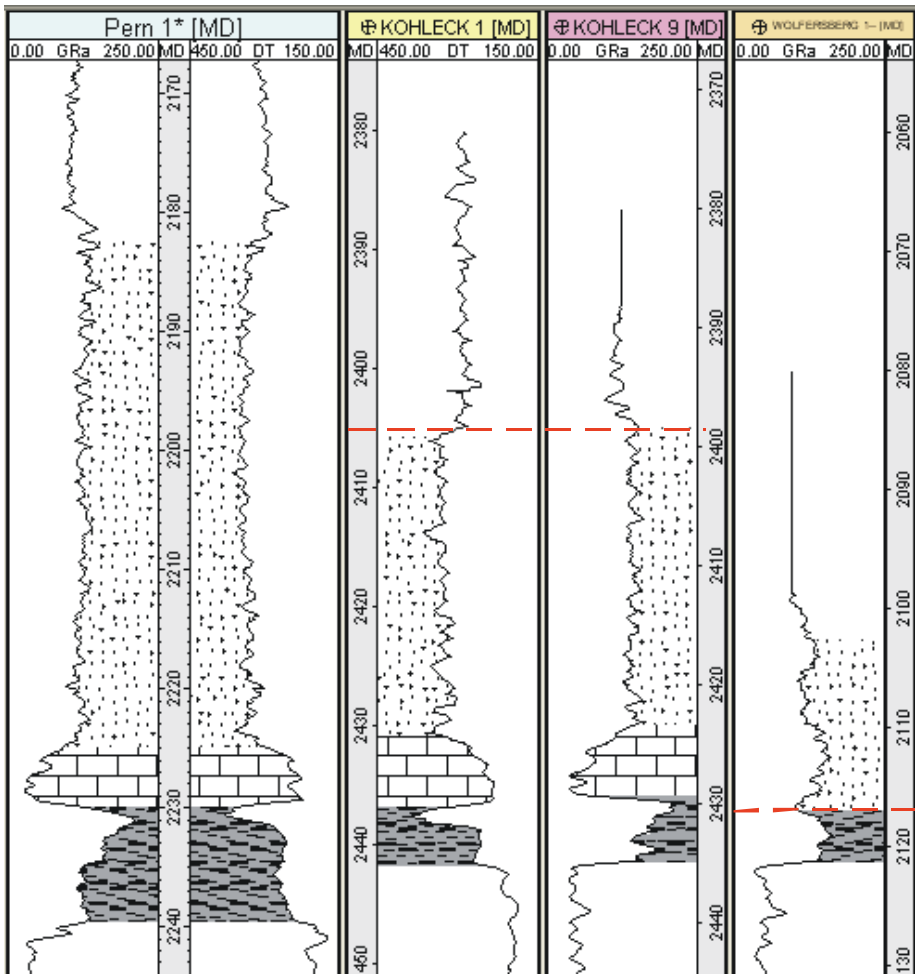

Fig. 44: Logs from the “Kohleck-Wolfersberg” area. Red lines show the position of missing material.

5.3.2.6 Puchkirchen

The Puchkirchen field is located in the central southern part of the study area (Fig. 45).

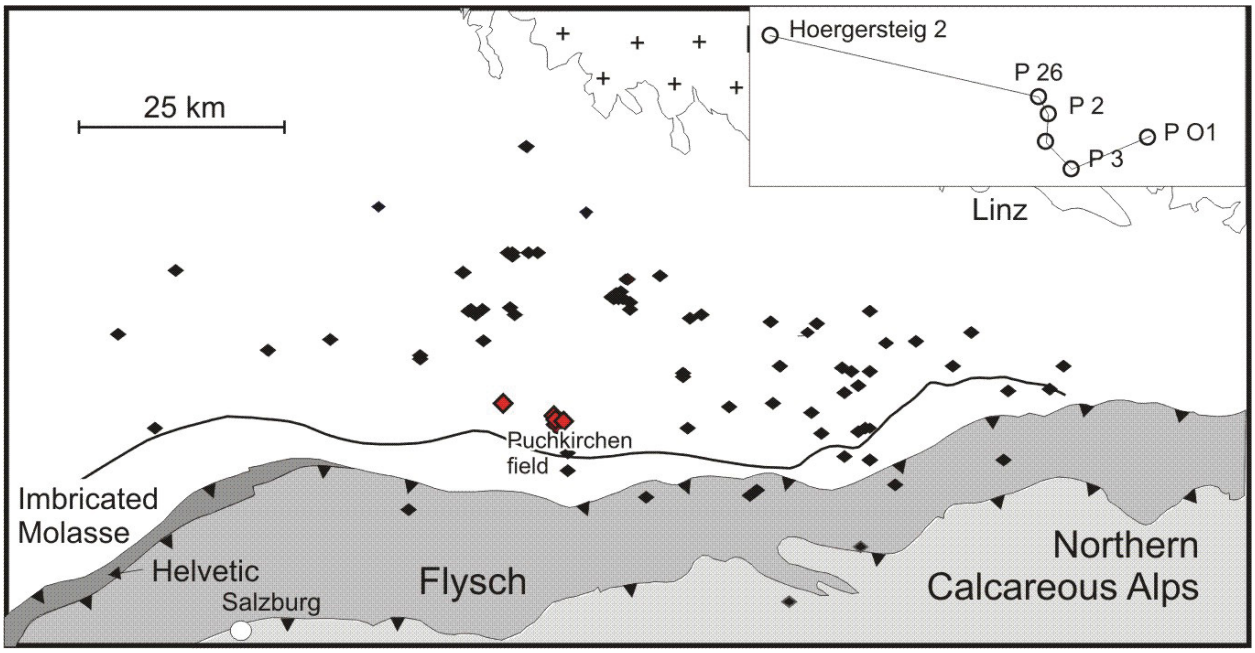

Fig. 45: Index map showing position of the Puchkirchen field. Inset shows position of the Puchkirchen (P) and the Hörgersteig (Hoerg) 2 wells.

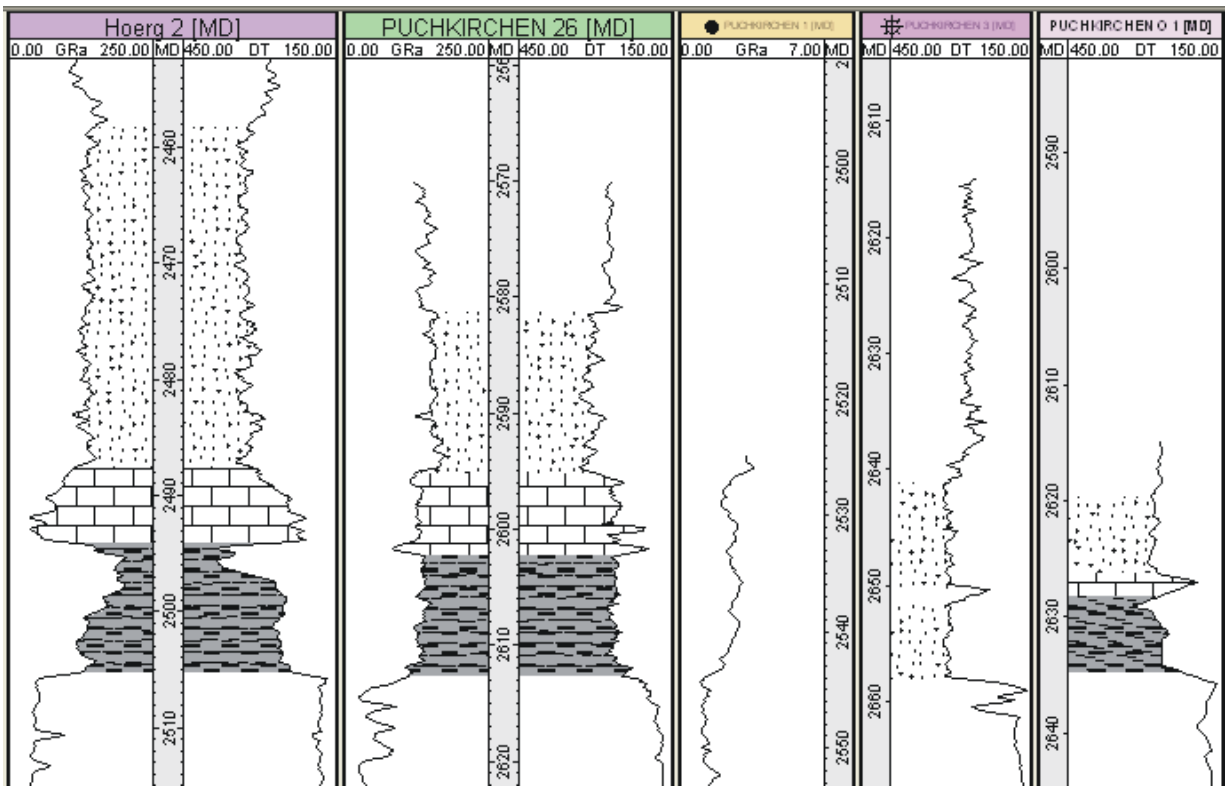

Fig. 46: Logs from the “Puchkirchen” area.

The Hörgersteig 1 well shows typical log patterns for Schöneck, Dynow and lower Eggerding Formation. The upper Eggerding Formation is missing, probably because of erosion.
Well Puchkirchen 26 exhibits typical log patterns for the lower Eggerding Formation, but logs of the Schöneck Formation and the Dynow Formation are abnormal. Because re-deposited material is known from a core in the Puchkirchen 2 well, the abnormal logs probably result from the deposition of re-deposited material.
The remaining Puchkirchen log patterns are also totally untypical and attest erosion and re-deposition.

5.3.2.7 Bachmanning - Aiterbach

The wells illustrated in Fig. 48 are located east of the Trattnach field and northwest of the Voitsdorf field (Fig. 47).

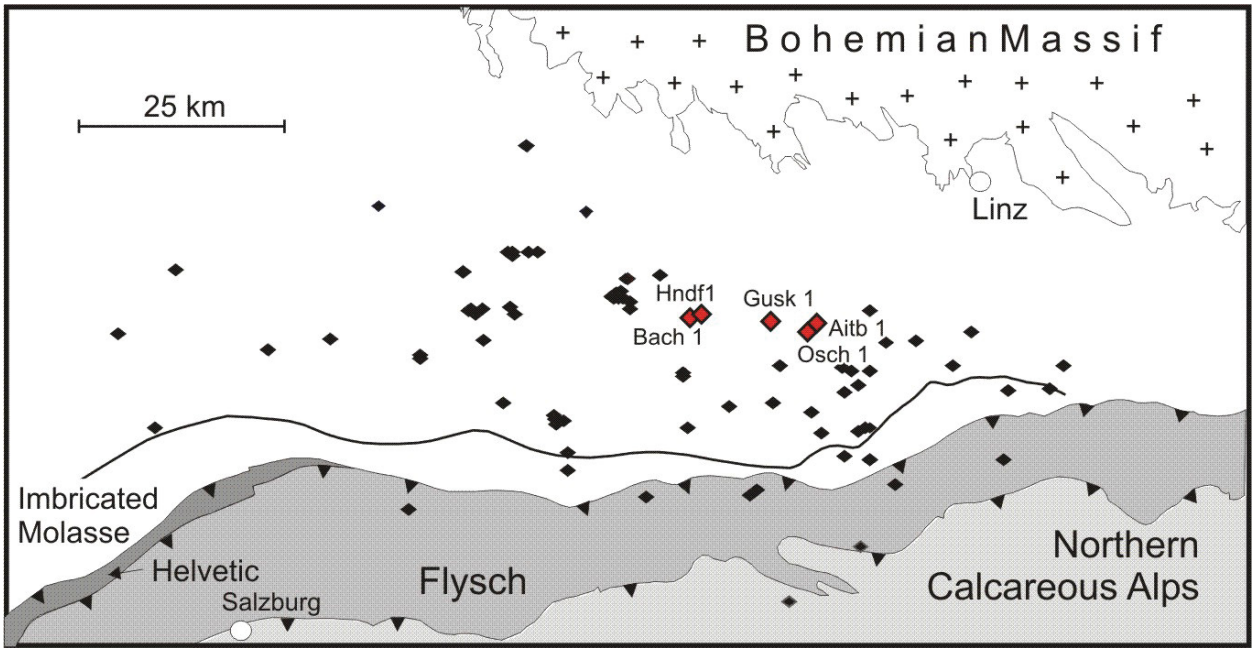

Fig. 47**:** Index map showing position of the the "Bachmanning - Aiterbach" area: Bachmaning (Bach) 1, Haindorf (Hndf) 1, Gunskirchen1 (Gusk1), Oberschauersberg 1 (Osch1), Aiterbach 1 (Aitb1).

All wells show typical Schöneck and Dynow formations. Variations in the thickness of the Schöneck Formation are significant. Moreover, sandy, turbiditic layers in well Oberschauersberg (e.g. Schulz et al., 2002) produce some untypical peaks. Similar peaks in the Gunskirchen well indicate the presence of similar sandy layers

The Eggerding Formation of Haindorf 1 seems complete and undisturbed from costal input. In Bachmaning 1 a great part of the upper Eggerding Formation and probably a few meters from its lower Zupfing Formation are missing. An erosion event can be assumed.

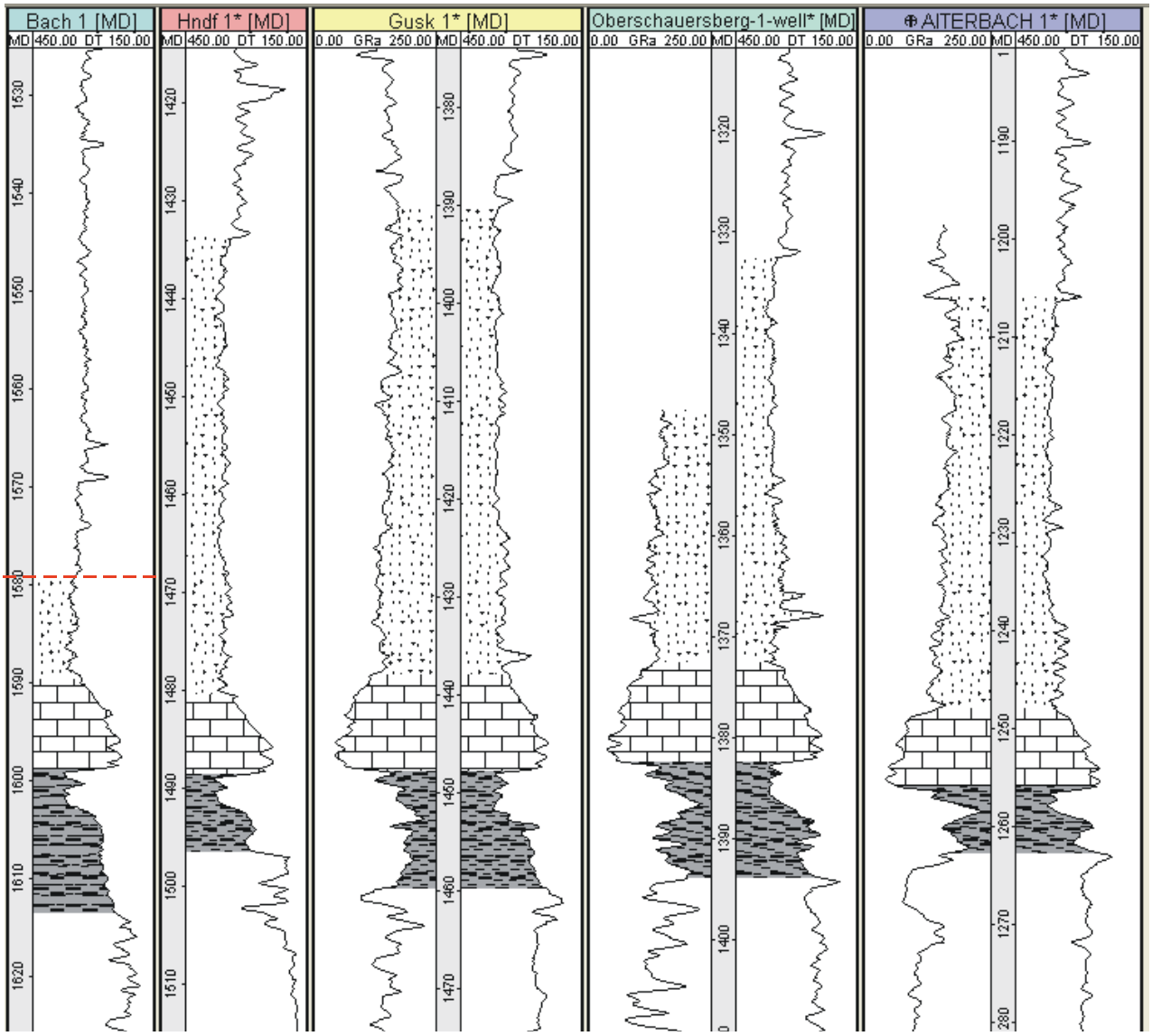

Fig. 48: Logs from the “Bachmanning - Aiterbach” area. Red line shows erosion horizon.

Logs of wells Gunskirchen 1 are compared with key well Haindorf 1 in Fig. 49. The rectangles in Fig. 49 show the similarities between both wells. The arrows point at intervals, which are present in only Gunskirchen 1.

Logs of wells Oberschauersberg 1 and Aiterbach 1 are compared with Haindorf 1 in Fig. 50. Here, the arrows point at locations where material is missing. These gaps lay in the same log position as the additional material in Gunskirchen 1. Perhaps the material missing at Oberschauersberg 1 and Aiterbach 1 has been eroded and re-deposited at Gunskirchen.

The lower Eggerding Formation in Oberschauersberg 1 and Gunskirchen 1 is characterized by layers with abnormal (high velocity) peaks in the DT log. Probably these result from sandstone or marlstone. Whereas in the Oberschauersberg well the peaks in the DT log correlate with peaks in the GR log (low gamma-ray responses), the DT peaks in Gunskirchen 1 have unchanged high gamma-ray responses. This combination could indicate feldspar-rich

sands or conglomerates/sandstones with a shale cementation.

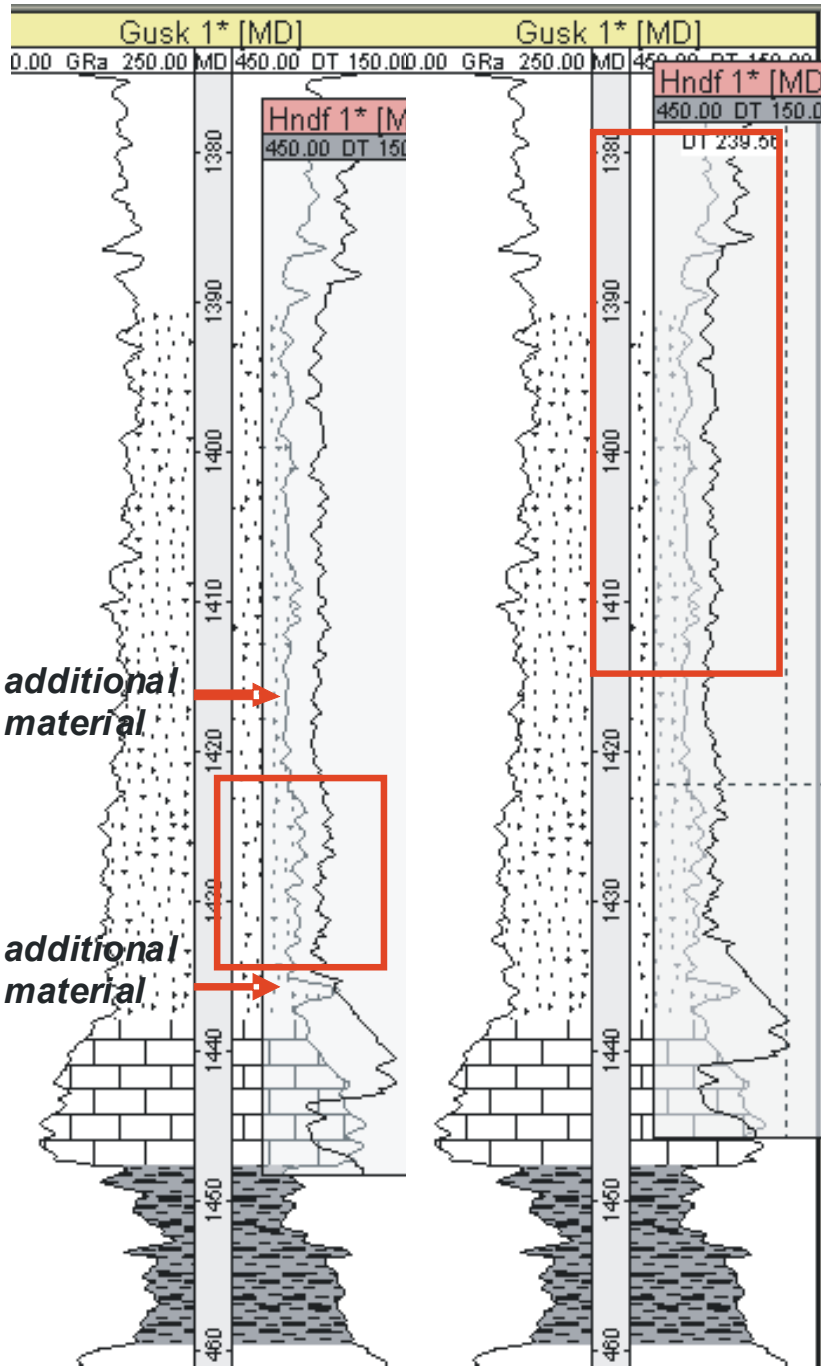

Fig. 49: The well Gunskirchen 1 is shown with the ghost of Haindorf 1. The red rectangles show the areas of congruence between the two wells. The red arrows show the positions of additional material in Gunskirchen 1.

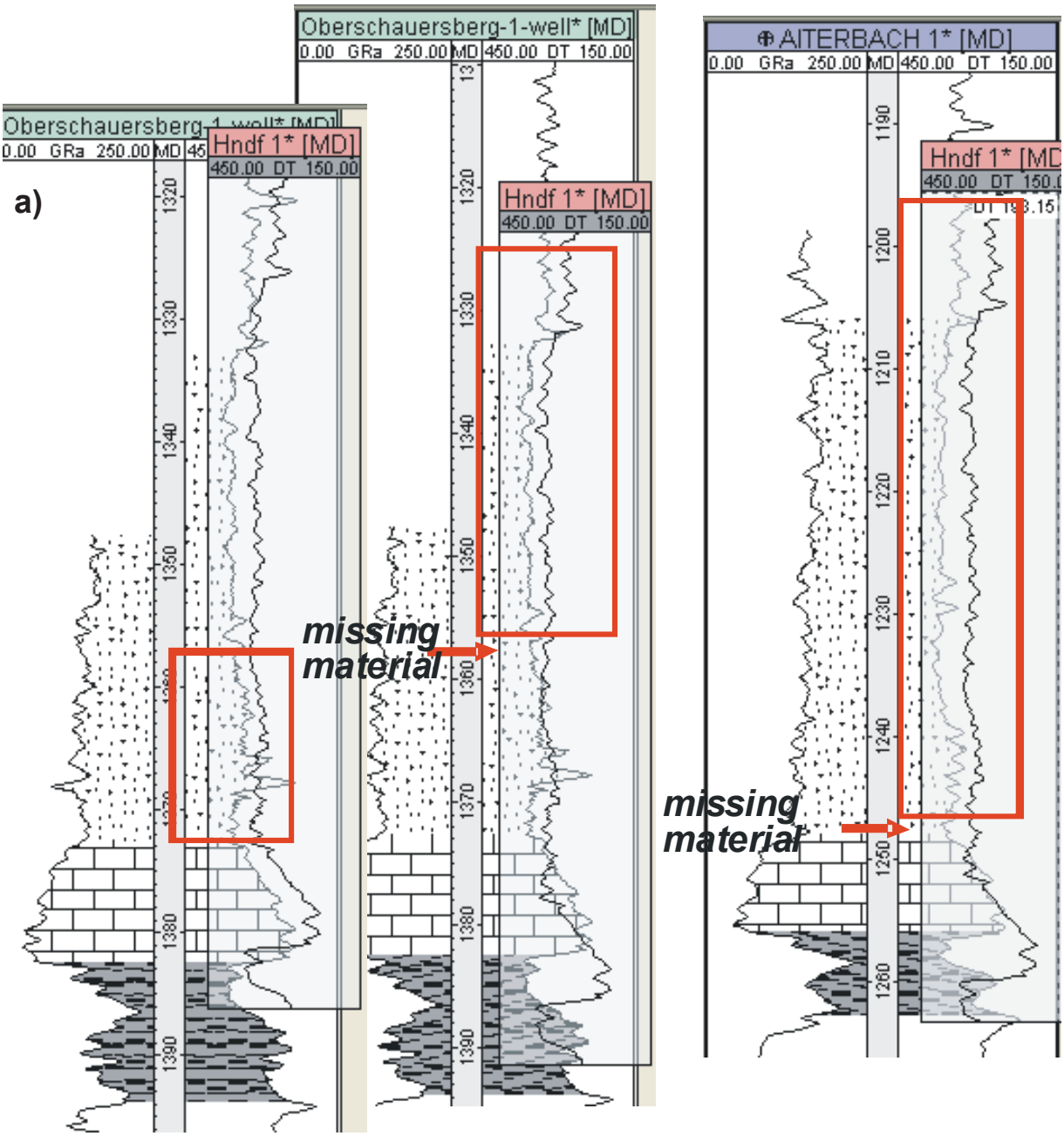

Fig. 50: a) Well Oberschauersberg 1 with ghost Haindorf 1. The red rectangles show the areas of congruence between the two wells. The red arrow shows the positions of missing material in Oberschauersberg 1. b) Well Aiterbach 1 with ghost Haindorf 1. The red rectangle shows the area of congruence between the two wells. The red arrow shows the positions of missing material in Aiterbach 1.

5.3.2.8 Schwanenstadt-Sattledt

The wells illustrated in Fig. 52 are located south of the wells from Central east 1 (Fig. 51).
The Schöneck Formation is present in all wells, but reaches a maximum thickness in the three western wells Schwanenstadt 18, 20 and Fischlham 1. The Dynow Formation is present in all wells, too. Only the Schwanenstadt 20 well seems to have an incomplete Dynow Formation. Probably its upper part is eroded.

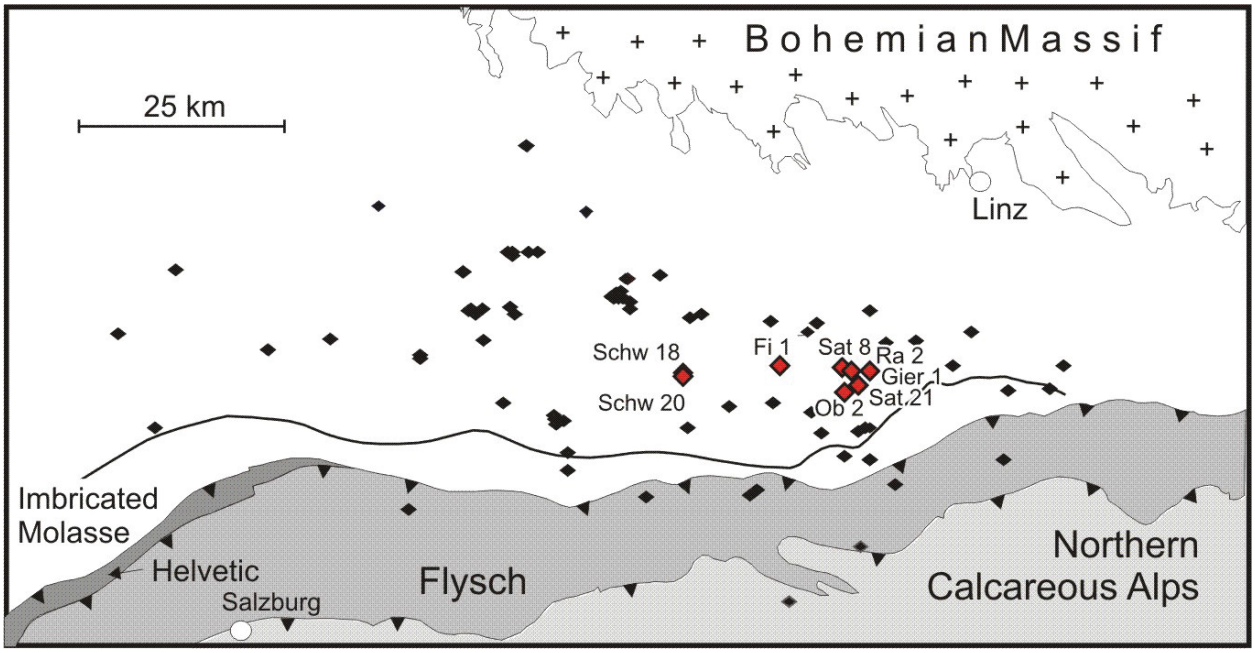

Fig. 51: Index map showing position of the the “Schwanenstadt - Sattledt” area: Schwanenstadt (Schw) 18, Schwanenstadt (Schw) 20, Fischlham (Fi) 1, Sattledt (Sat) 8, Oberaustall (Ob) 2, Rappersdorf (Ra) 2, Sattledt (Sat) 21, Giering (Gier) 1.

Oberaustall 2 is used as a key well for the investigation of the Eggerding Formation in the Schwanenstadt-Sattledt area.
The neighbouring wells Schwanenstadt 18 and 20 include relatively thin Eggerding Formation (~10 m). This suggests that large parts of the Eggerding Formation were removed by erosion. Whereas erosion did not affect the underlying Dynow Formation, it removed the upper part in Schwanenstadt 20.
Whereas the Eggerding Formation is complete in the wells Fischlham 1 and Oberaustall 2, the upper 8 m are missing in Rappersdorf 2. Only a density log is available from Sattledt 8, but it suggests that the entire Eggerding Formation is preserved. The Eggerding Formation in Giering 1 is relatively thick. Nevertheless a detailed peak-to-peak correlation shows that material is missing in its lower part (see red arrow in Fig. 52).

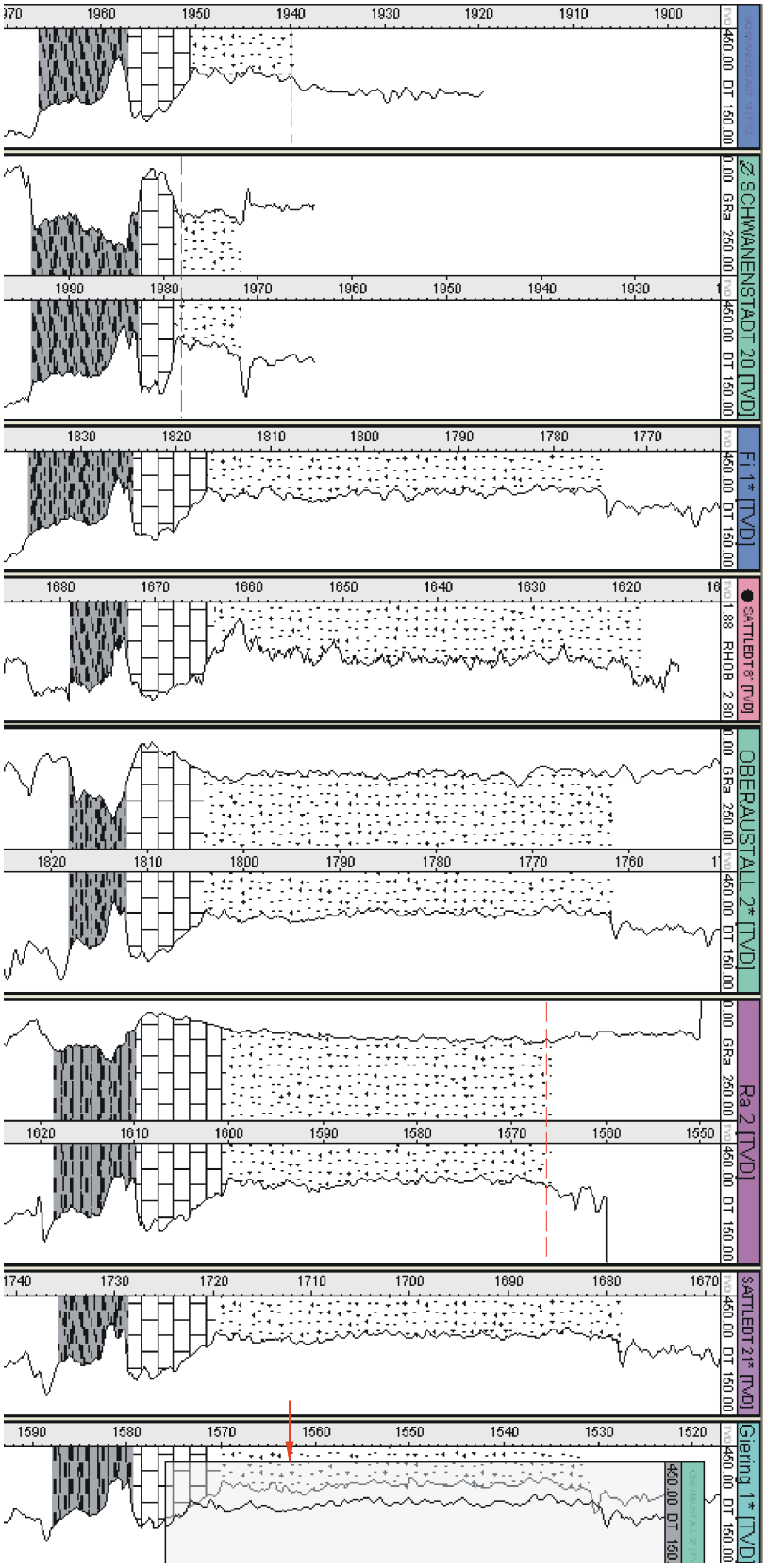

Fig. 52: Logs from the “Schwanenstadt - Sattledt” area. Red lines show erosion horizon. The red arrow shows the position of missing material.

5.3.2.9 Lindach -Voitsdorf

The wells illustrated in Fig. 54 are location south of the wells investigated in the previous chapter (Fig. 53).

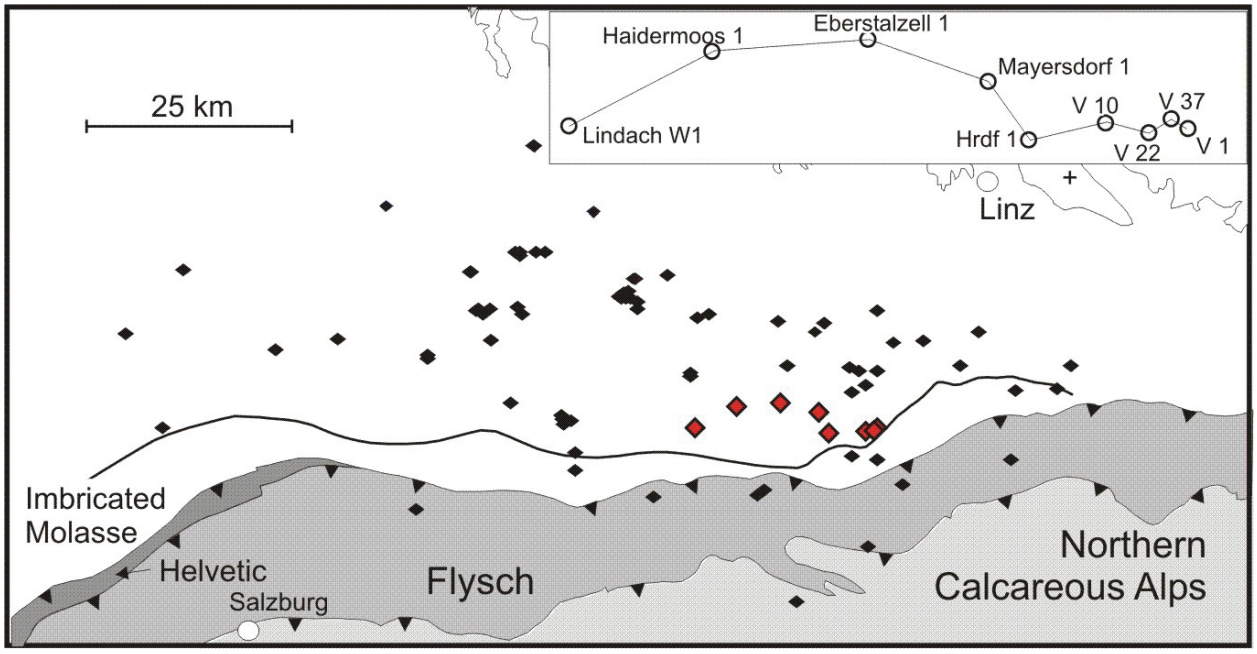

Fig. 53: Index map showing position of the “Lindach - Voitsdorf ” area. Inset shows position of the wells Lindach W 1, Haidermoos 1, Eberstalzell 1, Mayersdorf 1, Hermannsdorf (Hrdf)1, Voitsdorf (V) 10, Voitsdorf (V) 22, Voitsdorf (V) 37, Voitsdorf (V) 1, Voitsdorf (V) 41.

Schöneck and Dynow Formation are present in all wells. The base of the former formation is not always sharp. Except of possibly Mayersdorf 1, the Dynow Formation is in all wells complete.

- Lindach W1 shows a lack of the upper part of the Eggerding Formation and the lower part of the Zupfing Formation due to erosion. Considering the results of wells Schwanenstadt and Bachmaning 1, located directly to the north, which exhibit the same erosion features, it appears that erosion was not localized.
- The log from Haidermoos 1 is only available up to the lower Eggerding Formation. Up to this level all formations are present.
- In Eberstallzell 1 a few meters of the upper part of the Eggerding Formation are missing.

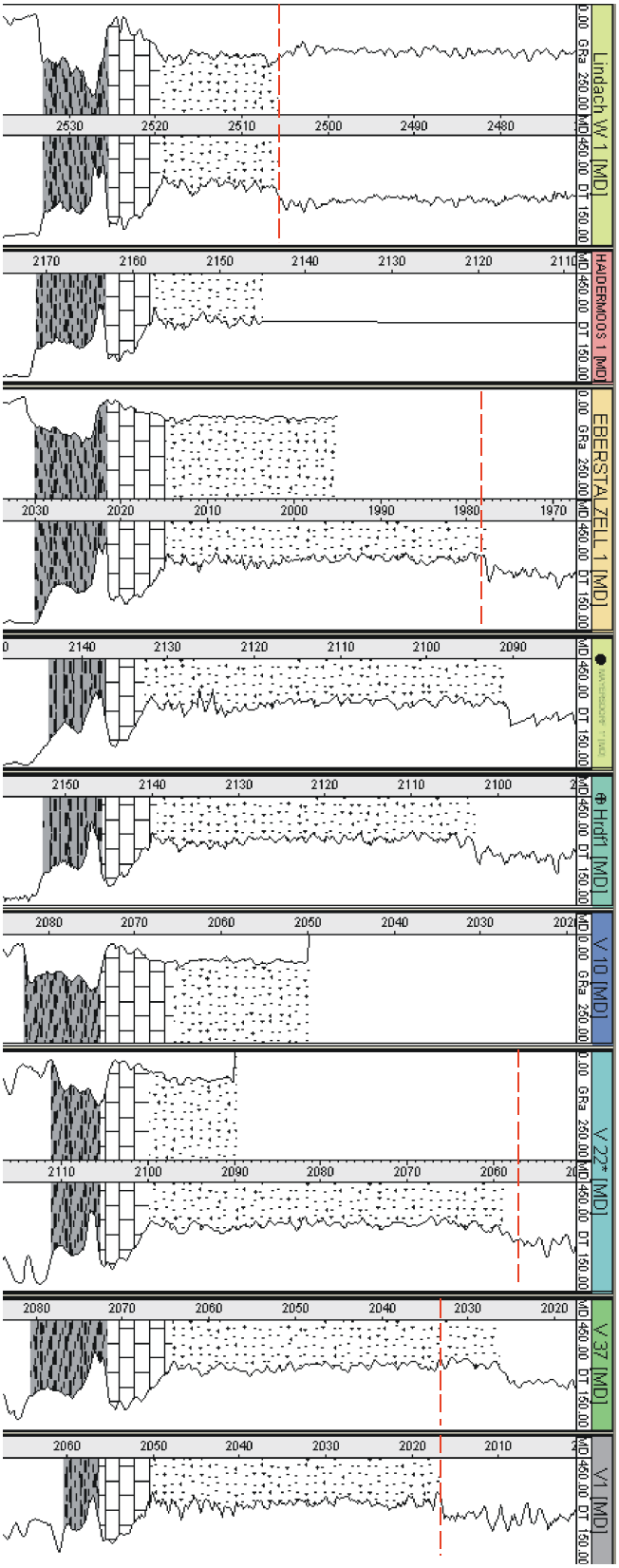

Fig. 54: Logs from the “Lindach -Voitsdorf” area. Red lines show erosion horizon. The red arrow shows the position of missing material.

- Mayersdorf shows some “strange” low-velocity layers in the lower part of the Eggerding Formation. However, because all characteristic features of the 43 m thick Eggerding Formation are present, it is likely that the Eggerding Formation is complete.
- The Eggerding Formation in Hermannsdorf 1 is about 37 m thick. Its log pattern corresponds to that of Oberaustall 2 both in the Zupfing Formation and in the upper Eggerding Formation (down to a depth of 2114 meters (MD)) (Fig. 55). The deeper Eggerding Formation diverges in some parts from the typical shape in this region. Especially in the lowest part of the Eggerding Formation is not really clear if the first peak is missing or if there is a lack of material, so that the two distinctive features melted together. After comparing the available wells in adjacent areas, it is probably a local event.

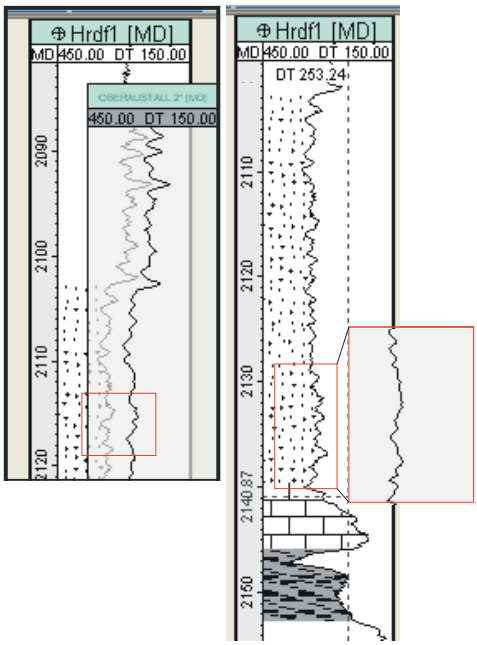

Fig. 55: Hermannsdorf (Hrdf) 1 together with the ghost of Oberaustall 2. The red rectangles show the areas different in both wells.

- The log of V 10 is available only for the lower part of the Eggerding Formation, but this part seems more or less comparable with the GR log from V 22.
- V 22 shows irregularities in the border zone between Eggerding and Zupfing formations: the lowermost five meters of the Zupfing Formation are missing; instead of these, two meters of additional material overlay the regular Eggerding Formation. Probably this is re-deposited material (Fig. 56).
- In V 37 the Eggerding Formation in V 37 is 36 m thick. The lower 31 m are complete and show typical log patterns. Above 2033 m depth (MD) the log of V 37 differs significantly from that of Oberaustall 2. Probably the upper 5 m of the Eggerding formation in V 37 is represented by re-deposited material. In addition a 1.5 m thick interval representing the base of the Zupfing Formation is missing in V 37 (Fig. 56).
- In V1 the lowermost 3 m of Zupfing Formation and the uppermost 8 m of Eggerding Formation are missing in comparison to Oberaustall 2 (Fig. 56).

From the information of the Voitsdorf wells the following history can be deduced:
Erosion started when 1.5 m (compressed, present day) of Zupfing Formation had been deposited. In the area of V 37, erosion removed sediments 12.5 m thick (1.5 m of Zupfing Fm., 11 m of Eggerding Fm.). 5 m of the resulting relief were filled with re-deposited material probably derived from the margins of the erosion channel.
Following this erosion event and deposition of another 2 m of Zupfing Formation, slumping/sliding removed the newly deposited material and, probably, re-deposited it further down-slope.

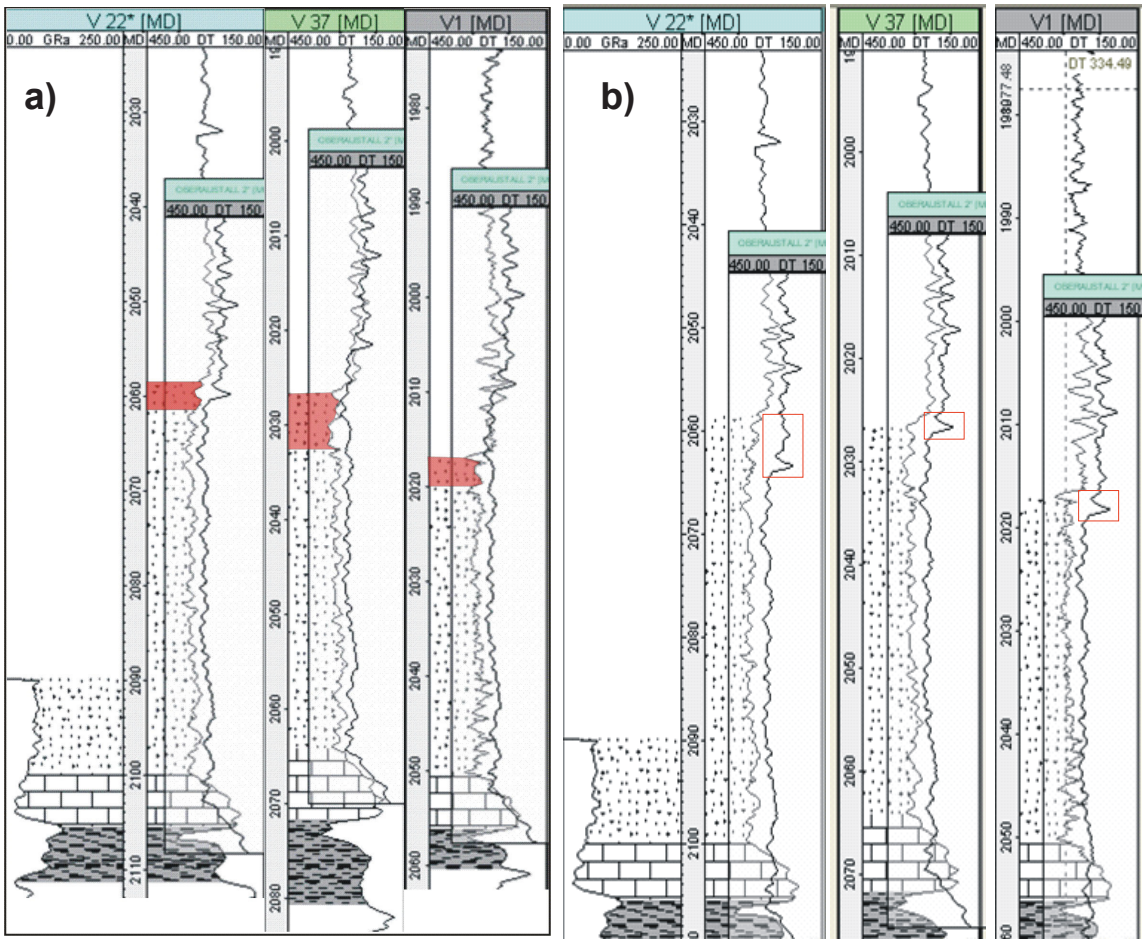

Fig. 56: The Voitsdorf 22, Voitsdorf 37 and Voitsdorf 1 together with the ghost of Oberaustall 2. a) In red the areas of re-deposited material. b) The red rectangles in the complete Oberaustall ghost show the missing Zupfing material of the Voitsdorf wells.

5.3.2.10 Ottsdorf - Dietach

The wells illustrated in Fig. 58 present a WNW to ESE section of the study area.

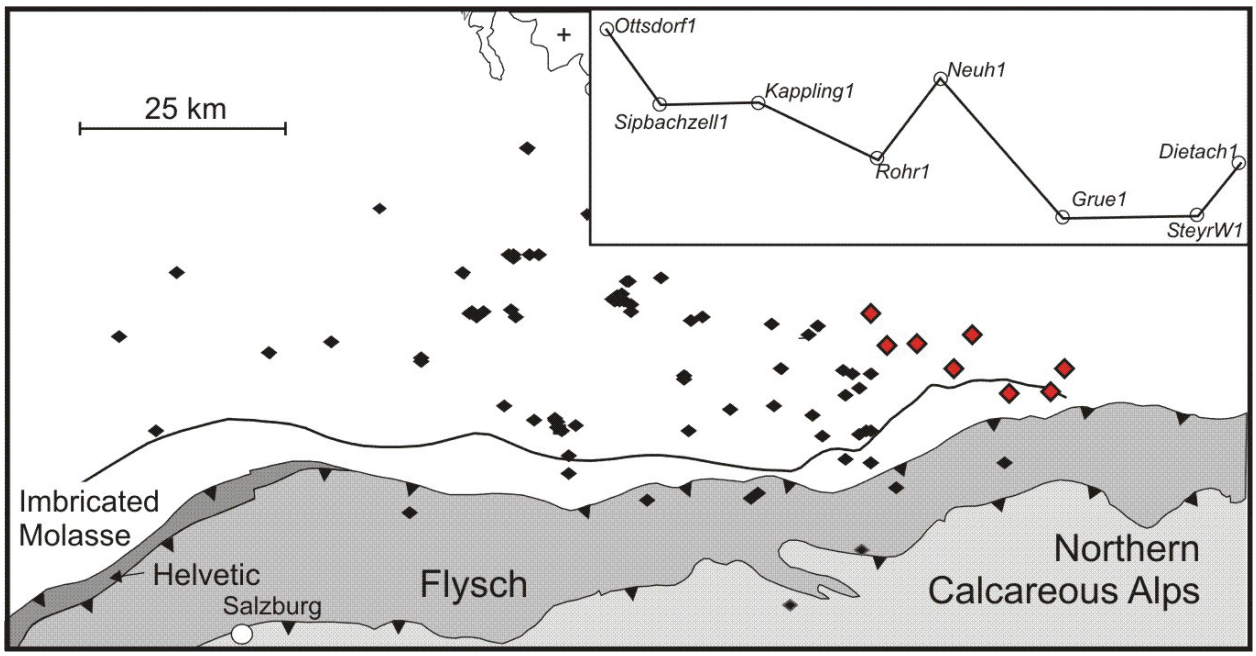

Fig. 57**:** Index map showing position of the "Ottsdorf - Dietach " area. Inset shows position of the wells Ottsdorf 1, Sippachzell 1, Kappling 1, Rohr 1, Neuhofen (Neuh) 1, Grue 1, Steyr W 1, Dietach 1.

As it can be seen in Fig. 58, the Schöneck Formation varies in thickness and in log pattern:
E.g. in wells Ottsdorf 1, Sippachzell 1 and Grue 1 the Schöneck Formation is up to 13 m thick. Its upper unit ("unit c" according to Schulz et al., 2002) with a low sonic velocity is relatively thick.
The Dynow Formation is relatively thick (about 10 m) in all wells, which is a typical feature of well located near the former basin margin (see also Sachsenhofer and Schulz, 2006). Perhaps the uppermost part of the Dynow Formation is missing in wells Neuhaus 1, Steyr W1 and Dietach 1 (Fig. 58).
The well Sippachzell 1 is used as key well for the Eggerding Formation in this area. In all eastern wells the Eggerding Formation varies in thickness, but is largely complete, at least in Ottsdorf 1, Sippachzell 1, Kappling 1, and Rohr 1.
The DT log of Neuhofen 1 is very "turbulent" and can hardly be correlated. According to the logs, the Eggerding Formation is at least 40 m thick. The DT log shows a high-velocity peak 26 m above the top of the Dynow Formation. Probably the peak results from a limestone or sandstone layer.

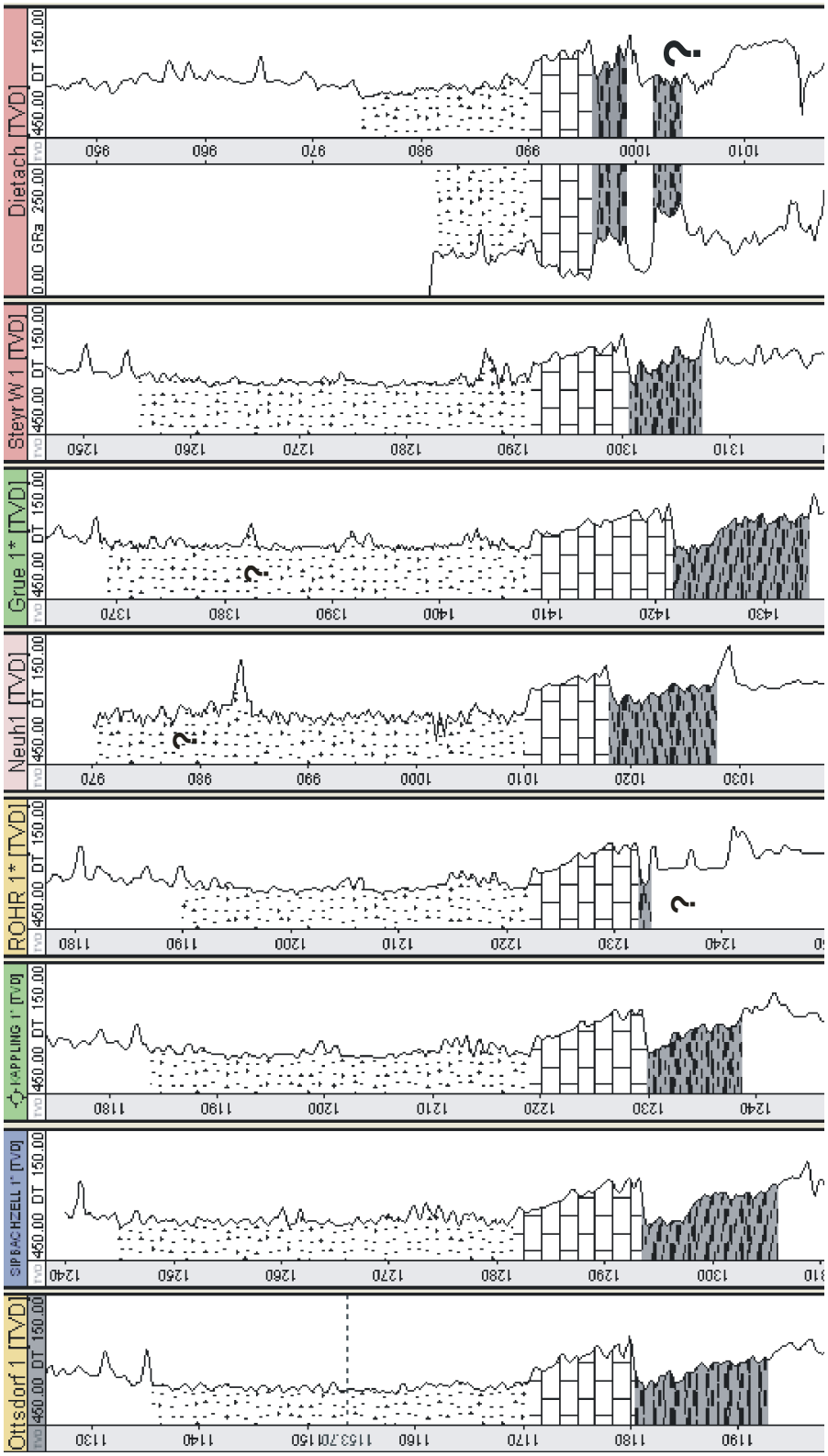

Fig. 58: Logs from the “Ottsdorf - Dietach” area. The question marks are showing incertitude in the interpretation.

Grue 1 shows except for a high-velocity peak at 1382 m (TVD) an Eggerding Formation, which can be correlated accurately with Sippachzell 1. A layer with even higher velocity occurs in a

similar stratigraphic position in well Neuhaus 1. Perhaps, these peaks represent the same (limestone or sandstone) layer.
The well Steyr West 1 shows a similar pattern as Sippachzell 1 except for its lower part. In Steyr West 1 the lower part of the Eggerding Formation exhibits log patterns with high-velocity peaks, comparable to Eggerding 2 (near-shore environment) and Oberschauersberg1 (Fig. 59). Probably they signalize the presence of sand layers.

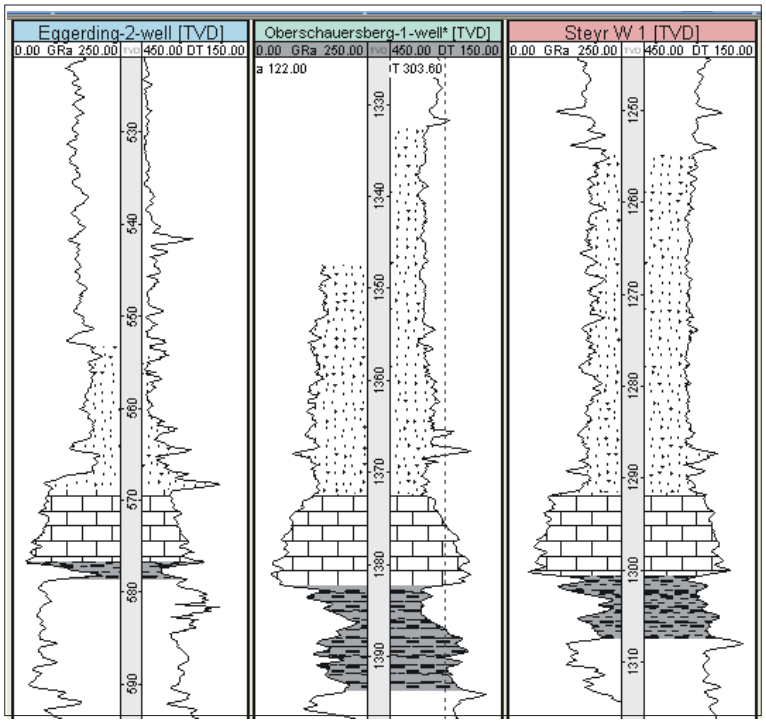

Fig. 59: Eggerding 2, Oberschauersberg 1and Steyr W 1 are near shore wells. They show typical high velocity pattern in the lower Eggerding Formation.

The log pattern of the Lower Oligocene succession in the shallow Dietach well is unique. The definition of the Schöneck Formation in this well is uncertain: After Schulz et al. (2002) the Schöneck Formation ranges from 995.8 m to 999.5 m (TVD) and overlies costal sands from the Bohemian Massif (Ampfing Sandstone). The log pattern under the sandstone shows a section with high values in both DT and GR logs. This probably indicates another part of the Schöneck Formation.
The Dynow Formation is about 8 m thick, whereas the Eggerding Formation is about 15 m thick. It cannot be decided whether the relatively low thickness of the Eggerding Formation is a result of erosion or due to the near-shore environment of the well.

5.3.2.11 South

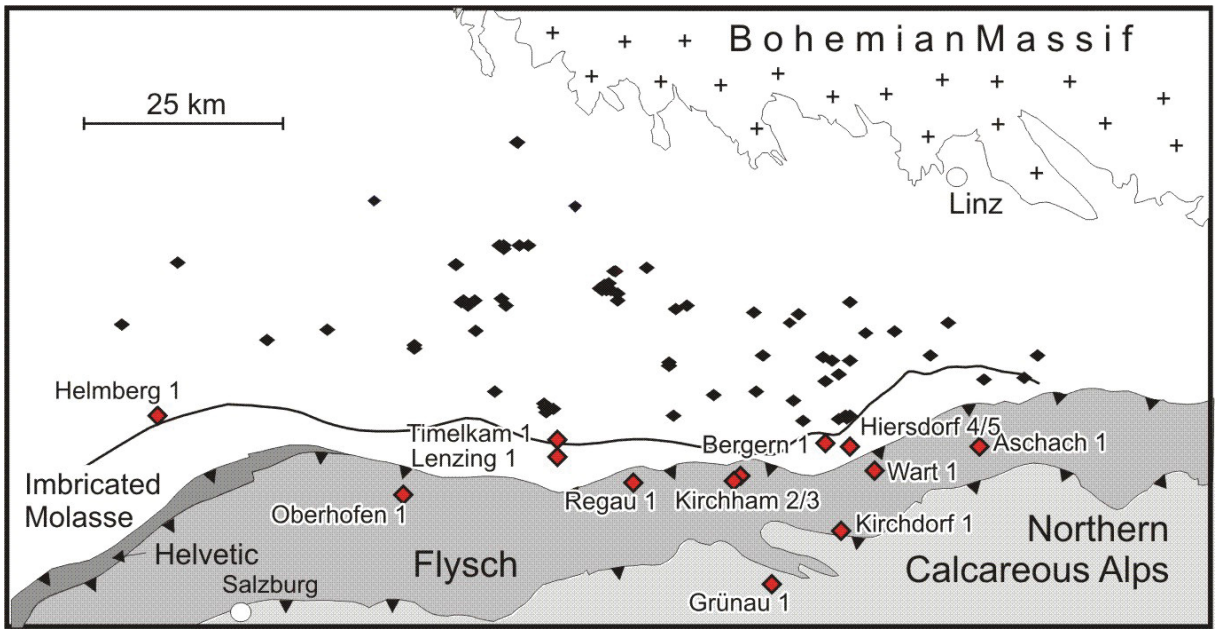

Fig. 60: Index map showing in the black rectangle the position of the southern area. From west to east: Helmberg 1, Oberhofen 1, Timelkam 1, Lenzing 1, regau 1, Lindach W 1, Kircham 2, Kircham 3, Grünau 1, Bergern 1, Bergern Süd 1, Kirchdorf 1, Hiersdorf 4, Wart 1, Aschach 1.

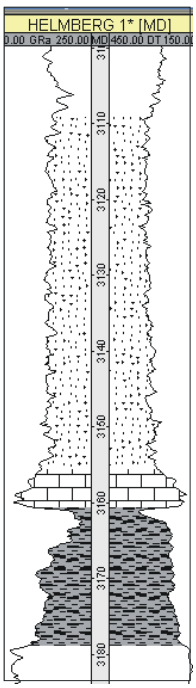

Fig. 61: The south western well Helmberg 1.

In the southern, deep part of the Molasse basin the true vertical depth (TVD) of the Eggerding Formation ranges from 2500 m to about 4800 m. Their bathymetric settings reach from the upper to the lower slope.

In the west there is Helmberg1 (Fig. 61) with a very thick (~ 47 m), complete and typical Eggerding Formation.

The Schöneck, Dynow and Eggerding formations in the wells of the central part of the southern study area show strange log patterns (Oberhofen – Regau; Fig. 62). Wagner (1986) and Schulz (2002) described the “Oberhofen facies” on the lower slope in the well Oberhofen 1. Sachsenhofer and Schulz (2006) described the Oberhofen facies in the Oberhofen 1 well based on its log pattern as a variety of the Lower Oligocene succession with the following characteristics:

- there is a low interval transit time in the Schöneck Formation, because of high carbonate content; in the middle there are olistholites containing Eocene material;
- relatively thick Dynow Formation with a blocky, non structured log motif;

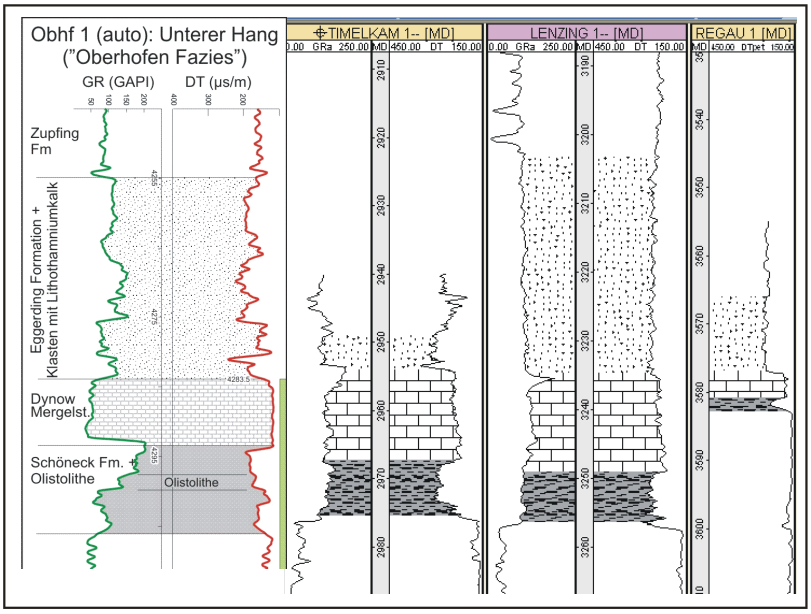

Fig. 62: The wells Oberhofen 1, Timelskam 1, Lenzing 1 and Regau 1 show an “Oberhofen facies”, especially in the Dynow Formation.

- the Eggerding Formation exhibits a highly structured log pattern. Lithothamnium limestone in cutting samples suggests re-deposited Eocene and Lower Oligocene material;

Timelkam 1 and Lenzing 1 show Dynow Formation in “Oberhofen facies” (Fig. 62). The distribution of the strange Dynow Formation can be explained by mobilization of coccolithophoride-bearing material in more northern positions (e.g. from Kemating W, the Puchkirchen wells, Wolfersberg…) and accumulation in the south. The Dynow Formation in Regau 1 has a similar blocky pattern but is relatively thin.

The part of well Lenzing 1, which has been interpreted as Eggerding Formation (see Fig. 63), has a relatively low interval transit time, similar to that in the Eggerding Formation of the Oberhofen well, but in contrast to the Oberhofen well, it is rather uniform.

If the Eggerding Formation in Timelkam1 is present at all, it is only 5 m thick.

Regau 1 shows a similar pattern as Lenzing 1. In both wells the transition to the Zupfing Formation is smooth.

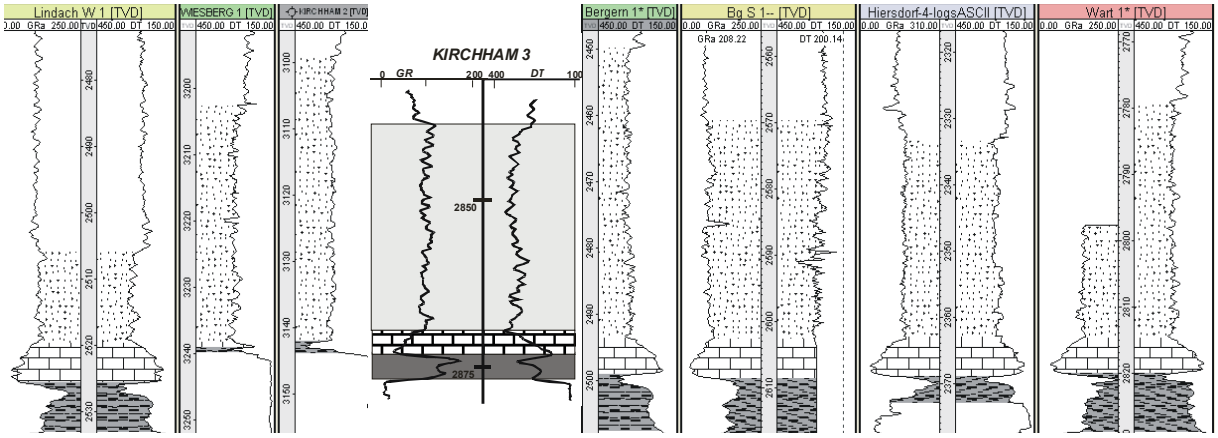

Fig. 63: The southern wells: Lindach W 1, Wiesberg 1, Kirchham 2, Kirchham 3, Bergern 1, Bergern Süd (BgS) 1, Hiersdorf 4, Wart 1.

The wells in the eastern part of the southern study area (see Fig. 63) exhibit following characteristics:

- In the well Lindach W1 (see also chapter 5.3.2.9) the Schöneck and Dynow formations and the lower part of the Eggerding Formation show typical development. The upper part of the Eggerding Formation (together with 8 m of the lower Zupfing Formation) is missing due to erosion.
- The DT log of Wiesberg 1 suggests that Schöneck and Dynow formations are very thin. The Eggerding Formation is nearly 40 m thick. An interval about 6 m thick is missing in the lower part of the Eggerding Formation.
- In Kirchham 2 a very thin Schöneck Formation is overlain by a more or less complete Eggerding Formation. Perhaps 1 or 2 m of its lowest part are missing.
- In Kirchham 3 (logs were not available in digital format) the Schöneck and Dynow formations are thin, but show log motifs characteristic for these formations. The Eggerding Formation is about 30 m thick.
- In the well Bergern1 the Lower Oligocene succession is completely developed and shows characteristic log patterns.
- The DT log from Bergern Süd is poor, but the GR log shows that Dynow and Schöneck formations are present. The thickness of the Eggerding Formation is about 30 m thick. It is difficult to decide, whether the DT log pattern results from logging problems or indicates non-uniform lithologies because of re-deposition.
- In Hiersdorf 4 the Schöneck Formation is thin. The Dynow Formation shows a typical and complete pattern. The upper part of Eggerding Formation together with the lower part of Zupfing Formation is missing (see also Voitsdorf wells).
- Wartberg 1 exhibits a more or less typical complete log pattern.

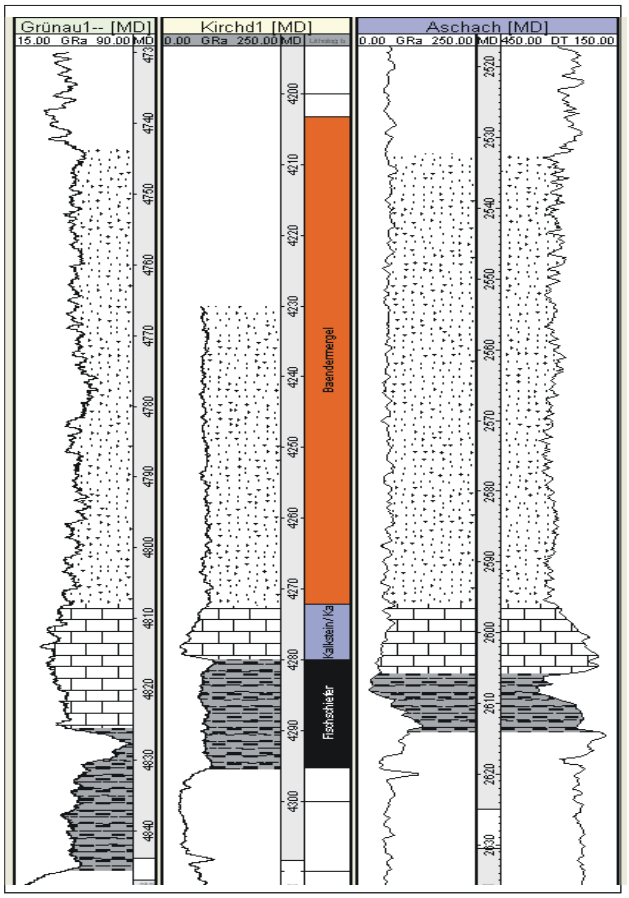

Fig. 64: The well Grünau 1, Kirchdorf (Kirchd) 1 and Aschach 1 exhibit an abnormal thick Eggerding Formation.

Grünau 1, Kirchdorf 1 and Aschach 1 are remarkable because of their thick Eggerding Formation (more than 60 m). The two former wells are the ones with the deepest position on the paleo-slope available for this study.

Grünau 1 has a complete Schöneck Formation. The Dynow and Eggerding formations are untypical and suggest that these units are developed in “Oberhofen facies” (see Fig. 62). This means that there is a lot of re-deposited material.

Probably the top of the Schöneck Formation (“unit c”) is missing in the Kirchdorf 1 well. Unfortunately log data from the upper Eggerding Formation are missing.

Borehole Aschach 1 is located in the south eastern part of the study area. Fig. 65 shows that the Eggerding Formation in this well is unusually thick (~65 m). It also demonstrates that the lower 40 m of the Eggerding Formation in the Aschach well fit quite well with the “model” log pattern of Pattigham Süd 1. In contrast, the DT log of the upper 25 m is strongly serrated and has no analogue in the “model” log. Perhaps, the upper 25 m represent re-deposited material, which has been eroded in shallower positions to the north.

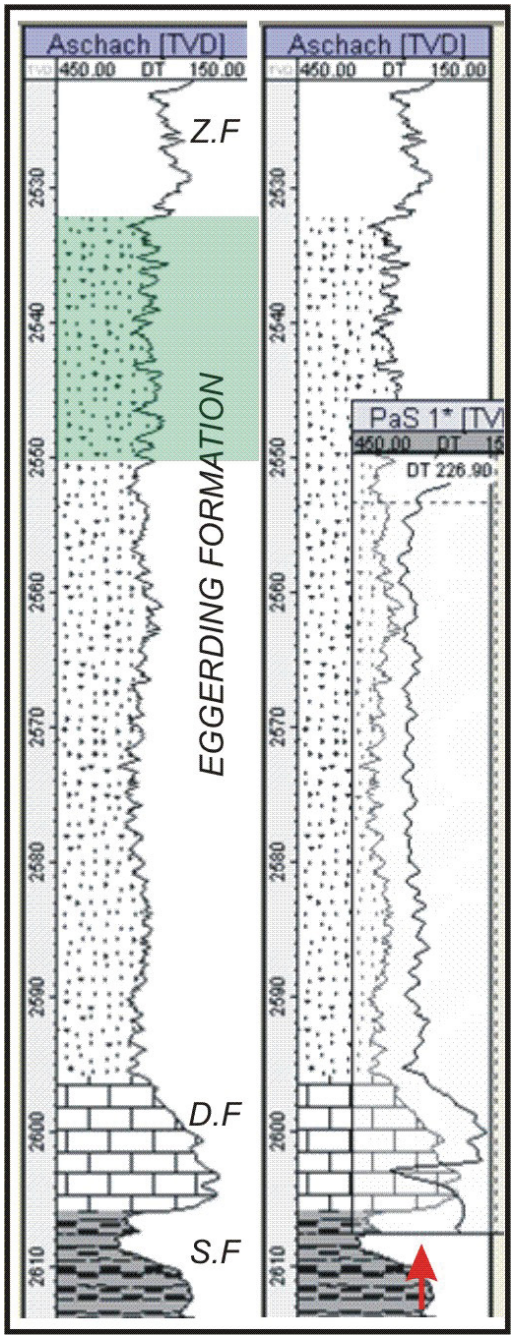

Fig. 65: DT log from Aschach 1 together with the “ghost” of PaS 1 (Pattigham Süd 1). In green: re-deposited material.

5.3.2.12 North

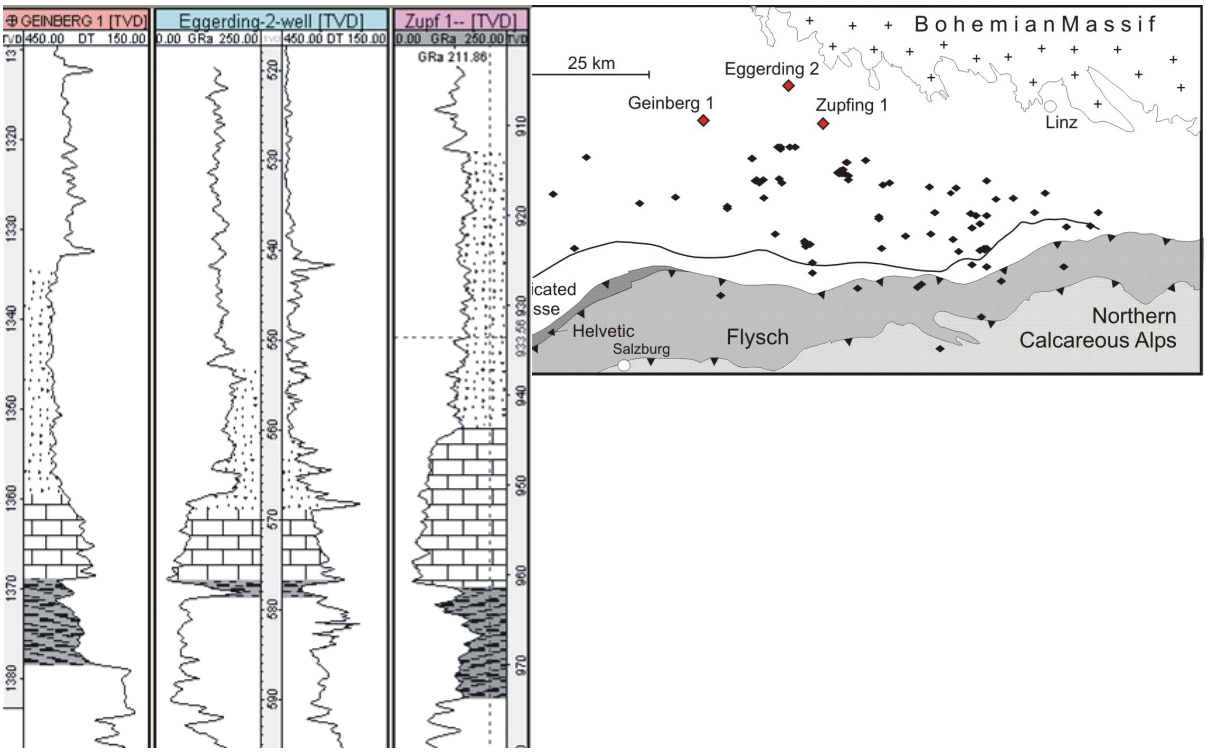

Fig. 66: The northern wells Geinberg 1, Eggerding 2 and Zupfing 1.

Wells Geinberg 1, Eggerding 2 and Zupfing 1 are located in the shallow northern part of the study area close to the paleo-shoreline.

The Schöneck and Dynow Formation are present in all three wells, but not uniform in facies and thickness.

In Geinberg 1 the Eggerding Formation is about 25 m thick. Typically the Eggerding Formation is about 40 m thick (e.g. nearby well Renging 1). It looks like that only the upper part is preserved. In any case, the lower Zupfing Formation is present.

The well Eggerding 2 is the type locality for the Eggerding Formation. Because of the shallow paleo-depth the formations, especially the Eggerding Formation is characterized by a lot of sandy input. Also the Schöneck Formation is characterized by sandy intervals and only the top part is represented by politic rocks. The Dynow Formation is similar to the one of Geinberg 1 and seems complete. Because of the sandy layers, the Eggerding Formation is not comparable with the typical Eggerding log pattern.

Zupfing 1 has a complete Schöneck Formation and a very thick Dynow Formation. The Eggerding Formation is about 30 m thick. It is not clear which part of it has been removed.

6. Interpretation

6.1 Depositional enviroment

6.1.1 Nannoflora

The interpretation of the nannoflora data follows an oral communication of Coric (21. 10. 2008):
The nannoplankton zone NP23 is defined as the period between the last appearance of Reticulofenestra umbilica and the initial appearance of Sphenolithus ciperoensis (Martini, 1971). The lack of these forms in the investigated samples confirms the classification into NP23. The stratigraphic classification of the upper NP23 /lower NP24 is based on the appearance of Reticulofenestra ornata. This taxa is found in the samples Osch 68 and P16.
The samples Osch 64 and Osch 68 from the lower part of the Eggerding Formation are rich in Braarudosphaera bigelowii. This form is especially frequent in near shore environments. Nagymarosy (1991) described the Braarudosphaera-bloom from Oligocene sediments and explained it with the partial separation of the Paratethys. Švábenická (1999) reported Braarudosphaera-rich sediments in the Turonian of the Bohemian Cretaceous Basin. Bukry (1974) used the high percentage of Braarudosphaera bigelowii in Holocene sediments from the Black Sea as an indication of low marine salinity. The enrichment of this cold, nutrient-rich-water-loving species in sediments suggests a short period of fresh water input and reduced salinity during deposition of the lower part of the Eggerding Formation.

6.1.2 Biomarker

Based on Biomarker data, the following observations are made:
The upper Eggerding Formation seems to be more similar with the lower Zupfing Formation (both investigated in well Puchkirchen 3) than with the lower Eggerding Formation (Oberschauersberg 1). However, an influence of the fact that samples from the upper Eggerding and lower Zupfing formations are more mature and belong to the same well can not be completely excluded.
Within the lower Eggerding Formation two sample groups can be separated. Group 1 includes the uppermost (Osch 72) and the lowermost sample (Osch 59). The second group includes three samples. Group 1 show higher CPI values (Tab. 2). In the Pr/ n-C_{17} - Ph/ n-C_{18} diagram Group 1 samples plots into field of type III kerogen, in contrast to apart all other samples (Fig. 19). They differ from group 2 also in the ternary sterane diagram (Fig. 83), where they have relatively high C_{27} contents similar to the upper Eggerding Formation. Also in the sterane/hopane versus TOC/S diagram (Fig. 25), they plot close to the upper Eggerding Formation.
The di-/tri- MTTC ratio indicates salinity fluctuations during deposition of the lower part of the Eggerding Formation (Fig. 28). The Schöneck Formation shows higher salinities in comparison to the Dynow Formation. Towards the Eggerding Formation the salinity increases again and reaches in the samples Osch 59 and Osch 61 the highest salinity before

it drops in the sample Osch 68 to a value similar to the Dynow Formation and remains low in Osch 72.
These results agree with nannoplankton data (see above), where the presence of Braarudosphaera bigelowii in samples Osch 64 and Osch 68 testifies reduced salinity.

From these observations the following can be deduced: During deposition of the lower part of the Eggerding Formation (well Oberschauersberg 1) environmental conditions fluctuated relative quickly: e.g. terrestrial input versus aquatic input, salinity, eH conditions.

6.1.3 TOC/S – ratio

In organic-rich sediments deposited in fresh water, much less pyrite is formed than in marine sediments. This is a consequence of the much lower concentrations of dissolved sulphate in fresh water compared to seawater. As a result, modern organic-rich freshwater sediments exhibit a much higher organic carbon-to-pyrite sulphur ratio (TOC/S) than marine sediments with similar organic contents. Aside the sulphate concentration, there are other limiting factors for the formation of reduced sulphur: the reduction rate in pore waters, the availability of reactive iron and the quantity and quality of organic matter (Berner, 1984).

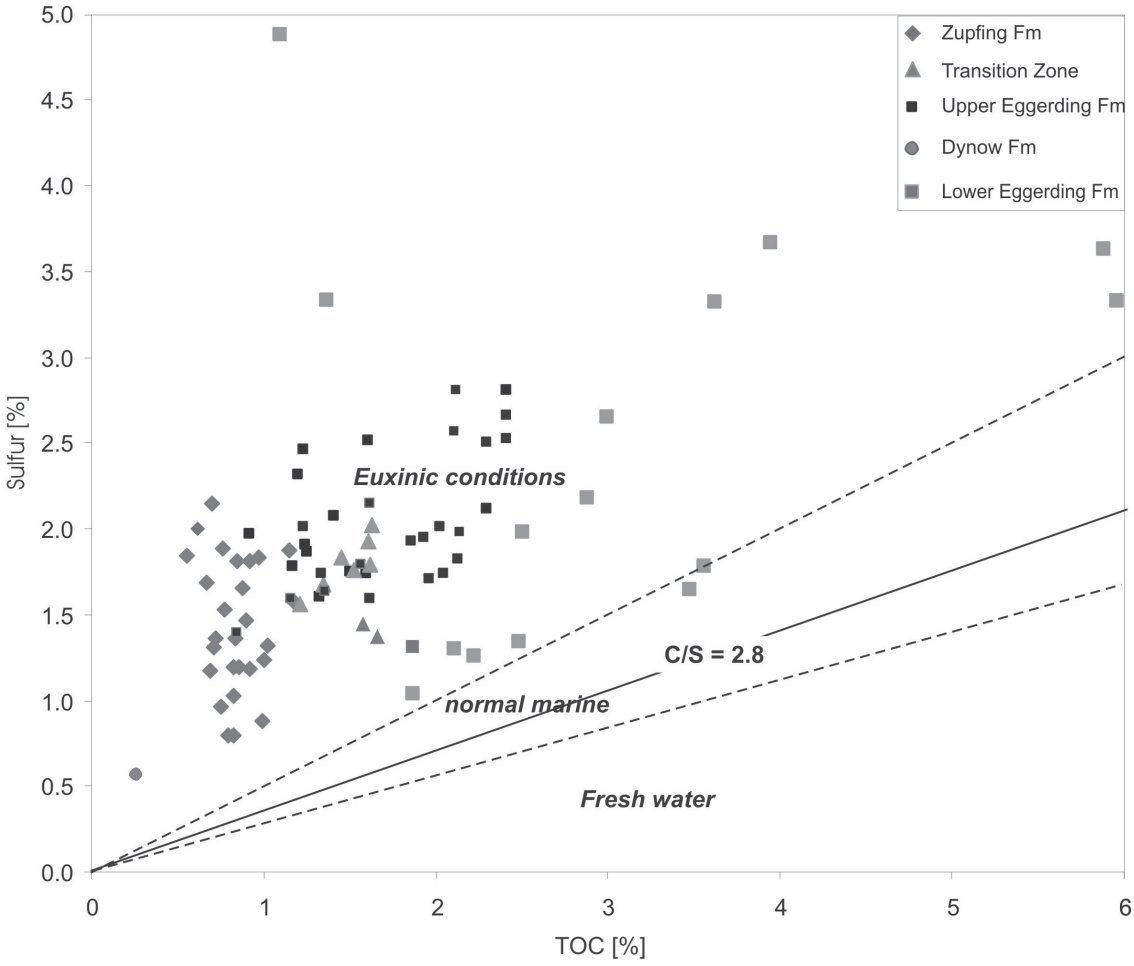

Fig. 67: Sulphur [%] content versus TOC [%] content.

The TOC/S approach (Berner & Raiswell, 1984) cannot distinguish brackish-water sediments deposited under salinities greater than half that of seawater from marine sediments. The method is also not applicable to nearly pure limestone or to rocks low in organic matter (<1% TOC).
In normal marine sediments the TOC/S ratio is about 2.8 ($\pm$ 0.8). Freshwater sediments obtain a higher TOC/S ratio (>10) (Berner & Raiswell, 1983). In euxinic depositional environment there are high amounts of sulphides, resulting in low TOC/S ratios. The limiting factor here is the availability of reactive iron.

Nearly all the samples have high sulphur contents (Zupfing Fm.: 0.8 -2.2%; Transition zone: 1.3 -2.0%; upper Eggerding Fm.: 1.6 -2.8%; lower Eggerding Fm.: Osch 1: 1 -3.6%; Egdg 2: up to 4.8%) and, therefore, plot into the euxinic area.
The samples from the lower part of the Eggerding Formation (Osch 1) show a positive linear correlation between TOC and S, but have slightly higher TOC/S-ratios than the rest of the samples. Therefore, the lower part of the Eggerding Formation plots near the normal marine trend. This might indicate either less euxinic conditions. However, pristane/phythane-ratios do not show significant differences between lower and upper Eggerding Formation in terms of eH-conditions. Moreover, lack of bioturbation suggests anoxic conditions.
For one of the samples (Osch 64), calcareous nannoplankton (Braarudosphaera bigelowii, small) suggests slightly reduced salinity in the lower part of the Eggerding Formation. Although slight variations in salinity are normally not visible in the TOC/S plot, the higher TOC/S-ratios might be related to slightly reduced salinity.

6.1.4 Variation of silicate, carbonate and TOC (after Ricken, 1993)

In this chapter the calcite equivalent – and TOC – values from each Formation are plotted in diagrams. The slope of the trend lines indicates three different deposition models:

In the carbonate deposition model carbonate supply is allowed to vary and deposition of siliciclastics and organic matter is assumed constant. An increase in carbonate supply would ideally result in diluting the organic carbon content to lower weight percentages, causing an increase in the carbonate content and simultaneous decrease in the organic carbon content in the sediment (Fig. 68a).
Carbonate deposition is decoupled from the organic matter flux. Increasing nannoplankton productivity in the surface water will only slightly increase the organic matter flux, as the organic matter is largely recycled, whereas the carbonate flux reaches uninfluenced the sea floor.

In the siliciclastic deposition model (Fig. 68b) silt and clay deposition varies and the supply of organic carbon and carbonate remains unchanged. With an increase of the clastic supply the carbonate and organic carbon concentration of the sediment decreases. In this model decreasing amounts of organic carbon and carbonate in the sediment suggest an increase in sedimentation rate.

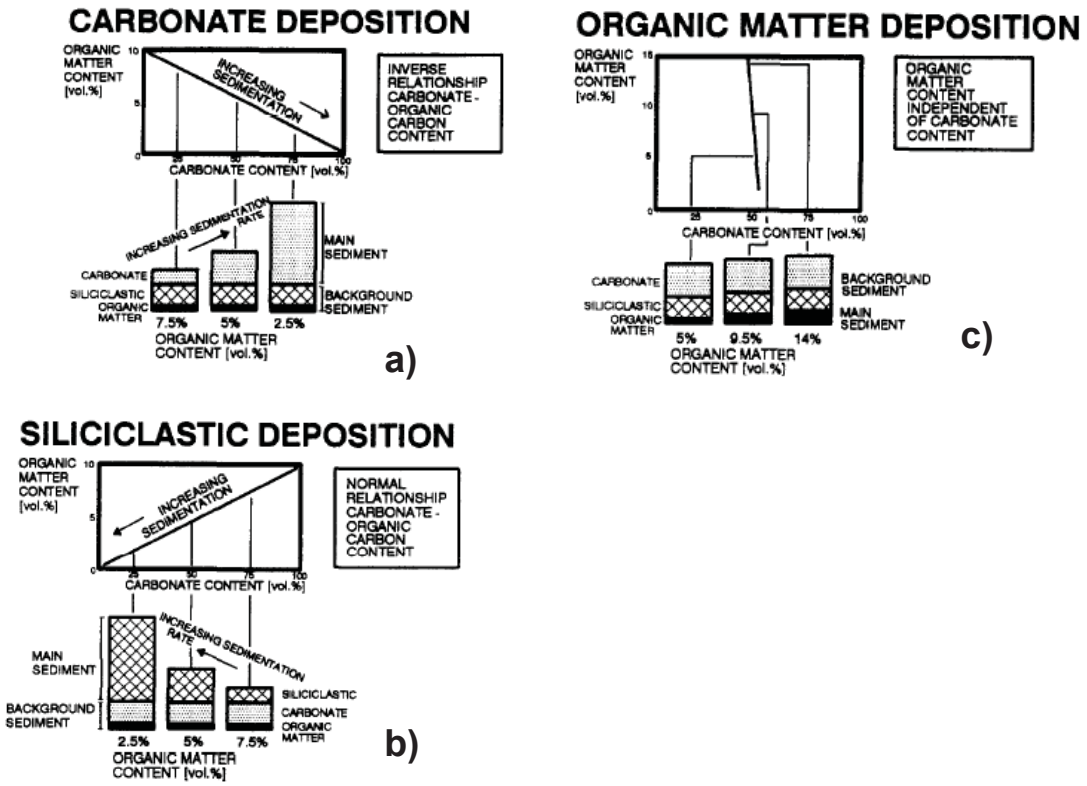

Fig. 68: Various deposition models (Ricken, 1993): a) carbonate deposition model; b) siliciclastic deposition model; c) organic matter deposition model.

In the organic matter deposition model (Fig. 68c) organic matter deposition varies and the supply of clastics and carbonate remains constant. Changes in the relatively small organic fraction have limited effects on the much larger carbonate and clastic fractions. As a result the organic matter-carbonate graph of Fig. 68c shows a steep negative correlation which is more or less independent of the carbonate content. Changes in the amount of deposition of organic matter have a limited influence on the sedimentation rate.

In all five wells (Figs. 69 -71) the Eggerding Formation shows more or less a trend line with no slope, which means constant carbonate and silicate supply and variation in organic matter deposition. The Transition zone in the wells Voitsdorf 1 and Puchkirchen 3 shows a positive correlation. This correlation stands for the variation of silt and clay input. The samples of Hiersdorf 5 seem to have a negative correlation. The difference of the results between the wells could depend on the small amount of data; the washing procedure of the Hiersdorf 5 samples could also have some effects. The Zupfing Formation shows only a “data cloud”.

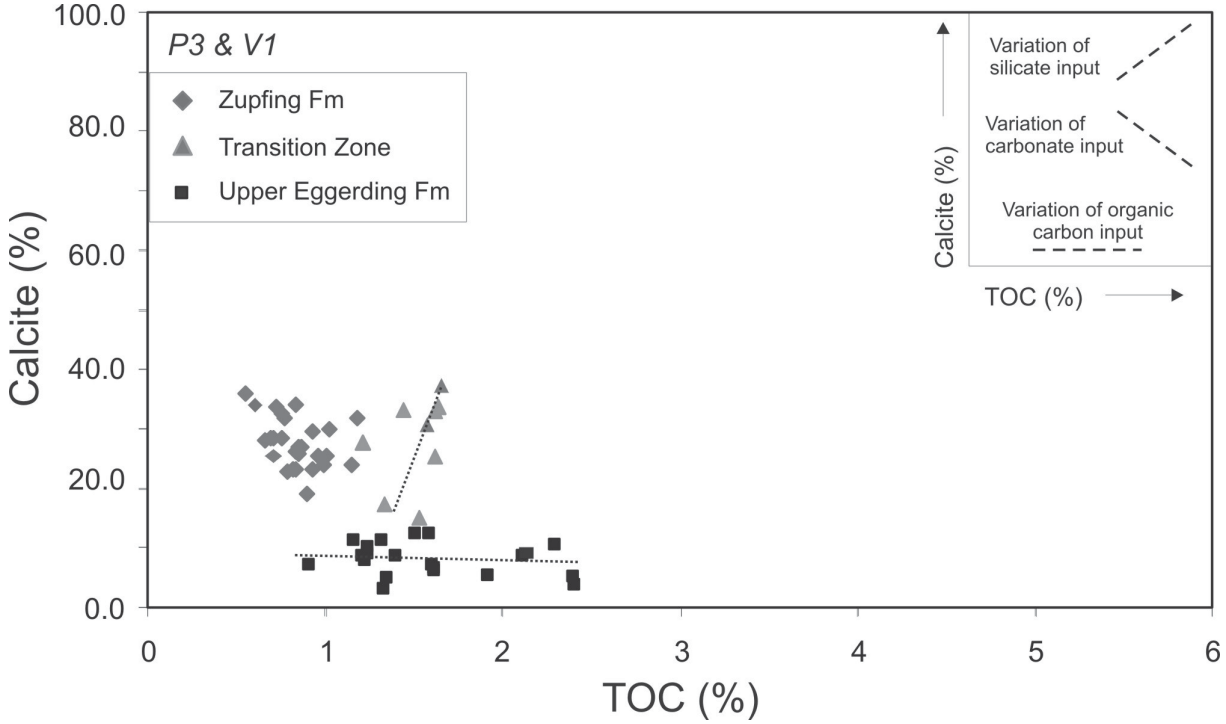

Fig. 69: Calcite [%] content versus TOC [%] content for the wells Puchkirchen 3 and Voitsdorf 1.

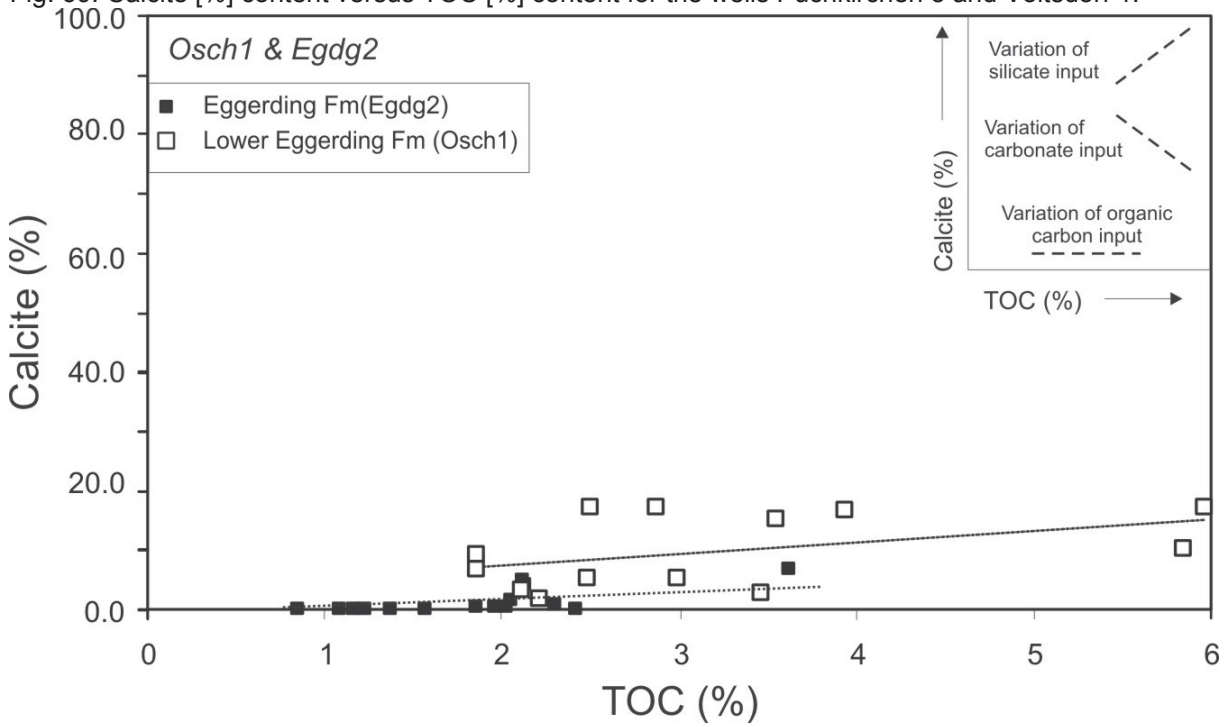

Fig. 70: Calcite [%] content versus TOC [%] content for the wells Oberschauersberg 1 and Eggerding 2.

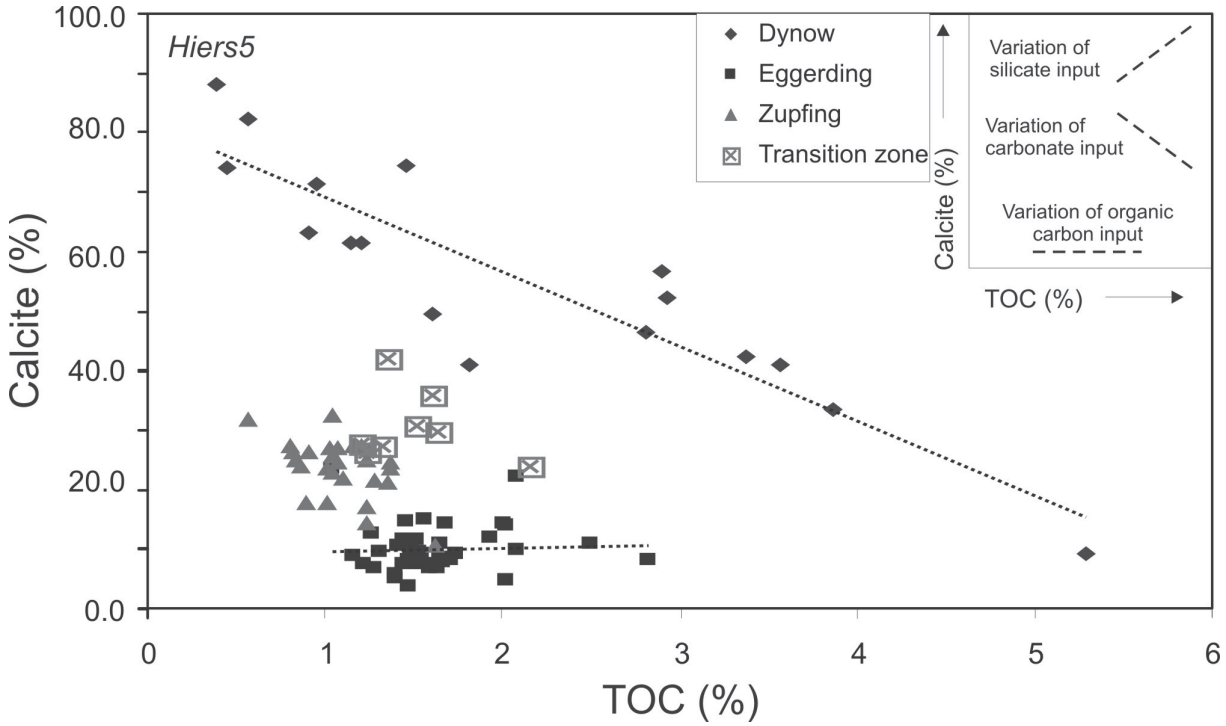

Fig. 71: Calcite [%] content versus TOC [%] content for the well Hiersdorf 5.

6.2 Post depositional events

The isopach map in Fig. 72 shows the thickness distribution of the Eggerding Formation (Sachsenhofer and Schulz, 2006). On the map are added additionally the wells, on which this study is based on. The wells with complete Eggerding Formation (black) show log patterns which can be traced over wide distances within the entire study area. This observation suggests uniform sedimentation in the early Oligocene Molasse Basin.
Because of the lateral continuity it was possible to decide whether the Eggerding Formation in a specific well is complete, absent, abnormally thick or if there is a missing part. Furthermore it allows identifying which part is missing (see chapter 5.3 and legend of Fig. 72).

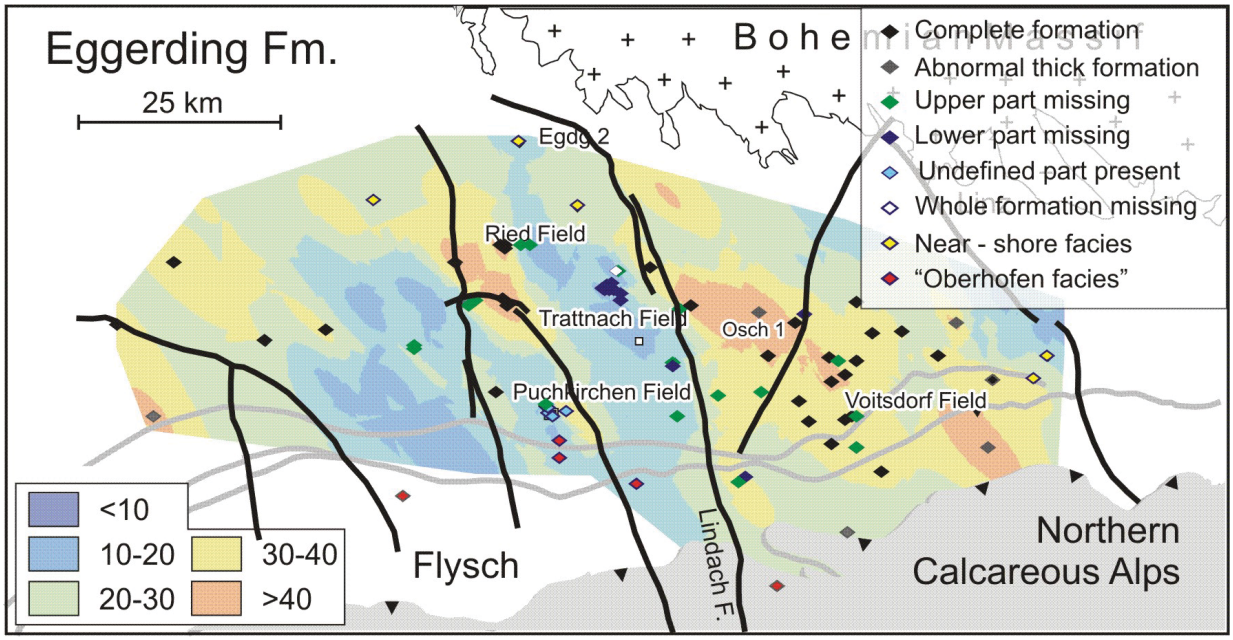

Fig. 72: Isopach map of the study area (after Sachsenhofer and Schulz, 2006). Investigated wells are included and categorized according to the completeness of the Eggerding Formation.

This detailed information shows a complicated erosion history. In some areas wells with missing parts are frequent. In these areas it has to be checked if the missing parts can be caused by one or several erosion events.
Within the study area two principal erosion events occurred:

- Event 1 occurred after deposition of the lower part of the Eggerding Formation, so that the upper Eggerding Formation directly overlies the Dynow Formation (e.g. Trattnach 8), the Schöneck Formation (e.g. Wolfersberg) or even the Lithothamnium Limestone (Trattnach 10). This event was most prominent in the Trattnach area (max. erosion ~ 50 m).
- Event 2 occurred after the deposition of the whole Eggerding Formation so, that the upper part of the Eggerding Formation is missing. In some wells also the lowermost part of the Zupfing Formation is missing (e.g. V 37). This could be a result of slumping

and sliding. Erosion during event 2 was more widespread and cut deeper into the subsurface than erosion during event 1 (max. erosion ~ 70 m).

Some additional small-scale local erosion events can be supposed (e.g. Aiterbach 1, Oberschauersberg 1, Gunskirchen 1, see chapter 5.3.2.7).
Erosion occurred mainly west of the Lindach Fault in the Ried – Schwanenstadt and Braunau blocks. These blocks experienced enhanced tectonic activity during Paleogene times suggesting that the gravity–induced movements were triggered by earthquakes (Sachsenhofer and Schulz, 2006).
Especially in the southern part of the basin are wells with untypical log pattern ("Oberhofen facies", see Fig. 74) or/and abnormal thick lithologies (e.g. Aschach 1, see Fig. 73). It can be assumed that the wells in this positions show formations with re-deposited material, that means eroded on the upper slope, transported, reworked and than deposited e.g. on the lower slope.

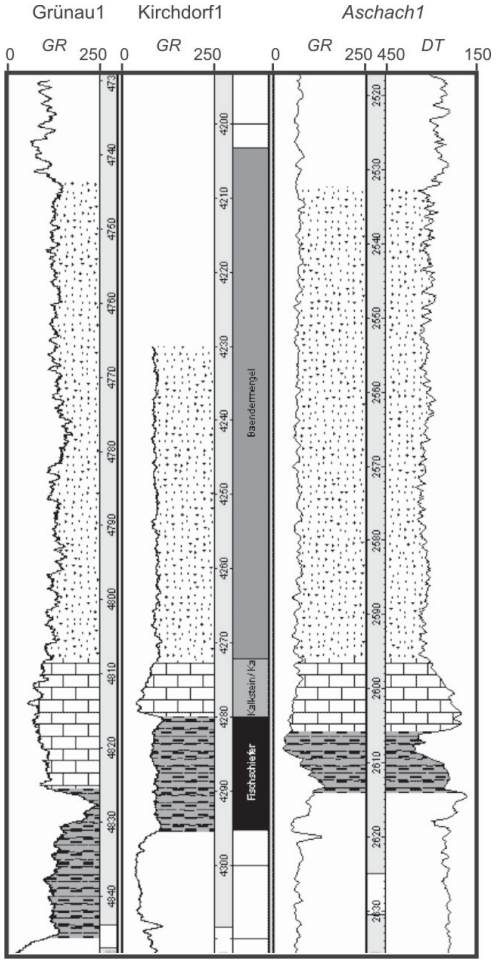

Fig. 73: Logs from the southern study area with abnormal thick Eggerding Formation: Grünau 1, Kirchdorf 1 and Aschach 1.

The lower Oligocene formations were deposited in several hundred metres of water depth (Wagner 1998). Therefore even the sea level fall between the early and late Oligocene (NP

24) could not establish sub aerial conditions. Consequently, all erosional events are considered as submarine processes (Sachsenhofer and Schulz, 2006).
Similar erosional features occurred in the western Carpathians during NP23 (“Sitborice Event”; Krhovský and Djurasinovic, 1993). Correlations of such events highlight that slope instability may have occurred basin-wide rather than being a local phenomenon (Sachsenhofer and Schulz, 2006).

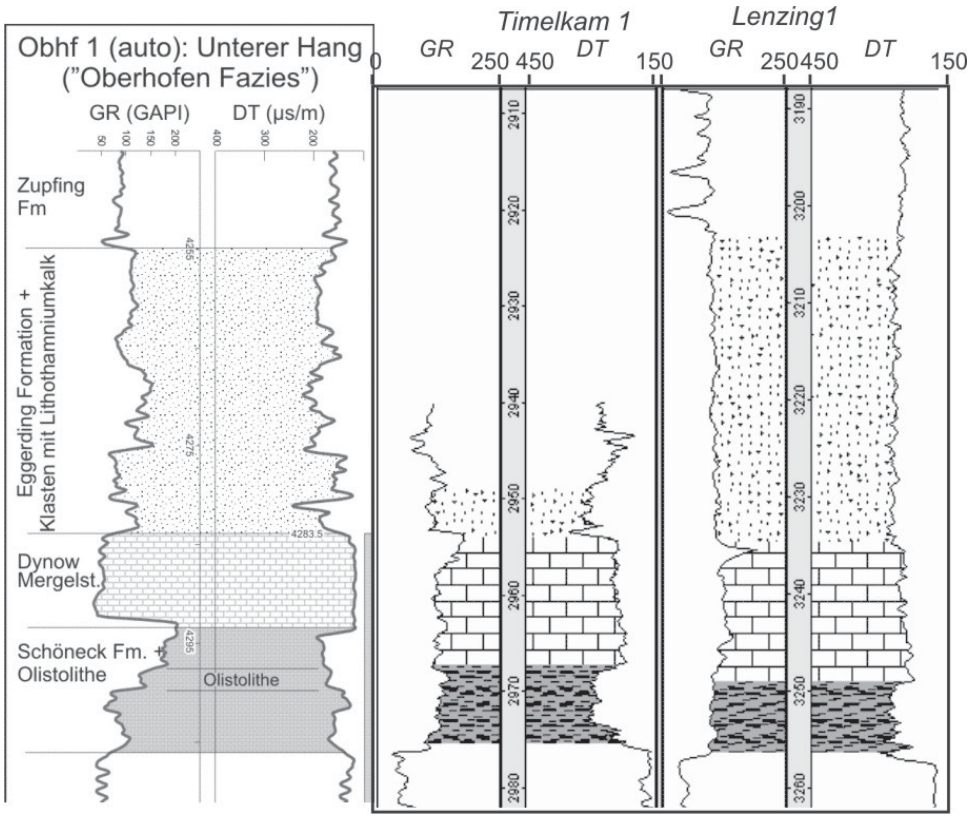

Fig.74: Logs with an “Oberhofen facies” (blocky Dynow Formation and highly structured Eggerding Formation): Oberhofen 1, Timelkam 1, Lenzing 1.

It was tried to detect some of these erosion and «secondary deposition» events on seismic lines. On Fig. 75 the NW-SE trending seismic line 2188 near the Trattnach field illustrates some interesting features.
The red line highlights the top of the Eggerding Formation; the strong horizons below mark the sequence of Dynow Formation, Schöneck Formation and Lithothamnium Limestone. At the northwestern end of the line thick Eggerding Formation is present. At about the middle of Fig. 75 the Eggerding Formation is eroded. Deformation (slumping?) features within the Eggerding Formation are visible near its erosional boundary. The blue arrow in Fig. 75 shows onlap of the basal Zupfing Formation onto the erosion surface. Chaotic reflection pattern on the right side of Fig. 75 demonstrate more erosion events. The seismic data in this part of the section probably show that (at least for this part of the basin) erosion was more complicated than log-correlation lets assume.

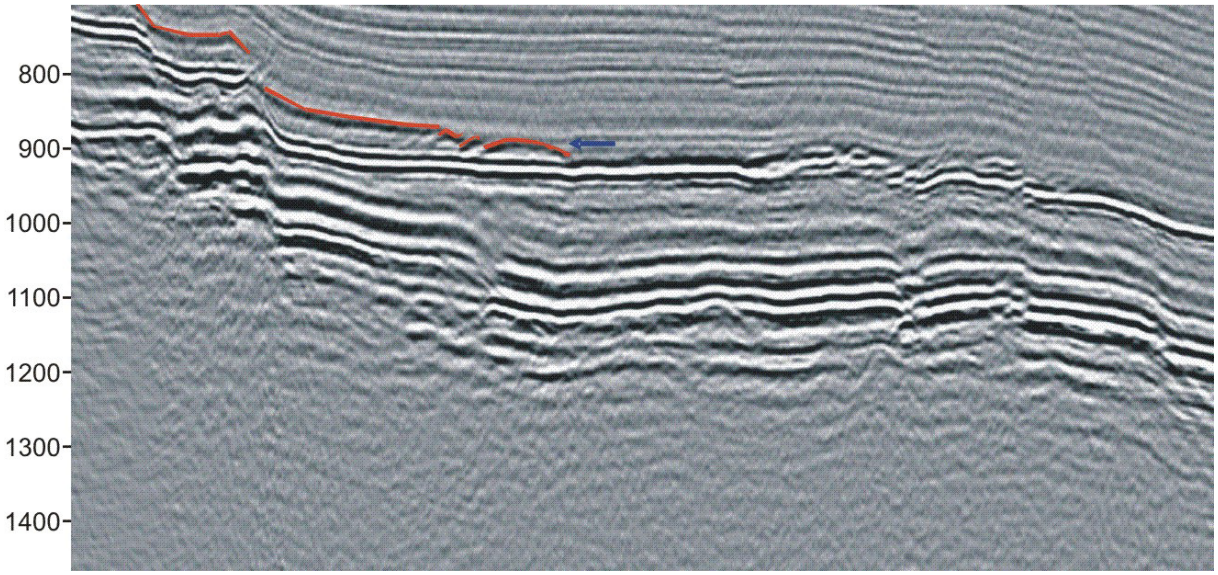

Fig. 75: Seismic section 2188 from NW to SE (near Trattnach). Vertical scale is in time.

6.3 Hydrocarbon Potential

The hydrocarbon potential of a formation depends mainly on its average TOC content and on the Rock-Eval parameter S2 (mgHC g^{-1}rock; parameter which reflects the amount of hydrocarbons generated by heating up to 550°C).
The genetic potential (S1+S2) gives the amount of hydrocarbons which is already generated and not yet expelled from the source rock together with the amount of hydrocarbons generated during pyrolysis.
A good source rock has a TOC content of 1 to 2 % (e.g. Peters, 1986). A TOC content of more than 2% describes a very good source rock.

Summarizing the outcomes for the Eggerding Formation from the individual wells (see chapter 5.2.1) results in following:
The Eggerding Formation reaches the highest TOC content (5.98%) and HI value (590 mgHC g^{-1}TOC, type II kerogen) in its lower part (well Oberschauersberg 1).
In the middle and upper part of the Eggerding Formation (wells Voitsdorf 1, Puchkirchen 3) the TOC content reaches a maximum of 2.4 %. The maximum hydrogen index is obtained in Puchkirchen 3 (401 mgHC g^{-1}TOC; type II kerogen).
Also in the near shore well Eggerding 2, high TOC (up to 3.6%) and HI values (up to 436 mgHC g^{-1}TOC, type II kerogen) occur in the non-sandy lower part of the Eggerding Formation.
Average values:

- lower Eggerding Formation: TOC content 3.2%
  HI 436 mgHC g^{-1}TOC
- upper Eggerding Formation: TOC content 1.5% (Puchkirchen 3); 1.8% (Voitsdorf 1)
  HI 300 mgHC g^{-1}TOC (Puchkirchen3); 303 (Voitsdorf 1)

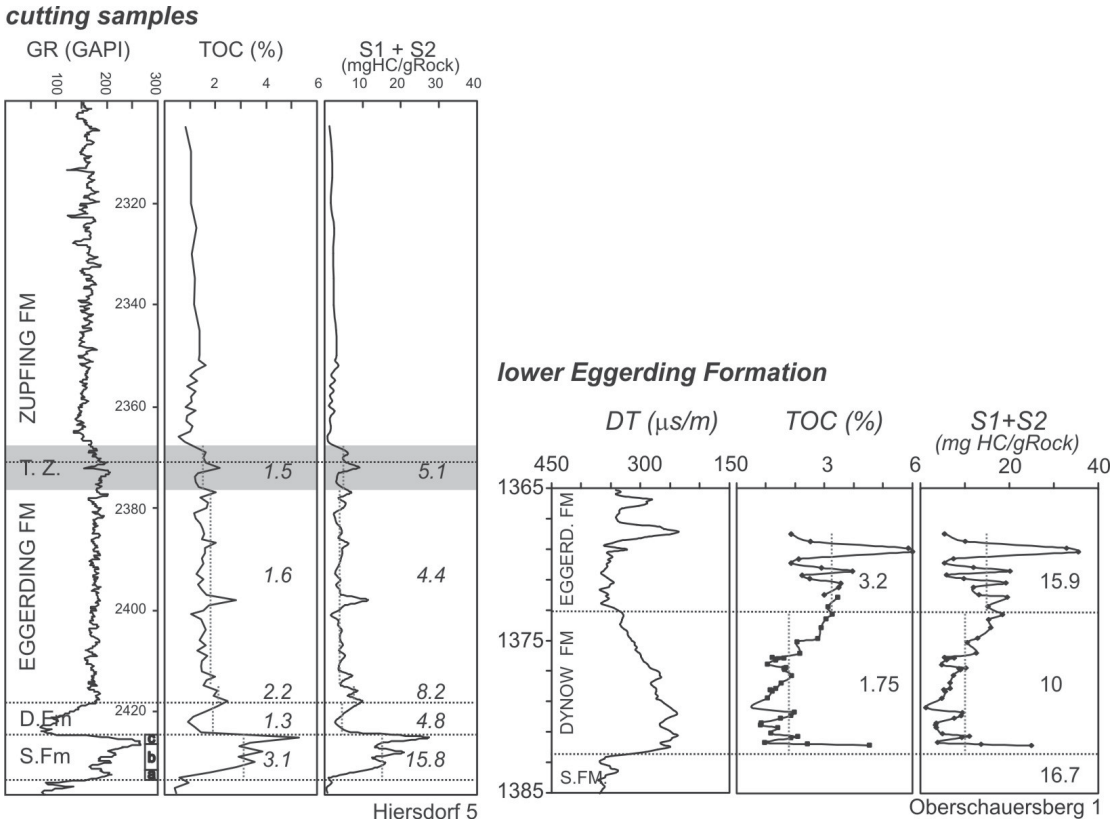

Fig. 76: TOC [%] and genetic potential (S1+ S2) from Hiersdorf 5 and Oberschauersberg 1.

In the Figs. 76, 77 and 78 the average TOC content of different stratigraphic units is highlighted in the respective wells. In the Transition zone an average value of 1.5 can be assumed. The upper Eggerding Formation exhibits a similar average TOC content of 1.65%. The lower Eggerding Formation reaches an average TOC content of 3.2.

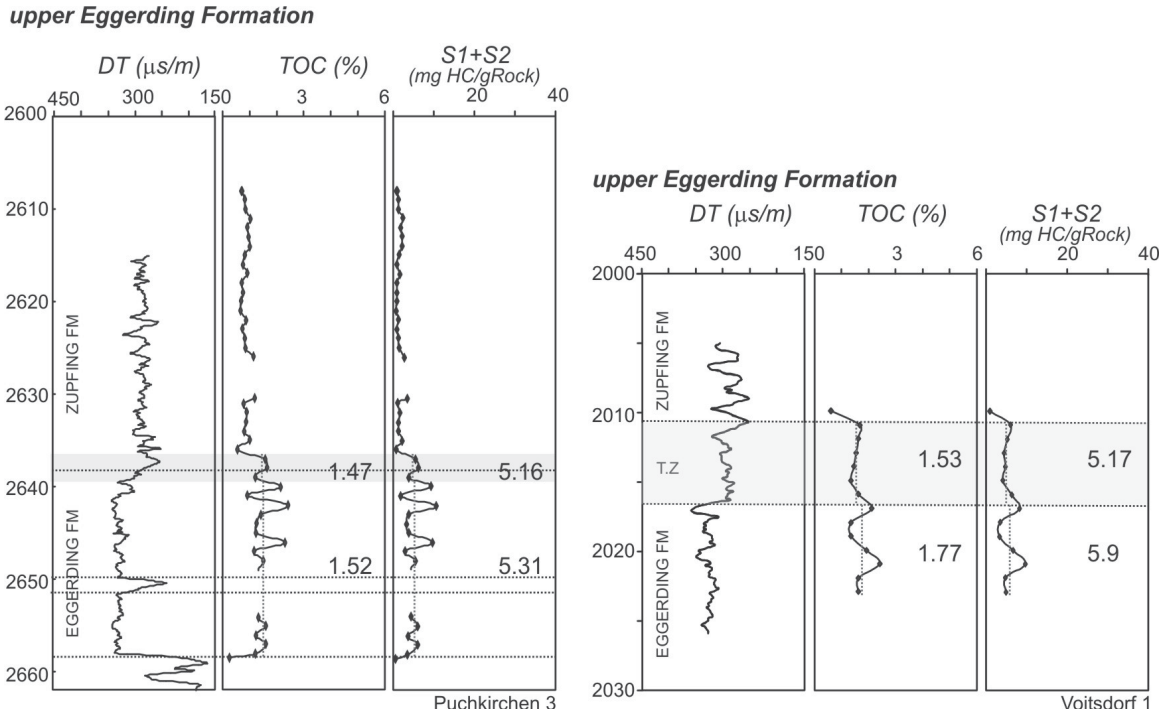

Fig. 77: TOC [%] and genetic potential (S1+ S2) from Puchkirchen 3 and Voitsdorf 1 wells.

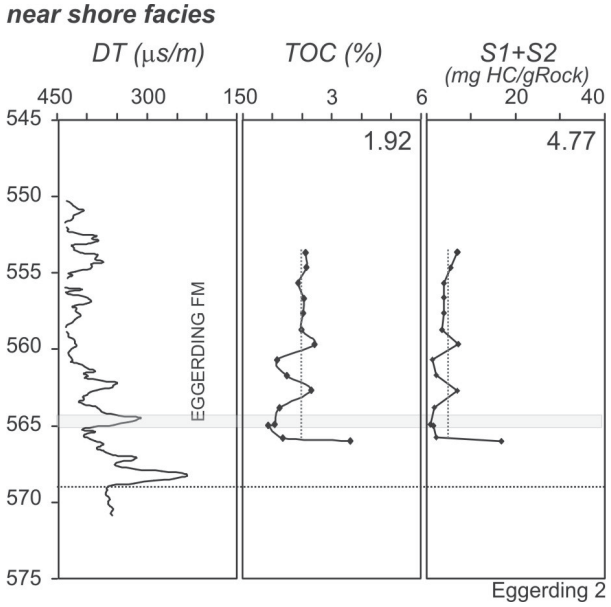

Fig. 78: TOC [%] and genetic potential (S1+ S2) from the near shore well Eggerding 2.

A quantitative determination of the hydrocarbon potential can be made using the source potential index (SPI; Demaison and Huizinga, 1994):

$$SPI\,(tHC/m^2) = \frac{h * (S1 + S2)}{1000} * \rho$$

h...*thickness*

ρ...*density*

$S1 + S2$...*genetic – potential*

It is calculated from the thickness and density of the formation and its genetic potential (S1+ S2), which is the amount of hydrocarbons in milligrams produced from a gram of the source rock during pyrolysis.

The average genetic potential of each well is illustrated in the Figs. 76 to 78. For the calculation of the SPI average values have to be used which are representative for the whole study area. Therefore the average values of the wells Voitsdorf 1, Oberschauersberg 1 and Puchkirchen 3 have been used. In comparison to the other wells the cutting material which was used for Hiersdorf 5 shows slightly lower results (Fig. 79), they consequently have not been included in the calculations. Because it represents a near shore facies, values from Eggerding 2 are also not useful for the estimation of the source potential of the whole study area.

Table 6 demonstrates the calculated SPI's. It shows that the Eggerding Formation (incl. the "Transition zone") has a higher source potential than the Schöneck Formation. This is mainly a result of the greater thickness of the Eggerding Formation. It shows that the Eggerding Formation could have contributed to the Molasse oil significantly.

formation	formation part	S1 + S2	thickness	density	SPI
	Transition zone	5.17	4	2	0.041
Eggerding	upper part	5.61	37	1.9	0.39
	lower part	15.87	5	1.9	0.15
					Σ 0.58
Dynow		10	8	2	0.16
Schöneck		16.7	10	2.1	0.35

Tab. 6: Genetic potential, thickness, density and source rock potential (SPI) of different Lower Oligocene formations.

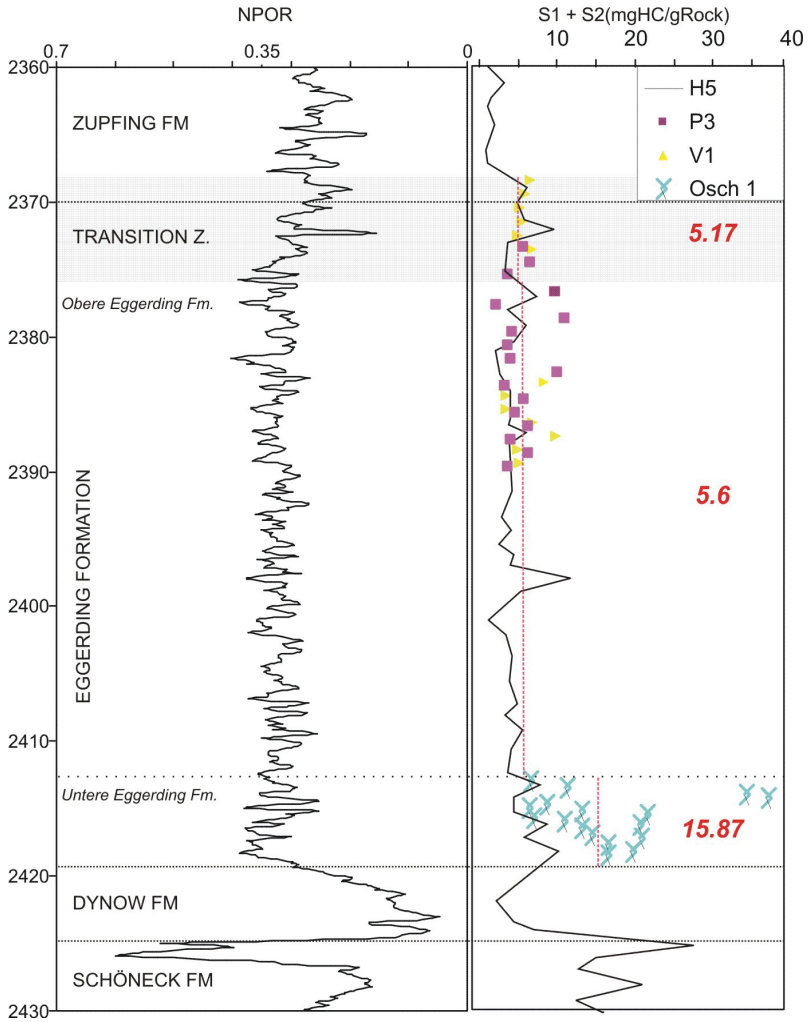

Fig. 79: Comparison of the genetic potential between the cutting samples of Hiersdorf 5 and the core samples of Puchkirchen 3, Oberschauersberg 1 and Voitsdorf 1 for the Transition zone and upper and lower Eggerding Formation. In addition the average values of the genetic potential.

The type of hydrocarbons, which will be generated in a source rock can be estimated using the Hydrogen index (HI), which calculated according to the formula (100*S2 TOC^{-1}). In other words, it predicts how many hydrocarbons (in mg) can be formed by 1 g of TOC. HI values in the range of 50 to 300 correspond to type III kerogen (gas prone) which derives mostly from terrestrial plants. HI values up to 600 belong to type II kerogen (oil prone). It originates from mixed phytoplankton, zooplankton and bacterial debris. A HI of 600 and more corresponds to type I kerogen (very oil prone) which has formed from extensive bacterial reworking of lipid rich algal debris.
Because of a mineral matrix effect (Langford and Blanc-Valleron, 1990) sometimes hydrocarbons are not fully released during Rock- Eval pyrolysis.
By plotting the samples in a TOC - S2 diagram, the true average HI can be derived:
slope of the trend line times 100.

The calculated average value for the Eggerding Formation in the well Eggerding 2 is 554 mgHC g^{-1} TOC (type II kerogen; Fig. 80), which is higher than the experimental average (~230 mgHC g^{-1}TOC).

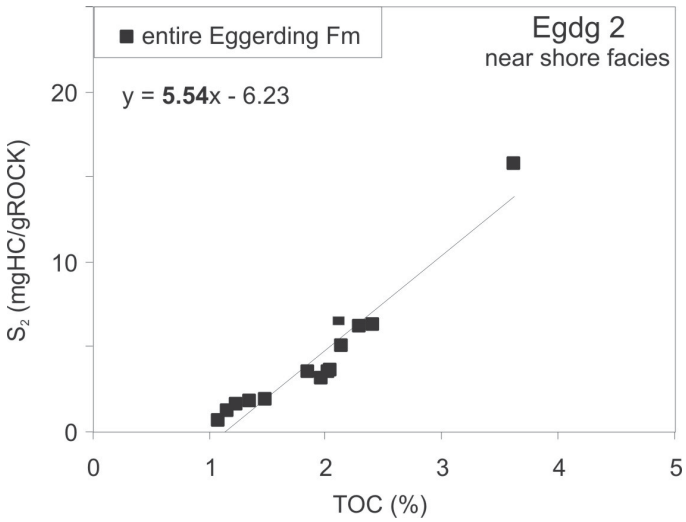

Fig. 80: Crossplot of S2 (mg HC g^{-1} rock; Rock Eval) versus TOC (%) from Eggerding 2. The slope of the trend lines times 100 results in the true Hydrogen index (554 mg HC g^{-1} TOC). Diagram after Langford and Blanc-Valleron (1990).

The calculated HI average value for the lower Eggerding Formation (Oberschauersberg 1) is 681 mgHC g^{-1}TOC (type I kerogen; Fig. 81), which is higher than the experimental average (436 mgHC g^{-1}TOC), too.

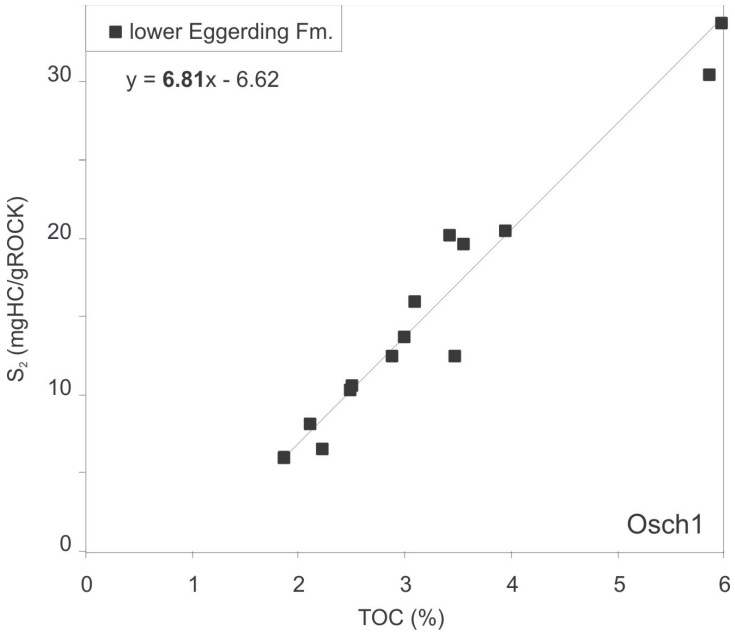

Fig. 81: Crossplot of S2 (mg HC g^{-1} rock; Rock Eval) versus TOC (%) from Oberschauersbach 1. The slope of the trend lines times 100 results in the true Hydrogen index (681 mg HC g^{-1} TOC). Diagram after Langford and Blanc-Valleron (1990).

The calculated average values for the Eggerding Formation, the "Transition zone" and the Zupfing Formation of the well Puchkirchen 3 (Fig. 82) belong with values of 553 mgHC g^{-1} TOC (experimental average: 298 mgHC g^{-1} TOC), 504 mgHC g^{-1} TOC (experimental average: 312 mgHC g^{-1} TOC) and 417 mgHC g^{-1} TOC (experimental average: 153 mgHC g^{-1} TOC) all to type II kerogen.

The calculated HI values of the well Voitsdorf 1 (Fig. 82) are with 581 mgHC g^{-1} TOC for the upper Eggerding Formation (experimental average: 303 mgHC g^{-1} TOC) and 581 mgHC g^{-1} TOC for the "Transition zone" (experimental average: 312 mgHC g^{-1} TOC) slightly higher as in the well Puchkirchen 3.

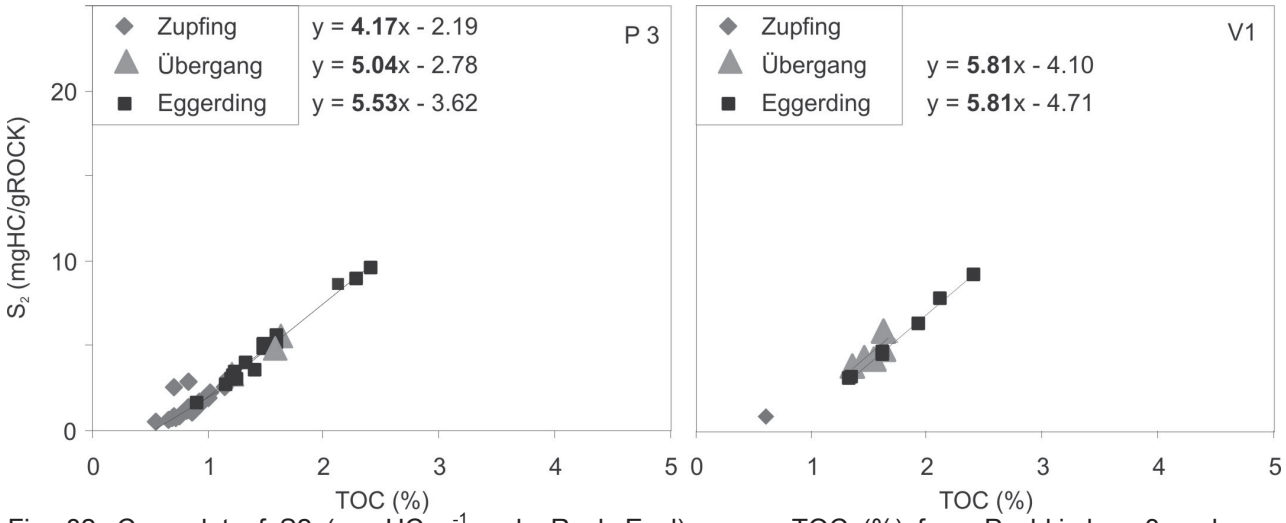

Fig. 82: Crossplot of S2 (mg HC g^{-1} rock; Rock Eval) versus TOC (%) from Puchkirchen 3 and Voitsdorf 1. The slope of the trend lines times 100 results in the true Hydrogen indices. Diagram after Langford and Blanc-Valleron (1990).

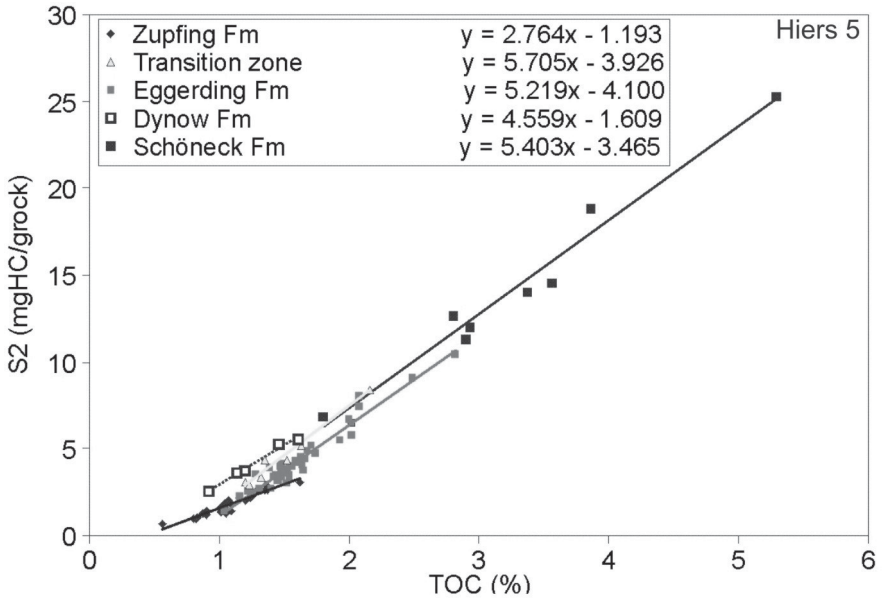

Fig. 83: Crossplot of S2 (mg HC g^{-1} rock; Rock Eval) versus TOC (%) from Hiersdorf 5. The slope of the trend lines times 100 results in the true Hydrogen index. Diagram after Langford and Blanc-Valleron (1990).

The "true" mean HI values of Hiersdorf 5 (Fig. 83) vary between 450 and 570 mgHC g^{-1}TOC. This suggests a prevalence of oil-prone type II kerogen. The "true" HI of the Zupfing Formation above the Transition zone is 277 mgHC g^{-1}TOC (Sachsenhofer, 2008).

From the "true" mean HI values can be deduced a Type I kerogen for the lower Eggerding Formation, a Type II kerogen for the upper Eggerding Formation and the "Transition zone". The calculated HI values are summarized in table 7.

	True average HI (mgHC / gTOC)
Zupfing Formation:	
P 3	417
V 1	
H 5	277
Zupfing Formation (basal part "Transition Zone"):	
P 3	504
V 1	581
H 5	570
Whole Eggerding Formation:	
H5	522
Egdg 2 (near shore position)	554
Upper part of Eggerding Formation:	
V 1	581
P 3	553
Lower part of Eggerding Formation:	
Osch 1	681

Tab. 7: Calculated Hydrogen indices (mgHC g^{-1}TOC) without matrix effect.

In Fig. 84 the HI and the T_{max} values are plotted in diagrams. T_{max} is a thermal maturity parameter based on the temperature at which the maximum amount of pyrolyzate (S2) is generated from the kerogen in a rock sample. The beginning and the end of the oil-generative window approximately correspond to T_{max} values of 435°C and 470°C (Peters, 1986).

The diagrams show the kerogen types of different formations in different wells. In addition it can be seen that the samples are immature or marginal mature (Puchkirchen 3).

With respect to thermal maturity the difference between Eggerding Formation and Schöneck Formation is irrelevant, because the Schöneck Formation underlies the top Eggerding Formation by maximal 50 m. Assuming a normal geothermal gradient 50 m make a temperature difference of only 1.5°C.

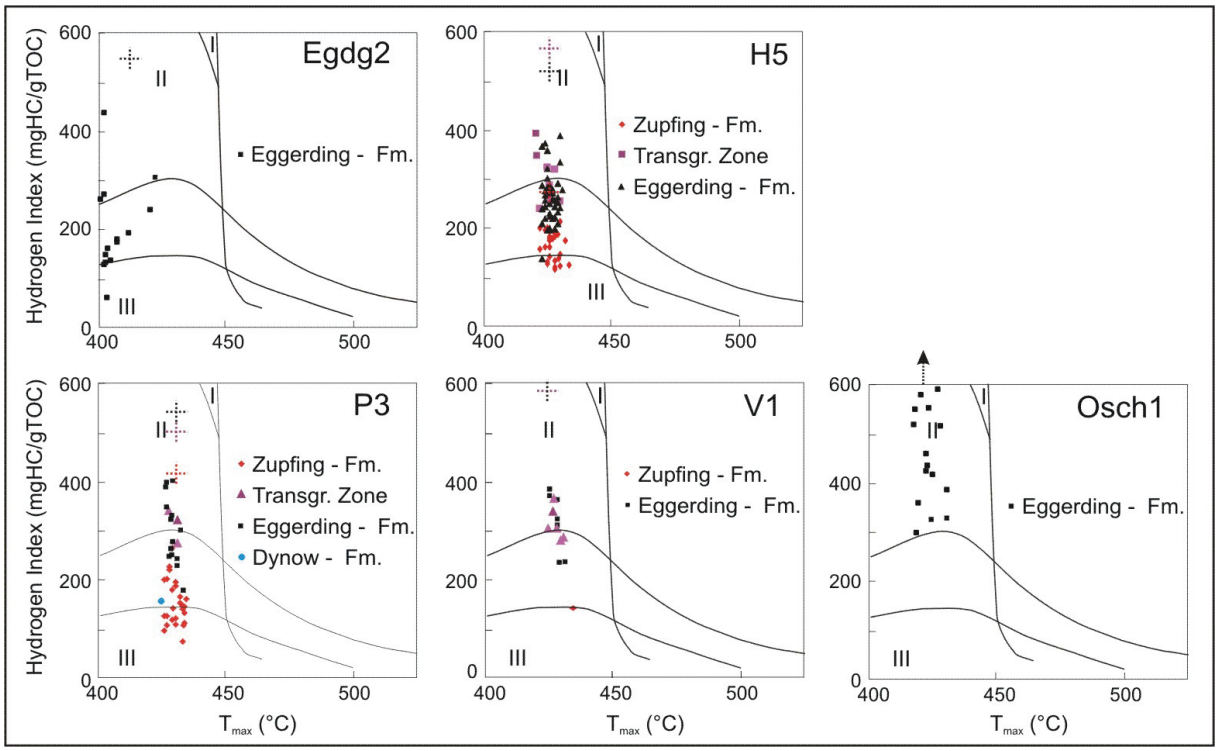

Fig. 84: Crossplots of Hydrogen index (mgHC g^{-1}TOC) versus Tmax (°C).

6.4 Source rock - oil correlation

In chapter 6.3 the hydrocarbon potential of the Eggerding Formation is qualitatively and quantitatively described. In this chapter it will be investigated whether hydrocarbons from the Eggerding Formation in fact make a significant contribution to the Molasse oil.
The Figs. 85 to 87 exhibit the results of the biomarker analysis of the Eggerding Formation (see chapter 5.2.2) together with the results for Dynow Formation, Schöneck Formation and Molasse oil (Gratzer, 2008). The sterane distribution plot shows that the Schöneck Formation and the upper Eggerding Formation correspond excellent with the Molasse oil. Dynow Formation and lower Eggerding Formation are richer in C_{28} steranes. Both formations could be the reason for a shift of the oil in the very direction.
In the pristane/phythane diagram (Fig. 87) the samples of the Schöneck Formation do not correspond so well with the Molasse oil as the samples of the Eggerding Formation. After this correlation the Dynow Formation can be excluded as a major contributor to the Molasse oil. This implies that the lower Eggerding Formation, although it is only a few meters thick, is alone responsible for the distortion of the Molasse oil in the sterane diagram towards C_{28}.

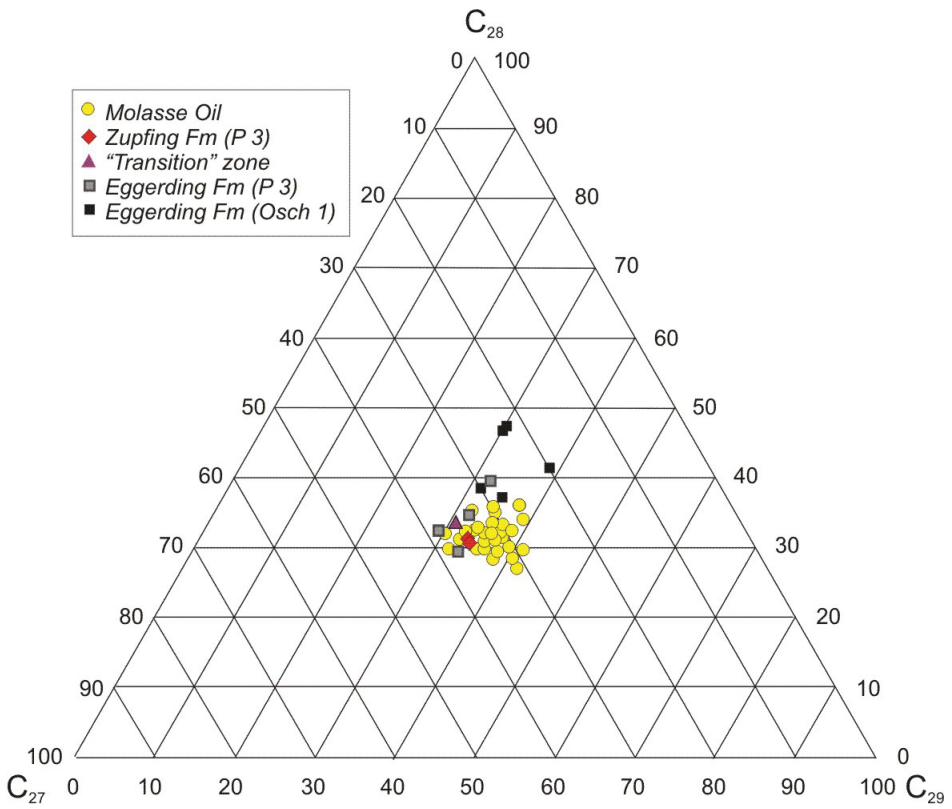

Fig. 85: Ternary diagram of the C_{27}, C_{28} and C_{29} steranes for Eggerding Formation, „Transition zone", Zupfing Formation and Molasse oil (Gratzer et al., 2008).

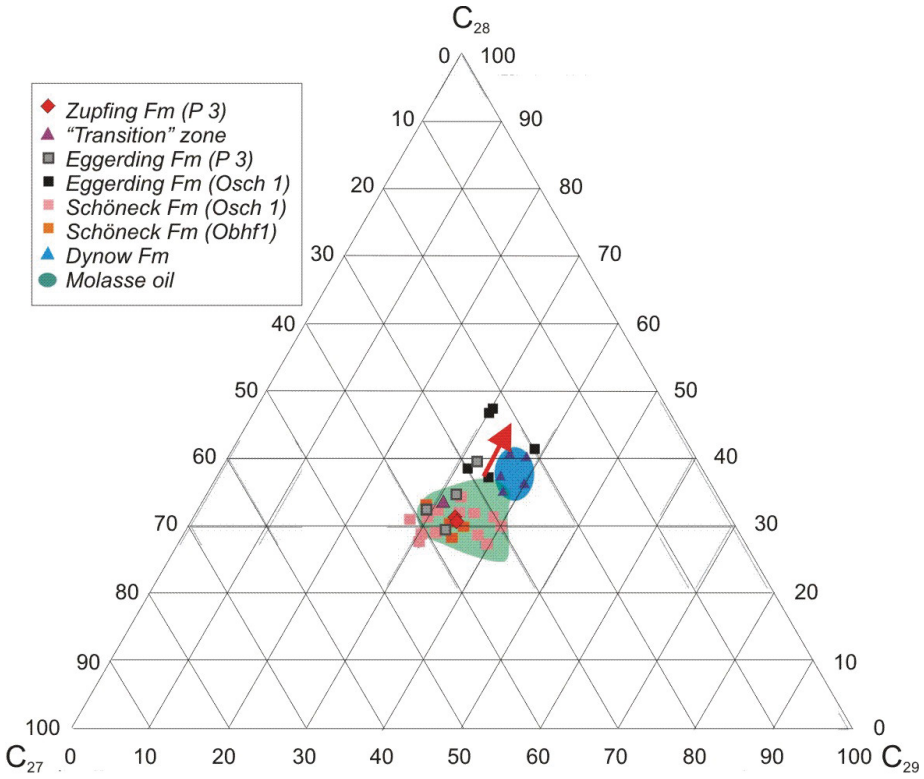

Fig. 86: Ternary diagram of the C_{27}, C_{28} and C_{29} steranes for Schöneck Formation, Dynow Formation and Molasse oil. The red arrow highlights a slight distortion of Molasse oils towards a C_{28}-rich composition.

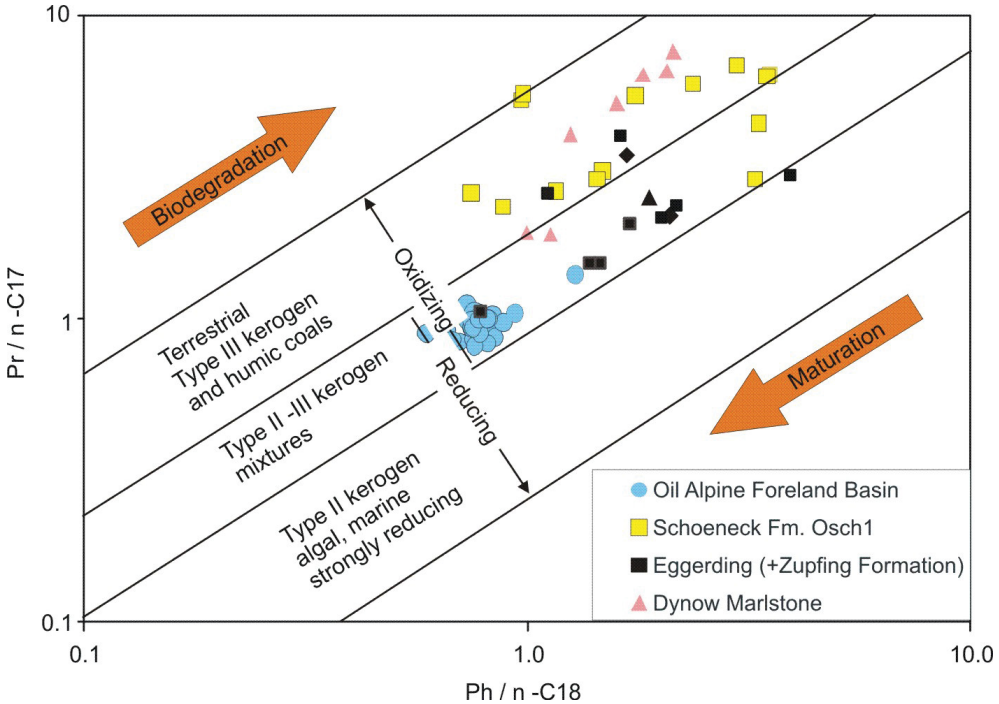

Fig. 87: Crossplot of Pr/*n*- C_{17} versus Ph/ *n*-C_{18}. Only a few samples of the Schöneck Formation match with the Molasse oil. The samples of the Dynow Formation do not correlate with the oil. The samples of the Eggerding Formation instead match surprisingly well with the Molasse oil.

7. Conclusion

The lower Oligocene sediments in the Molasse basin subdivided from bottom to top into Schöneck Formation, Dynow Formation, Eggerding Formation and Zupfing Formation.
The Dynow Formation and the lower part of the Eggerding Formation have been deposited during nannoplankton zone NP 23. No nannoplankton is present in the upper part of the Eggerding Formation. Nannoplankton blooms near the base of the Zupfing Formation are indicative for the NP 24. The Eggerding Formation, therefore, represents the upper part of NP23 and maybe the lowermost part of NP 24. In any case, it is part of the Kiscellian.
The lower part of the Eggerding Formation consists of dark grey laminated shaly marlstone with white bands from which the Eggerding Formation derived its old name ("banded marl"). The white bands are rich in coccolithophorides. The upper part of the Eggerding Formation consists of a homogenous sequence of marly shale and includes about 1.6 % TOC.
The Zupfing Formation consists of clay marl. It is generally low in organic carbon (<1 %), only its lowermost part, several meters thick, contains about 1.5 % TOC. Because this TOC value is similar to that in the Eggerding Formation, this interval is termed "Transition zone". In the DT log the "Transition zone" forms part of the Zupfing Formation.

The Eggerding Formation shows log patterns, which can be traced over the whole study area. Despite of the large E-W extension (~100 km), variances in the log pattern are very small. Consequently, laterally uniform depositional environments can be presumed. The continuity allows determining minor changes from the typical pattern, e.g. it enables to detect parts of the Eggerding Formation, which are missing due to non-deposition or erosion. Furthermore it was possible to date erosion events precisely.

Two major erosion events occurred.

- Erosion in the Trattnach area occurred during deposition of the Eggerding Formation and removed sediments up to 50 m thick.
- Even more important was erosion after deposition of the Eggerding Formation when sediments up to 70 m thick were removed (e.g. Ried area). Moreover, the second event had a wider lateral extent. Erosion was minor in the eastern part of the study area, where a maximum of 12 m of lowermost Zupfing and uppermost Eggerding Formation were removed. Therefore, in this part of the basin, Dynow and Schöneck formations were not affected by erosion.

The results of organic chemical investigation show a very good source rock potential in the lower part of the Eggerding Formation (TOC: 3.2%; HI: 436 mgHC g^{-1}TOC), and a good potential for the upper Eggerding Formation (TOC: 1.65 %; HI: 300 mgHC g^{-1}TOC). Therefore, and because the Eggerding Formation is about 40 m thick, the source potential index (SPI) of the entire Eggerding Formation (0.58 tHC m^{-2}) exceeds the SPI of the Schöneck Formation (0.35 tHC m^{-2}) significantly.
This, and a match of biomarker ratios in rock extracts and Molasse oils, suggests that the contribution of the Eggerding Formation to the formation of the Molasse oil has been underestimated.

8. References

Bachmann, G. H., Müller, M., Weggen, K. (1987). Evolution of the Molasse Basin (Germany, Switzerland). Tectonophysics, 137, 77–92.

Barakat, A.O., Rullkötter, J. (1997). A comparative study of molecular paleosalinity indicators: chromans, tocopherols and C20 isoprenoid thiophenes in Miocene lake sediments (Nördlinger Ries, Southern Germany). Aquatic Geochemistry, 3, 169–190.

Bechtel, A., Reischenbacher, D., Sachsenhofer, R.F., Gratzer, R., Lücke, A. (2007). Paleogeography and paleoecology of the upper Miocene Zillingdorf lignite deposit. Int. J. Coal Geol., 60, 119–143.

Berner, R. A., Raiswell, R. (1983). Burial of organic carbon and pyrite sulfur in sediments over Phanerozoic time: A new theory. Geochimica et Cosmochimica Acta, 47, 862–885.

Berner, R. A., Raiswell, R. (1984). C/S method for distinguishing freshwater from marine sedimentary rocks. Geology 12: 365-368.

Berner, R.A. (1984). Sedimentary pyrite formation: an update. Geochimica et Cosmochimica Acta, 12, 365–368.

Boigk, H. (1981). 4. Alpenvorland. In H. Boigk (Ed.), Erdöl und Erdölgas in der Bundesrepublik Deutschland (pp. 235–284). Stuttgart: Ferdinand Enke.

Bray, E. E., Evans, E. D. (1961). Distribution of *n*-paraffins as a clue to recognition of source beds.*Geochim. Cosmochim. Acta,* 22, 2–15.

Bruch, A. A. (1998). Palynologische Untersuchungen im Oligozän Sloweniens—Paläo-Umwelt und Paläoklima im Ostalpenraum. Tübinger Mikropaläontologische Mitteilungen, 18, 1–193.

Bukry, D. (1974). Coccoliths as paleosalinity indicators: evidence from the Black Sea. American Association of Petroleum Geologists, Memoir, 20, 303–327.

Connan, J. & Cassou, A. M. (1980). Properties of gases and petroleum lipids derived from terrestrial kerogen at various maturation levels. *Geochimica et Cosmochimica Acta,* 44, 1-23.

Demaison, G., Huizinga, B.J. (1994). Genetic classification of petroleum systems using three factors: charge, migration and entrapment. In: Magoon, L.B., Dow, W.G. (eds.) The petroleum system, from source to trap. AAPG Memoir 60, 73-89.

Dohmann, L. (1991). Die unteroligozänen Fischschiefer im Molassebecken. PhD thesis, Ludwig-Maximilian-Universität, Munich.

Espitalie´, J., Laporte, J. L., Madec, M., Marquis, F., Leplat, P., Paulet, J., Boutefeu, A. (1977). Methode rapide de caracterisation des roches meres, de leur potentiel petrolier et de leur degre d'evolution. Revue de l'Institut Francais du Petrole, 32, 23–42.

Friebe, J.G. (1994). Serpulid–bryozoan–foraminiferal biostromes controlled by temperature, climate and reduced salinity. Facies 30, 51–62.

Grantham P.J., Wakefield, L.L. (1988). Vatiations in the sterane carbon number distributions of marine source rock derived crude oils through geological time. *Organic Geochemistry* 12, 61–73.

Gratzer, R., Sachsenhofer, R.F., Bechtel, A., Schulz, H.-M., Smuk, A. (2008) Öl-Öl und Öl-Muttergesteinskorrelation im Alpinen Molassebecken Österreichs. Journal of Alpine Geology, 49, 32-33.

Haq, B., Hardenbol, J., Vail, P. R. (1987). Chronology of fluctuating sea levels since the Triassic (250 million years ago to present) Science, 235, 1156-1167

Harzhauser,M., Piller,W.E. (2004). The Early Sarmatian—hidden seesaw changes. Courier Forschungsinstitut Senckenberg, 246, 89–111.

Hunt, J.M. (1995). Petroleum Geochemistry and Geology, W.H. Freeman and Co., New York.

Jin, J., Aigner, T., Luterbacher, H.P., Bachmann, G.H., Müller, M. (1995). Sequence stratigraphy and depositional history in the southeastern German Molasse Basin. Mar. Pet. Geol., 12, 929–940.

Kollmann, K. (1977). Die Öl- und Gasexploration der Molassezone Oberösterreichs und Salzburgs aus regional-geologischer Sicht. Erdoel- Erdgas Zeitschrift, 74(12), 414–420.

Krhovsky, J., Djurasinovic, M. (1993). The nannofossil chalk layers in the Early Oligocene Stiborice Member in Velke Nemcice (the Menilitic Formation, Zdanice Unit, South Moravia): orbitally forced changes in paleoproductivity. *Knih. Zem. Plyn. Nafta,* 15, 33–53.

Kroh, A. (2007). Climate Changes in the Early to Middle Miocene of the Central Paratethys and the Origin of its Echinoderm Fauna. - Palaeogeography, Palaeoclimatology, Palaeoecology, 253, 185-223.

Langford, F. F., & Blanc-Valleron, M.-M. (1990). Interpreting Rock-Eval pyrolysis data using graphs of pyrolyzable hydrocarbons vs. total organic carbon. American Association of Petroleum Geologists Bulletin, 74, 799–804.

Li, M., Larter, S.R., Taylor, P., Jones, D.M., Bowler, B., Bjorøy, M. (1995). Biomarkers or not biomarkers? A new hypothesis for the origin of pristine involving derivation from methyltrimethyltridecylchromans (MTTCs) formed during early diagenesis from chlorophyll and alkylphenols. Organic Geochemistry, 23, 159–167.

Moldowan, J. M., Seifert, W. K., Gallegos E. J. (1985). Relationship between petroleum composition and depositional environment of petroleum source rocks: AAPG Bulletin, v. 69, 1255-1268.

Nagymarosy, A. (1991). The response of the calcareous nannoplankton to the Earlyv Oligocene separation of the Paratethys, 13, 62, 63

Ourisson, G., Albrecht, P., Rohmer, M. (1979). The hopanoids.Palaeochemistry and biochemistry of a group of natural products. Pure Appl. Chem., 51, 709 -729.

Peters, K. E. (1986). Guidelines for evaluating petroleum source rock using programmed pyrolysis, American Association of Petroleum Geologists, 70, pp. 318–329.

Peters, K.E., Moldowan, J.M. (1993). The Biomarker Guide. Prentice-Hall, Englewood Cliffs, NJ, 363 pp.

Peters, K. E., Fraser, T. H., Amris, W., Rustanto, B., Hermanto, E. (1999). Geochemistry of crude oils from eastern Indonesia. AAPG Bulletin, 83, 1927-1942.

Philp, R.P. (1985). Fossil fuel biomarkers. Applications and spectra, Methods Geochem. Geophys., 23, 1–294.

Piller,W.E., Harzhauser, M. (2005). The myth of the brackish Sarmatian Sea. Terra Nova, 17, 450–455.

Prothero, D. (1994). The Eocene–Oligocene transition—Paradise lost. New York: Columbia University Press.

Radke, M., Willsch, H., Welte, D. H. (1980). Preparative hydrocarbon group type determination by automated medium pressure liquid chromatography. Analytical Chemistry, 52, 406–411.

Rider, M.H. (1996). The Geological Interpretation of Well Logs (2nd ed.): Caithness (Whittles Publishing).

Ricken, W. (1993). Sedimentation as a three component system: organic carbon, carbonate, noncarbonate. Lect. Notes Earth Sci., 51, 211 pp.

Rögl, F. (1996). Stratigraphic correlation of the Paratethys Oligocene and Miocene. In: Decker, K. (Ed.), PAN-CARDI Workshop 1996 — Dynamics of the Pannonian–Carpathian–Dinaride System. Mitteilungen der Gesellschaft der Geologie und Bergbaustudenten Österreichs, vol. 41, 65–74.

Rögl, F., Steininger, F.F. (1983). Vom Zerfall der Tethys zu Mediterran und Paratethys. Annalen des Naturhistorischen Museums in Wien 85/A, 135–163.

Sachsenhofer, R.F., Schulz, H.-M. (2006). Architecture of Lower Oligocene source rocks in the Alpine Foreland Basin: a model for syn- and postdepositional source rock features in the Paratethyan Realm. Petroleum Geoscience 12, 363–377.

Sachsenhofer, R.F., Geissler, M., Mobarakhabad, A. (2008). Source potential of Lower Oligocene rocks in the Hiersdorf area (Upper Austria) - Are cuttings useful for source rock studies? Unpubl. Report for RAG, Leoben, 15 pp.

Schulz, H.-M., Sachsenhofer, R.F., Bechtel, A., Polesny, H., Wagner, L. (2002). Origin of hydrocarbon source rocks in the Austrian Molasse Basin (Eocene–Oligocene transition). Marine and Petroleum Geology 19 (6), 683–709.

Schulz, H.-M., Bechtel, A., Rainer, T., Sachsenhofer, R.F., Struck, U. (2004). Paleoceanography of the western Central Paratethys during nannoplankton zone NP

23 the Dynow Marlstone in the Austrian Molasse Basin. Geologica Carpathica 55 (4), 311 – 323.

Schulz, H.-M., Bechtel, A., Sachsenhofer, R.F. (2005). The birth of the Paratethys during the Early Oligocene: From Tethys to an ancient Black Sea analogue? Global and Planetary Change, 49, 163-176.

Seifert, W. K., Moldowan, J. M. (1986). Use of biological markers in petroleum exploration, in R. B Johns, ed., Methods in Geochemistry and Geophysics, v. 24, 261-290.

Sinninghe Damste´, J.S., Keely, B.J., Betts, S.E., Baas, M., Maxwell, J.R., de Leeuw, J.W. (1993). Variations in abundances and distributions of isoprenoid chromans and longchain alkylbenzenes in sediments of the Mulhouse Basin: a molecular sedimentary record of palaeosalinity. Organic Geochemistry, 20, 1201–1215.

Sissingh, W. (1997). Tectonostratigraphy of the Northern Alpine Foreland Basin: Correlation of Tertiary depositional cycles and orogenic phases. Tectonophysics, 282, 223–256.

Steininger, F., Rögl, F. (1979). The Paratethys history - a contribution towards the Neogene Geodynamics of the Alpine orogene. Ann. Geol. Pays. Hellen., Tome hors serie, fasc. III, 1153-1165, Athens.

Steininger, F.F., Wessely, G. (2000). From the Tethyan Ocean to the Paratethys Sea: Oligocene to Neogene stratigraphy, paleogeography and paleobiogeography of the circum-Mediterranean region and the Oligocene to Neogene Basin evolution in Austria. Mitteilungen der Österreichischen Geologischen Gesellschaft 92 (1999), 95–116.

Švábenická L. (1999). Braarudosphaera-rich sediments in the Turonian of the Bohemian Cretaceous Basin, Czech Republic. Cretaceous Research, 20, 773-782.

Tissot, B.P. and Welte, D.H. (1984). Petroleum Formation and Occurrence, Springer Verlag Heidelberg, 699 pp.

Wagner, L. R. (1980). Geologische Charakteristik der wichtigsten Erdöl und Erdgasträger der oberösterreichischen Molasse. Teil I: Sandsteine des Obereozäns. Erdöl-Erdgas Zeitschrift, 96, 338–346.

Wagner, L. R. (1998). Tectono-stratigraphy and hydrocarbons in the Molasse Foredeep of Salzburg, Upper and Lower Austria. A. Mascle, C. Puigdefa`bregas, H. P. Luterbacher, Geological Society Special Publications, 134, 339–369.

Ziegler, P. A. (1987). Late Cretaceous and Cenozoic intraplate compressionaldeformations in the Alpine foreland. Tectonophysics, 137, 389–420.

Zweigel, J., Aigner, T., Luterbacher, H. (1998). Eustatic versus tectonic controls on Alpine foreland basin fill: sequence stratigraphy and subsidence analysis in the SE-German Molasse.-in: Muscle, A. (ed.): Cenozoic foreland basins of Western Europe- Geol. Soc. Lond. Spec. Publ.

9. APPENDIX

APPENDIX I – sample list

Samples studied within the frame of the present study.
Sample list with sample code, depth, core number, Formation, and used analysis. Wells are arranged from bottom to top (and not necessarily according to sample number).

APPENDIX I (cont´d)- Samples studied within the frame of the present study.

Sample code	Depth (m)	Core	Formation	Leco	Rock -Eval	Biomarker	Nannoflora
Eggerding 2							
Egdg 73	566.02	2	Eggerding	x	x		
Egdg 74	565.79	2	Eggerding	x	x		
Egdg 75	565.00	2	Eggerding	x	x		
Egdg 76	564.91	2	Eggerding	x	x		
Egdg 77	563.82	2	Eggerding	x	x		
Egdg 78	562.70	1	Eggerding	x	x		
Egdg 79	561.70	1	Eggerding	x	x		
Egdg 80	560.70	1	Eggerding	x	x		
Egdg 81	559.70	1	Eggerding	x	x		
Egdg 82	558.70	1	Eggerding	x	x		
Egdg 83	557.65	1	Eggerding	x	x		x
Egdg 84	556.65	1	Eggerding	x	x		
Egdg 85	555.65	1	Eggerding	x	x		x
Egdg 86	554.65	1	Eggerding	x	x		
Egdg 87	553.65	1	Eggerding	x	x		x
Oberschauersberg 1							
Osch 59	1371.98	2	Eggerding	x	x	x	
Osch 60	1371.52	2	Eggerding	x	x		x
Osch 61	1371.22	2	Eggerding	x	x	x	x
Osch 62	1370.95	2	Eggerding	x	x		
Osch 63	1370.69	2	Eggerding	x	x		x
Osch 64	1370.45	2	Eggerding	x	x		x
Osch 65	1370.20	2	Eggerding	x	x	x	
Osch 66	1369.90	2	Eggerding	x	x		x
Osch 67	1369.65	2	Eggerding	x	x		
Osch 68	1369.17	2	Eggerding	x	x	x	x
Osch 70	1368.96	2	Eggerding	x	x		
Osch 71	1368.50	2	Eggerding	x	x		x
Osch 72	1368.00	2	Eggerding	x	x	x	x
Voitsdorf 1							
V 45	2021	1	Eggerding	x	x		
V 46	2020	1	Eggerding	x	x		
V 47	2019	1	Eggerding	x	x		
V 48	2018	1	Eggerding	x	x		
V 49	2017	1	Eggerding	x	x		
V 50	2016	1	Eggerding	x	x		
V 51	2015	1	Eggerding	x	x		
V 52	2014	1	"Transition Zone"	x	x		
V 53	2013	1	"Transition Zone"	x	x		
V 54	2012	1	"Transition Zone"	x	x		
V 55	2011	1	"Transition Zone"	x	x		
V 56	2010	1	"Transition Zone"	x	x		
V 57	2009	1	"Transition Zone"	x	x		
V 58	2008	1	Zupfing	x	x		

APPENDIX I (cont´d) - Samples studied within the frame of the present study.

Sample code	Depth (m)	Core	Formation	Leco	Rock -Eval	Biomarker	Nannoflora
Puchkirchen 3							
P 1	2655.5	3	Dynow	x	x		
P 2	2655.0	3	Eggerding	x	x	x	
P 3	2654.0	3	Eggerding	x	x		x
P 4	2653.0	3	Eggerding	x	x		x
P 5	2652.0	3	Eggerding	x	x		x
P 6	2651.0	3	Eggerding	x	x		x
P 7	2650.0	3	Eggerding	x	x	x	x
P 8	2649.0	3	Eggerding	x	x		x
P 9	2648.0	3	Eggerding	x	x	x	x
P 10	2647.0	3	Eggerding	x	x		x
P 11	2646.0	2	Eggerding	x	x		x
P 12	2645.0	2	Eggerding	x	x		x
P 13	2644.0	2	Eggerding	x	x		x
P 14	2643.0	2	Eggerding	x	x		x
P 15	2642.0	2	Eggerding	x	x	x	x
P 16	2641.0	2	"Transition Zone"	x	x		x
P 17	2640.0	2	"Transition Zone"	x	x	x	x
P 18	2639.0	2	"Transition Zone"	x	x		x
P 19	2638.0	2	Zupfing	x	x		x
P 20	2637.0	2	Zupfing	x	x		
P 21	2636.0	2	Zupfing	x	x		x
P 22	2635.0	2	Zupfing	x	x		x
P 23	2634.0	2	Zupfing	x	x		
P 24	2633.0	2	Zupfing	x	x		
P 25	2632.5	2	Zupfing	x	x		
P 26	2628.0	1	Zupfing	x	x		x
P 27	2627.0	1	Zupfing	x	x		
P 28	2626.0	1	Zupfing	x	x		x
P 29	2625.0	1	Zupfing	x	x		
P 30	2624.0	1	Zupfing	x	x	x	x
P 31	2623.0	1	Zupfing	x	x		
P 32	2622.0	1	Zupfing	x	x		
P 33	2621.0	1	Zupfing	x	x		
P 34	2620.0	1	Zupfing	x	x		
P 35	2619.0	1	Zupfing	x	x		
P 36	2618.0	1	Zupfing	x	x		x
P 37	2617.0	1	Zupfing	x	x		
P 38	2616.0	1	Zupfing	x	x		x
P 39	2615.0	1	Zupfing	x	x		x
P 40	2614.0	1	Zupfing	x	x		x
P 41	2613.0	1	Zupfing	x	x	x	
P 42	2612.0	1	Zupfing	x	x		x
P 43	2611.0	1	Zupfing	x	x		
P 44	2610.0	1	Zupfing	x	x		

APPENDIX I (cont´d) – Samples (cuttings) studied within the frame of the present study (Sachsenhofer, 2008).

Sample	Depth (m)	Formation	Leco	Rock -Eval
Hiersdorf 5				
	2436	Eocene	x	x
	2435	Eocene	x	x
	2434	Eocene	x	x
	2433	Eocene	x	x
	2432	Schöneck	x	x
	2431	Schöneck	x	x
	2430	Schöneck	x	x
	2429	Schöneck	x	x
	2428	Schöneck	x	x
	2427	Schöneck	x	x
	2426	Schöneck	x	x
	2425	Schöneck	x	x
	2424	Dynow	x	x
	2423	Dynow	x	x
	2422	Dynow	x	x
	2421	Dynow	x	x
	2420	Dynow	x	x
	2419	Eggerding	x	x
	2418	Eggerding	x	x
	2417	Eggerding	x	x
	2416	Eggerding	x	x
	2415	Eggerding	x	x
	2414	Eggerding	x	x
	2413	Eggerding	x	x
	2412	Eggerding	x	x
	2411	Eggerding	x	x
	2410	Eggerding	x	x
	2409	Eggerding	x	x
	2408	Eggerding	x	x
	2407	Eggerding	x	x
	2406	Eggerding	x	x
	2405	Eggerding	x	x
	2404	Eggerding	x	x
	2403	Eggerding	x	x
	2402	Eggerding	x	x
	2401	Eggerding	x	x
	2400	Eggerding	x	x
	2399	Eggerding	x	x
	2398	Eggerding	x	x
	2397	Eggerding	x	x
	2396	Eggerding	x	x
	2395	Eggerding	x	x
	2394	Eggerding	x	x
	2393	Eggerding	x	x
	2391	Eggerding	x	x
	2390	Eggerding	x	x
	2389	Eggerding	x	x

Sample	Depth (m)	Formation	Leco	Rock -Eval
Hiersdorf 5				
	2388	Eggerding	x	x
	2387	Eggerding	x	x
	2386	Eggerding	x	x
	2385	Eggerding	x	x
	2384	Eggerding	x	x
	2383	Eggerding	x	x
	2382	Eggerding	x	x
	2381	Eggerding	x	x
	2380	Eggerding	x	x
	2379	Eggerding	x	x
	2378	Eggerding	x	x
	2377	Eggerding	x	x
	2376	"Transition zone"	x	x
	2375	"Transition zone"	x	x
	2374	"Transition zone"	x	x
	2373	"Transition zone"	x	x
	2372	"Transition zone"	x	x
	2371	"Transition zone"	x	x
	2370	"Transition zone"	x	x
	2369	"Transition zone"	x	x
	2367	Zupfing	x	x
	2366	Zupfing	x	x
	2365	Zupfing	x	x
	2364	Zupfing	x	x
	2363	Zupfing	x	x
	2362	Zupfing	x	x
	2361	Zupfing	x	x
	2360	Zupfing	x	x
	2359	Zupfing	x	x
	2358	Zupfing	x	x
	2357	Zupfing	x	x
	2356	Zupfing	x	x
	2355	Zupfing	x	x
	2354	Zupfing	x	x
	2353	Zupfing	x	x
	2352	Zupfing	x	x
	2351	Zupfing	x	x
	2350	Zupfing	x	x
	2345	Zupfing	x	x
	2340	Zupfing	x	x
	2335	Zupfing	x	x
	2330	Zupfing	x	x
	2325	Zupfing	x	x
	2320	Zupfing	x	x
	2315	Zupfing	x	x
	2310	Zupfing	x	x
	2305	Zupfing	x	x

APPENDIX II – bulk organic chemistry

Analytical data: Samples studied within the frame of the present study.
Sample number, depth and analytical results (S1, S2, HI, OI, Tmax, S1+S2, C TOC, TIC, S and TOC/S; for explanation see table below).

Abbreviations:

Calcite equiv.	Calcite equivalent = (C-TOC)*8.34 [wt%]
S1	Free and adsorbed hydrocarbons [mg HC/g rock]
S2	Hydrocarbons generated during pyrolysis [mg HC/g rock]
HI	Hydrogen Index = (S2*100)/TOC [mg HC/g TOC]
OI	Oxygen Index = (100*S3)/TOC [mg HC/g TOC]
Tmax	temperature at which the S2 generation peak occurs [C°]
S1 + S2	Genetic potential in [mg HC/g TOC]
C	Total carbon content
TOC	Total Organic Carbon [%]
TIC	Total Inorganic Carbon [%]
S	Sulphur [%]
TOC/S	Organic carbon / Sulphur ratio

APPENDIX II (cont´d) - Analytical data: Samples studied within the frame of the present study.

Eggerding 2 ***Rock Eval pyrolysis***

Sample nr.	Depth (m)	S1	S2	HI	OI	Tmax	S1+S2
73	566.02	0.99	15.8	436.2	17.8	406	16.8
74	565.79	0.22	1.8	109.0	35.3	399	2.1
75	565.00	0.16	1.2	117.8	31.2	407	1.4
76	564.91	0.12	0.6	104.9	56.1	402	0.8
77	563.82	0.18	1.6	309.0	35.0	403	1.8
78	562.70	0.68	6.2	177.7	30.7	402	6.9
79	561.70	0.23	1.9	106.6	35.3	402	2.1
80	560.70	0.14	1.2	321.4	54.1	400	1.4
81	559.70	0.81	6.3	260.7	25.3	401	7.1
82	558.70	0.29	3.1	159.9	24.7	404	3.4
83	557.65	0.37	3.5	173.8	23.4	402	3.9
84	556.65	0.27	3.7	178.8	25.2	412	3.9
85	555.65	0.38	3.6	191.7	28.3	404	3.9
86	554.65	0.26	5.1	239.3	22.7	420	5.4
87	553.65	0.36	6.4	304.3	29.7	421	6.8

Eggerding 2 ***Leco analysis***

Sample nr.	Depth (m)	C %	TOC %	TIC %	S %	TOC / S
73	566.02	4.43	3.62	0.81	3.32	1.1
74	565.79	1.34	1.37	-0.04	3.33	0.4
75	565.00	0.84	0.85	-0.01	1.39	0.6
76	564.91	1.08	1.09	-0.01	4.86	0.2
77	563.82	1.23	1.23	0.00	2.01	0.6
78	562.70	2.37	2.30	0.08	2.51	0.9
79	561.70	1.46	1.57	-0.11	1.79	0.9
80	560.70	1.15	1.16	-0.02	1.60	0.7
81	559.70	2.40	2.41	-0.01	2.66	0.9
82	558.70	1.99	1.96	0.03	1.71	1.1
83	557.65	2.08	2.03	0.05	2.01	1.0
84	556.65	2.24	2.05	0.19	1.74	1.2
85	555.65	1.91	1.85	0.06	1.93	1.0
86	554.65	2.65	2.13	0.51	1.83	1.2
87	553.65	2.68	2.12	0.56	2.80	0.8

APPENDIX II (cont´d) - Analytical data: Samples studied within the frame of the present study.

Oberschauersberg 1		***Rock Eval pyrolysis***					
Sample nr.	*Depth (m)*	*S1*	*S2*	*HI*	*OI*	*Tmax*	*S1+S2*
59	1371.98	0.37	13.76	458.8	8.3	423	14.1
60	1371.52	0.43	12.51	359.3	10.5	420	12.9
61	1371.22	0.62	19.68	575.9	8.7	424	20.3
62	1370.95	0.26	10.37	416.5	9.6	425	10.6
63	1370.69	0.20	6.62	297.4	9.9	419	6.8
64	1370.45	0.74	20.48	518.2	12.8	418	21.2
65	1370.20	0.42	12.53	434.5	13.4	423	12.9
66	1369.90	0.16	6.06	325.0	14.5	425	6.2
67	1369.65	0.19	8.16	386.0	9.7	431	8.3
68	1369.17	2.10	34.64	578.3	9.8	421	36.7
70	1368.96	1.84	32.22	549.2	8.5	418	34.1
71	1368.50	0.40	10.64	424.2	15.0	423	11.0
72	1368.00	0.20	6.11	347.8	12.8	431	6.3

Oberschauersberg1		***Leco analysis***				
Sample nr.	*Depth (m)*	*C %*	*TOC %*	*TIC %*	*S %*	*TOC / S*
59	1371.98	3.59	3.00	0.59	2.64	1.1
60	1371.52	3.76	3.48	0.28	1.65	2.1
61	1371.22	5.38	3.56	1.82	1.78	2.0
62	1370.95	3.11	2.49	0.62	1.34	1.9
63	1370.69	2.38	2.22	0.16	1.25	1.8
64	1370.45	5.91	3.95	1.96	3.67	1.1
65	1370.20	4.91	2.88	2.03	2.18	1.3
66	1369.90	2.95	1.86	1.08	1.03	1.8
67	1369.65	2.49	2.11	0.38	1.30	1.6
68	1369.17	8.01	5.99	2.02	3.33	1.8
70	1368.96	7.04	5.87	1.17	3.62	1.6
71	1368.50	4.55	2.51	2.04	1.98	1.3
72	1368.00	2.63	1.87	0.76	1.31	1.4

APPENDIX II (cont´d) - Analytical data: Samples studied within the frame of the present study.

Voitsdorf 1		***Rock Eval pyrolysis***					
Sample nr.	*Depth (m)*	*S1*	*S2*	*HI*	*OI*	*Tmax*	*S1+S2*
45	2021	0.29	4.70	290.5	11.4	429	5.0
46	2020	0.31	4.51	277.7	14.5	429	4.8
47	2019	0.53	9.21	382.1	12.9	426	9.7
48	2018	0.38	6.37	330.0	13.7	429	6.7
49	2017	0.20	3.11	233.2	15.4	429	3.3
50	2016	0.24	3.18	234.9	20.3	432	3.4
51	2015	0.51	7.80	369.6	19.2	426	8.3
52	2014	0.52	5.90	364.6	20.4	427	6.4
53	2013	0.23	3.84	285.7	25.7	431	4.1
54	2012	0.39	4.40	303.5	24.5	428	4.8
55	2011	0.24	4.26	278.5	21.9	430	4.5
56	2010	0.38	4.89	303.1	25.1	425	5.3
57	2009	0.40	5.63	338.8	30.1	427	6.0
58	2008	0.10	0.87	141.3	148.6	435	1.0

Voitsdorf 1		***Leco analysis***				
Sample nr.	*Depth (m)*	*C %*	*TOC %*	*TIC %*	*S %*	*TOC / S*
45	2021	2.36	1.62	0.74	1.59	1.0
46	2020	2.41	1.62	0.79	2.15	0.8
47	2019	3.02	2.41	0.61	2.52	1.0
48	2018	2.58	1.93	0.65	1.95	1.0
49	2017	1.71	1.33	0.38	1.74	0.8
50	2016	1.94	1.35	0.58	1.63	0.8
51	2015	3.15	2.11	1.04	2.57	0.8
52	2014	5.56	1.62	3.94	1.80	0.9
53	2013	3.43	1.34	2.08	1.67	0.8
54	2012	5.41	1.45	3.96	1.83	0.8
55	2011	3.33	1.53	1.81	1.76	0.9
56	2010	4.65	1.61	3.04	1.93	0.8
57	2009	6.14	1.66	4.48	1.37	1.2
58	2008	4.68	0.61	4.07	2.00	0.3

APPENDIX II (cont´d) - Analytical data: Samples studied within the frame of the present study.

Puchkirchen 3		***Rock Eval pyrolysis***					
Sample nr.	*Depth (m)*	*S1*	*S2*	*HI*	*OI*	*Tmax*	*S1+S2*
1	2655.5	0.13	0.41	155.0	63.1	425	0.5
2	2655.0	0.47	2.97	246.5	25.7	428	3.4
3	2654.0	0.79	5.16	321.3	21.5	429	6.0
4	2653.0	0.46	3.22	262.4	20.0	429	3.7
5	2652.0	0.53	5.55	347.8	14.4	427	6.1
6	2651.0	0.39	3.98	299.2	13.6	433	4.4
7	2650.0	0.47	4.97	330.2	11.0	429	5.4
8	2649.0	0.28	2.65	227.4	20.6	431	2.9
9	2648.0	0.78	8.92	388.5	16.1	427	9.7
10	2647.0	0.37	3.43	276.6	13.7	430	3.8
11	2646.0	0.33	3.02	241.5	17.6	431	3.3
12	2645.0	0.38	3.51	249.5	19.9	429	3.9
13	2644.0	1.07	9.59	397.4	8.5	427	10.7
14	2643.0	0.21	1.63	177.0	9.8	434	1.8
15	2642.0	0.74	8.59	401.0	36.9	430	9.3
16	2641.0	0.42	3.33	275.5	17.8	431	3.7
17	2640.0	0.65	5.56	340.2	13.5	428	6.2
18	2639.0	0.45	5.08	321.4	16.5	431	5.5
19	2638.0	0.13	0.53	105.8	20.1	433	0.7
20	2637.0	0.18	1.94	194.6	11.5	431	2.1
21	2636.0	0.12	1.12	140.9	18.3	430	1.2
22	2635.0	0.17	1.13	131.4	28.6	434	1.3
23	2634.0	0.16	1.55	178.7	7.8	429	1.7
24	2633.0	0.19	0.97	126.0	29.9	426	1.2
25	2632.5	0.32	3.11	263.5	15.3	429	3.4
26	2628.0	0.23	2.59	226.4	12.2	428	2.8
27	2627.0	0.14	1.24	145.7	17.1	433	1.4
28	2626.0	0.13	1.15	140.1	14.0	433	1.3
29	2625.0	0.12	0.77	106.1	19.4	427	0.9
30	2624.0	0.17	1.17	126.1	16.0	427	1.3
31	2623.0	0.11	0.64	95.7	21.1	426	*0.7*
32	2622.0	0.10	0.74	106.9	19.6	434	0.8
33	2621.0	0.14	0.83	108.8	32.3	431	1.0
34	2620.0	0.13	0.83	118.2	31.3	429	1.0
35	2619.0	0.16	1.49	160.7	26.5	435	1.6
36	2618.0	0.10	0.83	110.8	32.0	434	0.9
37	2617.0	0.16	1.37	164.4	34.9	432	1.5
38	2616.0	0.19	1.92	199.6	16.9	426	2.1
39	2615.0	0.24	1.94	200.6	22.2	427	2.2
40	2614.0	0.17	1.73	186.7	15.7	431	1.9
41	2613.0	0.21	2.25	220.1	21.6	428	2.5
42	2612.0	0.11	1.21	144.8	23.9	434	1.3
43	2611.0	0.14	1.18	152.3	15.7	432	1.3
44	2610.0	0.13	0.85	120.5	30.5	431	1.0

APPENDIX II (cont´d) - Analytical data: Samples studied within the frame of the present study.

Puchkirchen 3		***Leco analysis***				
Sample nr.	*Depth (m)*	*C %*	*TOC %*	*TIC %*	*S %*	*TOC / S*
1	2655.5	10.36	0.26	10.10	0.57	0.5
2	2655.0	2.22	1.20	1.02	2.31	0.5
3	2654.0	2.46	1.61	0.85	2.51	0.6
4	2653.0	2.17	1.23	0.94	2.46	0.5
5	2652.0	3.07	1.59	1.48	1.74	0.9
6	2651.0	2.69	1.33	1.36	1.60	0.8
7	2650.0	3.01	1.51	1.51	1.75	0.9
8	2649.0	2.53	1.17	1.37	1.78	0.7
9	2648.0	3.56	2.29	1.27	2.11	1.1
10	2647.0	2.30	1.24	1.06	1.90	0.7
11	2646.0	2.47	1.25	1.22	1.87	0.7
12	2645.0	2.43	1.41	1.03	2.07	0.7
13	2644.0	2.86	2.41	0.45	2.81	0.9
14	2643.0	1.78	0.92	0.86	1.96	0.5
15	2642.0	3.23	2.14	1.09	1.97	1.1
16	2641.0	4.54	1.21	3.33	1.57	0.8
17	2640.0	5.68	1.63	4.04	2.02	0.8
18	2639.0	5.28	1.58	3.70	1.45	1.1
19	2638.0	4.86	0.55	4.31	1.84	0.3
20	2637.0	3.86	1.00	2.86	0.87	1.1
21	2636.0	3.53	0.79	2.74	0.80	1.0
22	2635.0	4.11	0.86	3.25	1.19	0.7
23	2634.0	3.19	0.90	2.29	1.47	0.6
24	2633.0	4.61	0.77	3.84	1.53	0.5
25	2632.5	5.00	1.18	3.83	1.57	0.8
26	2628.0	4.02	1.14	2.88	1.88	0.6
27	2627.0	3.94	0.85	3.09	1.81	0.5
28	2626.0	3.63	0.82	2.80	0.79	1.0
29	2625.0	4.76	0.72	4.04	1.36	0.5
30	2624.0	4.11	0.87	3.24	1.65	0.5
31	2623.0	4.02	0.66	3.36	1.69	0.4
32	2622.0	4.10	0.69	3.41	1.18	0.6
33	2621.0	4.17	0.76	3.41	1.88	0.4
34	2620.0	4.13	0.70	3.43	2.15	0.3
35	2619.0	4.46	0.92	3.53	1.18	0.8
36	2618.0	4.68	0.75	3.93	0.96	0.8
37	2617.0	4.92	0.83	4.09	1.20	0.7
38	2616.0	4.06	1.01	3.05	1.24	0.8
39	2615.0	4.04	0.97	3.07	1.83	0.5
40	2614.0	3.72	0.92	2.80	1.81	0.5
41	2613.0	4.63	1.02	3.61	1.32	0.8
42	2612.0	3.63	0.84	2.80	1.36	0.6
43	2611.0	3.97	0.83	3.15	1.03	0.8
44	2610.0	3.78	0.71	3.08	1.31	0.5

APPENDIX II (cont´d) - Analytical data: Samples studied within the frame of the present study.

Hiersdorf 5		Rock Eval pyrolysis					Leco analysis	
Sample	Depth (m)	S1	S2	HI	Tmax	S1+S2	TOC %	TIC %
	2436	0.15	0.55	123.1	426	0.7	0.45	8.89
	2435	0.08	0.36	94.0	431	0.4	0.38	10.59
	2434	0.37	1.49	157.6	423	1.9	0.95	8.57
	2433	0.24	0.91	160.4	426	1.2	0.57	9.86
	2432	0.70	6.79	376.2	424	7.5	1.80	4.91
	2431	1.14	12.69	452.5	427	13.8	2.80	5.59
	2430	1.34	14.58	409.1	422	15.9	3.56	4.93
	2429	1.19	11.32	391.2	424	12.5	2.89	6.81
	2428	1.93	18.76	486.8	430	20.7	3.86	4.00
	2427	1.28	12.00	409.7	423	13.3	2.93	6.29
	2426	1.25	13.81	417.5	429	15.1	3.37	5.07
	2425	1.94	24.90	478.1	431	26.8	5.29	1.09
	2424	1.62	5.26	362.0	425	6.9	1.45	8.94
	2423	0.45	3.74	312.4	429	4.2	1.20	7.37
	2422	0.24	2.53	278.3	432	2.8	0.91	7.56
	2421	0.40	3.61	317.0	430	4.0	1.14	7.36
	2420	0.44	5.58	346.5	429	6.0	1.61	5.94
	2419	0.52	7.44	356.9	424	8.0	2.08	1.17
	2418	0.90	9.06	363.9	425	10.0	2.49	1.30
	2417	0.56	5.49	284.0	423	6.1	1.93	1.44
	2416	0.68	8.00	385.4	426	8.7	2.08	2.65
	2415	0.33	3.94	255.1	430	4.3	1.54	1.11
	2414	0.36	4.44	269.2	428	4.8	1.65	1.32
	2413	0.58	6.65	332.5	427	7.2	2.00	1.71
	2412	0.34	3.40	230.0	430	3.7	1.48	1.11
	2411	0.26	3.46	239.5	429	3.7	1.44	0.89
	2410	0.34	4.09	276.9	430	4.4	1.48	0.46
	2409	0.47	4.86	289.4	427	5.3	1.68	1.74
	2408	0.25	3.50	274.3	429	3.8	1.28	0.82
	2407	0.36	4.62	276.4	421	5.0	1.63	0.91
	2406	0.26	3.89	280.0	431	4.2	1.39	0.63
	2405	0.38	3.59	241.1	425	4.0	1.49	0.88
	2404	0.42	4.06	248.1	424	4.5	1.64	0.84
	2403	0.48	3.03	199.3	426	3.5	1.52	1.41
	2402	0.46	3.18	219.9	426	3.6	1.45	1.38
	2401	0.16	1.42	136.0	428	1.6	1.04	2.81
	2400	0.46	3.43	222.7	423	3.9	1.54	1.06
	2399	0.63	4.75	273.3	426	5.4	1.74	1.12
	2398	0.90	10.46	370.7	424	11.4	2.82	1.00
	2397	0.52	3.78	229.0	424	4.3	1.65	1.01
	2396	0.45	3.57	240.8	426	4.0	1.48	1.26
	2395	0.34	2.82	207.2	428	3.2	1.31	1.15
	2394	0.34	3.83	250.3	423	4.2	1.53	1.14
	2393	0.32	2.49	197.0	429	2.8	1.26	1.50
	2391	0.55	3.36	217.6	428	3.9	1.54	0.89
	2390	0.31	3.98	269.9	427	4.3	1.47	0.99
	2389	0.39	4.19	261.7	426	4.6	1.60	0.88

APPENDIX II (cont´d) - Analytical data: Samples studied within the frame of the present study.

Hiersdorf 5		Rock Eval pyrolysis					Leco analysis	
Sample	Depth (m)	S1	S2	HI	Tmax	S1+S2	TOC %	TIC %
	2388	0.32	4.28	269.1	429	4.6	1.59	0.81
	2387	0.49	5.77	285.3	426	6.3	2.02	0.59
	2386	0.48	3.17	217.7	423	3.7	1.46	1.75
	2385	0.54	3.96	254.0	424	4.5	1.56	1.81
	2384	0.41	3.87	257.7	422	4.3	1.49	1.22
	2383	0.37	2.71	193.4	427	3.1	1.40	0.69
	2382	0.25	2.52	206.7	426	2.8	1.22	0.91
	2381	0.26	2.26	194.6	429	2.5	1.16	1.05
	2380	0.47	4.41	265.8	425	4.9	1.66	0.93
	2379	0.40	5.14	300.6	424	5.5	1.71	0.97
	2378	0.31	3.36	237.1	425	3.7	1.42	1.29
	2377	0.55	6.48	320.1	423	7.0	2.02	1.67
	2376	0.37	4.34	321.1	425	4.7	1.35	5.02
	2375	0.24	2.86	236.5	429	3.1	1.23	3.15
	2374	0.25	3.04	253.3	430	3.3	1.20	3.31
	2373	0.39	3.41	257.4	426	3.8	1.32	3.28
	2372	0.71	8.54	390.6	420	9.3	2.16	2.88
	2371	0.43	5.18	317.9	428	5.6	1.63	3.57
	2370	0.39	4.33	285.2	426	4.7	1.52	3.67
	2369	0.44	5.54	344.5	421	6.0	1.61	4.32
	2367	0.16	0.94	117.9	428	1.1	0.80	3.26
	2366	0.11	0.66	115.0	427	0.8	0.56	3.81
	2365	0.18	1.34	132.1	428	1.5	1.01	2.81
	2364	0.19	1.39	128.8	427	1.6	1.09	2.61
	2363	0.11	1.25	144.2	430	1.4	0.87	2.87
	2362	0.22	1.43	158.9	426	1.7	0.90	3.16
	2361	0.23	2.45	198.3	425	2.7	1.24	3.01
	2360	0.15	1.01	123.3	433.5	1.2	0.82	3.17
	2359	0.18	1.86	172.9	432	2.0	1.08	2.94
	2358	0.14	1.26	120.5	430	1.4	1.05	2.76
	2357	0.19	2.18	176.2	427	2.4	1.24	2.06
	2356	0.14	1.25	135.1	429	1.4	0.90	2.14
	2355	0.25	2.54	199.0	422	2.8	1.28	2.58
	2354	0.18	1.62	159.6	424	1.8	1.01	2.12
	2353	0.23	2.19	180.5	431	2.4	1.23	1.74
	2352	0.51	3.10	191.3	428	3.6	1.62	1.28
	2351	0.19	2.64	194.4	432	2.8	1.35	2.52
	2350	0.27	2.89	212.1	430	3.2	1.36	2.95
	2345	0.39	2.60	189.3	428	3.0	1.37	2.84
	2340	0.25	2.08	189.3	429	2.3	1.15	3.30
	2335	0.30	2.06	171.6	426	2.4	1.20	3.26
	2330	0.25	1.99	185.6	429	2.2	1.07	3.23
	2325	0.28	2.26	180.7	428	2.5	1.25	3.18
	2320	0.23	1.43	140.3	428	1.7	1.03	3.25
	2315	0.22	1.96	177.9	428	2.2	1.04	3.87
	2310	0.20	1.61	156.2	425	1.8	1.04	3.09
	2305	0.18	1.04	124.6	425	1.2	0.83	3.00

APPENDIX III – biomarker analysis

Organic-geochemical parameters for facies characterisation, oil-source rock correlation and maturity assessment: Formation, sample code, depth and analytical results

Abbreviations:

Aliphatic HC	Saturated Hydrocarbons [wt. % (rock)]
Aromatic HC	Aromatized Hydrocarbons [wt. % (rock)]
Asphaltene	Asphaltenes [wt. % (rock)]
n-$C_{15\text{-}31}$	Normal Alkane series
CPI	Carbon Preference Index
Pr	Pristane
Ph	Phytane
Ts/Tm	18α (H)-Trisnorneohopane/17α (H)-Trisnorhopane
DBT	Dibenzothiophene
Ph	Phenanthrene
MPh	Methylphenanthrene
MPI 1	Methylphenanthrene Index
Rc	Calculated Vitrinite Reflectance [%]

APPENDIX III (cont´d) - Organic-geochemical results of samples investigated for facies characterisation, oil-source rock correlation and maturity assessment.

FORMATION	*SAMPLE*	*DEPTH (m)*	*Aliphaten HC (wt.%)*	*Aromatic HC (wt.%)*	*Asphaltene (wt.%)*
Zupfing Fm	P41	2613	0.007	0.009	0.002
Zupfing Fm	P30	2624	0.001	0.001	0.003
"Transition zone"	P17	2640	0.018	0.012	0.004
upper Eggerding Fm	P15	2642	0.018	0.008	0.005
upper Eggerding Fm	P 9	2648	0.053	0.020	0.007
upper Eggerding Fm	P 7	2650	0.023	0.010	0.005
upper Eggerding Fm	P 2	2655	0.015	0.004	0.007
lower Eggerding Fm	Osch 72	1368	0.014	0.009	0.005
lower Eggerding Fm	Osch 68	1369.17	0.054	0.036	0.009
lower Eggerding Fm	Osch 65	1370.2	0.002	0.019	0.008
lower Eggerding Fm	Osch 61	1371.22	0.020	0.020	0.008
lower Eggerding Fm	Osch 59	1371.98	0.018	0.014	0.007

FORMATION	*SAMPLE*	*n-C $_{15-19}$ / n-Alkanes*	*n-C $_{21-25}$ / n-Alkanes*	*n-C $_{27-31}$ / n-Alkanes*	*CPI*	*Pr / n-C $_{17}$*	*Ph / n-C $_{18}$*	*Pr / Ph*
Zupfing Fm	P41	0.21	0.32	0.34	1.32	3.59	1.67	1.38
Zupfing Fm	P30	0.12	0.31	0.43	1.07	2.29	2.09	0.86
"Transition zone"	P17	0.19	0.34	0.34	1.14	2.65	1.88	1.10
upper Eggerding Fm	P15	0.21	0.30	0.38	1.13	2.10	1.71	1.26
upper Eggerding Fm	P 9	0.10	0.47	0.27	1.19	1.54	1.49	0.96
upper Eggerding Fm	P 7	0.15	0.35	0.37	1.18	1.54	1.47	1.08
upper Eggerding Fm	P 2	0.12	0.33	0.41	0.78	1.07	0.79	0.88
lower Eggerding Fm	Osch 72	0.16	0.31	0.43	2.00	2.63	1.11	1.25
lower Eggerding Fm	Osch 68	0.19	0.34	0.33	1.20	3.03	3.95	0.61
lower Eggerding Fm	Osch 65	0.10	0.35	0.43	1.87	2.41	2.18	0.89
lower Eggerding Fm	Osch 61	0.19	0.28	0.38	0.59	2.18	2.02	1.19
lower Eggerding Fm	Osch 59	0.13	0.25	0.53	2.41	4.11	1.63	2.32

SATURATED ACYCLIC HYDROCARBONS

APPENDIX III (cont´d) - Organic-geochemical results of samples investigated for facies characterisation, oil-source rock correlation and maturity assessment.

FORMATION	*SAMPLE*	C_{27} *-Sterane / Steranes*	C_{28} *-Sterane / Steranes*	C_{29} *-Sterane / Steranes*	C_{27} *Diasterane / Sterane*	*20S/(20S+20R) αααC* $_{29}$ *-Steranes*	*20Rαββ /20Rααα C* $_{29}$ *-Steranes*	*20S/20Rααα C* $_{29}$ *-Steranes*
Zupfing Fm	P41	0.35	0.31	0.34	0.32	0.19	0.35	0.24
Zupfing Fm	P30	0.35	0.31	0.33	0.45	0.16	0.14	0.19
"Transition zone"	P17	0.35	0.34	0.31	0.30	0.22	0.37	0.28
upper Egdg Fm	P15	0.33	0.35	0.32	0.32	0.21	0.41	0.26
upper Egdg Fm	P 9	0.38	0.32	0.30	0.17	0.26	0.44	0.35
upper Egdg Fm	P 7	0.28	0.39	0.32	0.27	0.20	0.39	0.25
upper Egdg Fm	P 2	0.38	0.29	0.33	0.46	0.30	0.52	0.43
lower Egdg Fm	Osch 72	0.30	0.39	0.31	0.35	0.06	0.46	0.06
lower Egdg Fm	Osch 68	0.20	0.42	0.38	0.30	0.04	0.48	0.04
lower Egdg Fm	Osch 65	0.23	0.47	0.30				
lower Egdg Fm	Osch 61	0.22	0.47	0.30	0.66	0.00	0.40	0.00
lower Egdg Fm	Osch 59	0.28	0.37	0.35	0.32	0.07	0.49	0.07

SATURATED CYCLIC HYDROCARBONS

FORMATION	*SAMPLE*	*Hopane / Moretane*	*Oleanane / (Ole+Hop)*	$C_{35}/(C_{31}$ *-* $C_{35})$ *Hopanes*	*22S/(22S+22R)* C_{31} *-Hopanes*	C_{29} */* C_{29} *Ts Hopane*	*Ts / Tm*	*Steranes / Hopanes*
Zupfing Fm	P41	5.80	0.27	0.11	0.57	3.03	0.55	1.29
Zupfing Fm	P30	2.60	0.33	0.11	0.56	24.41	0.35	0.79
"Transition zone"	P17	5.95	0.32	0.10	0.55	22.21	0.57	2.07
upper Egdg Fm	P15	6.06	0.25	0.14	0.57	2.08	0.71	1.36
upper Egdg Fm	P 9	7.67	0.12	0.12	0.57	2.18	0.59	0.87
upper Egdg Fm	P 7	5.96	0.17	0.12	0.56	2.55	0.57	1.10
upper Egdg Fm	P 2	4.79	0.19	0.22	0.57	113.62	0.42	0.44
lower Egdg Fm	Osch 72	6.18	0.08	0.08	0.31	1.53	0.58	1.47
lower Egdg Fm	Osch 68	5.39	0.08	0.23	0.38	49.27	0.56	2.73
lower Egdg Fm	Osch 65							
lower Egdg Fm	Osch 61	7.09	0.12	0.18	0.32	1.56	0.61	3.40
lower Egdg Fm	Osch 59	3.84	0.05	0.07	0.34	2.26	0.52	1.34

SATURATED CYCLIC HYDROCARBONS

APPENDIX III (cont´d) - Organic-geochemical results of samples investigated for facies characterisation, oil-source rock correlation and maturity assessment.

FORMATION	*SAMPLE*	*Tri-/(Tri- + Mono-) Arom. Steroide*	*DBT / Ph*	*Ph / Sum MPh*	*MPI 1*	*Rc (%)*	*di-/tri- MTTC*
Zupfing Fm	P41	0.71	0.05	0.56	0.51	0.70	x
Zupfing Fm	P30	0.60	0.07	0.57	0.58	0.75	x
"Transition zone"	P17	0.58	0.17	0.13	0.64	0.79	x
upper Eggerding Fm	P15	0.62	0.12	0.56	0.47	0.68	x
upper Eggerding Fm	P 9	0.68	0.05	0.47	0.57	0.74	x
upper Eggerding Fm	P 7	0.71	0.19	0.34	0.61	0.77	x
upper Eggerding Fm	P 2	0.69	0.05	0.68	0.40	0.64	x
lower Eggerding Fm	Osch 72	0.10	0.20	0.22	0.62	0.77	0.11
lower Eggerding Fm	Osch 68	0.07	0.28	0.50	0.54	0.72	0.14
lower Eggerding Fm	Osch 65	x	x	x	x	x	x
lower Eggerding Fm	Osch 61	0.09	0.29	0.23	0.49	0.69	0.73
lower Eggerding Fm	Osch 59	0.10	0.24	0.78	0.44	0.66	0.72

AROMATIC HYDROCARBONS

FORMATION	*SAMPLE*	*di-/tri- MTTC*	*Pristan/ Phytan*
Eggerding Fm	D31	0.24	3.02
Dynow Fm	D25	0.08	3.07
Dynow Fm	D21	0.05	1.98
Dynow Fm	D17	0.08	2.74
Dynow Fm	D8	0.04	1.90
Dynow Fm	D6	0.05	2.02
Dynow Fm	D1	0.16	2.01
Schöneck Fm	118	0.12	2.75
Schöneck Fm	113	0.10	2.94
Schöneck Fm	111	0.07	3.60
Schöneck Fm	106	0.25	1.21
Schöneck Fm	105	0.41	1.16
Schöneck Fm	104	0.36	1.28
Schöneck Fm	95	0.29	1.49
Schöneck Fm	91	0.37	1.31
Schöneck Fm	80	0.34	0.76
Schöneck Fm	70	0.28	1.34
Schöneck Fm	50	0.34	1.35
Schöneck Fm	44	0.23	1.28
Schöneck Fm	26	0.18	1.68
Schöneck Fm	18	0.07	2.10
Schöneck Fm	6	0.08	2.45

Schulz et al. (2005)

APPENDIX IV - nannoflora

Determination of the nannoflora: Samples studied within the frame of the present study. Well, sample code, formation, coccolithophorides.

Abbreviations:

r	rare
c	common
f	frequent

APPENDIX IV (cont´d) - Determination of the nannoflora: Samples studied within the frame of the present study.

Puchkrichen 3

P 42 – 2612 m, Zupfing Fm.
C, G

Autochtonous Oligocene: Coccolithus pelagicus r, Cyclicargolithus abisectus r, Cyclicargolithus floridanus c, Pontosphaera multipora r, Reticulofenetra bisecta r, R. small f, R. scripsae r, R. stavensis r, Sphenolithus cf. dissimilis r

Re-deposited Palaeocene /Eocene: Lanternithus minutus r, Micula decussata r, Reticulofenetra dictyoda r

Re-deposited Cretaceous: Arkhangelskiella cymbiformis r, Eiffellithus gorkae r, Watznaueria barnesae r

Stratigraphic classification: NP24/25?

P 40 – 2614 m, Zupfing Fm.
C, G

Autochtonous Oligocene: Coccolithus pelagicus r, Cyclicargolithus flloridanus f/c, Helicosphaera compacta cf. recta r, Pontosphaera cf. decussata r, P. dsicopora r, Reticulofenestra bisecta f, R. lockeri r, R. stavensis r, R. small c, Sphenolithus moriformis r, Sphenolithus sp. r, Thoracosphaera heimii r, Th. saxea r, Umbilicosphaera sp. r, Zygrhablithus bijugatus r.

Re-deposited Palaeocene /Eocene: Blackites sp. r, Chiasmolithus sp. r, Chiasmolithus grandis r, Ericsonia sp. r, Helicosphaera seminulum r, Toweius sp. r, Micula decussata r.

Re-deposited Cretaceous: Arkhangelskiella cymbiformis r, Ceratolithus sesquipedalis r, Cribrosphaeralla ehrenbergii r, Placozygus fibuliformis r, Prediscosphaera cretacea r, Watznaueria barnesae r, W. brittanica r.

Stratigraphic classification: NP24/25?

P 39 – 2615 m, Zupfing Fm.
C, G

Autochtonous Oligocene: Braarudosphaera bigelowii r, Coccolithus pelagicus f/c, Cyclicargolithus floridanus f, Pontosphaera dessueta r, Pontosphaera latelliptica r, P. multipora r, Reticulofenetra bisecta r, R. lockeri r, R. small r, Sphenolithus distentus r, S. moriformis r, Sphenolithus sp. r, Thoracosphaera saxea r, Zygrhablithus bijugatus r,

Re-deposited Palaeocene /Eocene: Clausiococcus fenestratus r, Ericsonia formosa r, Lanternithus minutus r, Micula decussata r, Reticulofenestra hillae r, Toweius sp. r

Re-deposited Cretaceous: Eiffellithus gorkae r, Placozygus fibuliformis r, Watznaueria barnesae f

Stratigraphic classification: NP24/25?

P 38 – 2616 m, Zupfing Fm.
F/C, G

Autochtonous Oligocene: Braarudosphaera bigelowii f, Coccolithus pelagicus c, Cyclicargolithus floridanus c, Pontosphaera dessueta r, Reticulofenestra bisecta r, R.

dictyoda r, R. lockeri r, R. scripsae r, R. small f, Reticulofenestra cf. ornata r, Sphenolithus cf. conicus r, Zygrhablithus bijugatus r.

Re-deposited Palaeocene /Eocene: Cyclicargolithus luminis r, Ericsonia formosa r, Isthmolithus recurvus r, Lanternithus minutus r, Micula decussata r, Reticulofenestra hillae r, Toweius sp. r

Re-deposited Cretaceous: Arkhangelskiella cymbiformis r, Eiffellithus gorkae r, Retecapsa crenulata r, Z. ehrenbergii r, Watznaueria barnesae f

Stratigraphic classification: NP24/25?

P 36 – 2618 m, Zupfing Fm.

C,G

Autochtonous Oligocene: Braarudosphaera bigelowii r, Coccolithus pelagicus r, Cyclicargolithus abisectus r, Cyclicargolithus floridanus c/a, Pontosphaera multipora r, Reticulofenestra bisecta r, R. daviesii r, R. lockeri r, R. stavensis r, Reticulofenestra sp. r, Sphenolithus sp. r, S. moriformis r, Thoracosphaera saxea r, Zygrhablithus bijugatus r,

Re-deposited Palaeocene /Eocene: Ericsonia formosa r, Pontosphaera exilis r, Reticulofenestra hillae r, Toweius sp. r

Re-deposited Cretaceous: Arkhangelskiella maastrichtiana r, Cribrosphaerella ehrenbergii r, Calculithe ovalis r, Retecapsa crenulata r, Watznaueria barnesae r,

Stratigraphic classification: NP24/25?

P 30 – 2624 m, Zupfing Fm.

C, G

Autochtonous Oligocene: Braarudosphaera bigelowii r, Coccolithus pelagicus c, Cyclicargolithus abisectus r, Cy. floridanus f/c, Reticulofenestra bisecta r, R. small f, R. locker r, Reticulofenestra sp. r, R. ornata r, S. moriformis r, Thoracosphaera saxea r

Re-deposited Palaeocene /Eocene: Toweius sp. r

Re-deposited Cretaceous: Watznaueria barnesae f, W. brittanica r

Stratigraphic classification:NP24/25?

P 28 – 2626 m, Zupfing Fm.

C, G Cy. fl. bloom

Autochtonous Oligocene: Coccolithus miopelagicus r, C. pelagicus r, Cyclicargolithus floridanus c, Reticulofenestra bisecta f, R. lockerii f/c, R. stavensis r, Reticulofenestra sp. r, Sphenolithus moriformis r, Thoracosphaera saxea r, Zygrhablithus bijugatus r

Re-deposited Palaeocene /Eocene: Chiasmolithus gigas r, Micula decussata r

Re-deposited Cretaceous: Ceratolithus arcuatus r, Retecapsa crenulata r, Watznaueria barnesae r

Stratigraphic classification:NP24/25?

P 26 – 2628 m, Zupfing Fm.

C, G

Autochtonous Oligocene: Braarudosphaera bigelowii r, Coccolithus pelagicus f/c, Cyclicargolithus abisectus r, Cy. floridanus c, Helicosphaera recta r, Pontosphaera dessueta r, P. multipora r, Reticulofenestra bisecta f, R. clatrata r, R. lockeri f, R. small f, R. stavensis r, Thoracosphaera saxea r, Zygrhablithus bijugatus r

Re-deposited Palaeocene /Eocene: Reticulofenestra umbilica r,

Re-deposited Cretaceous: Eiffelithus gorkae r, Micula decussata r, Watznaueria barnesae r

Stratigraphic classification: NP24/25?

P 22 – 2635 m, Zupfing Fm.
C, G Cy. fl. bloom

Autochtonous Oligocene: Coccolithus pelagicus f, Cyclicargolithus floridanus c, Helicosphaera recta r, Pontosphaera dessueta r, P. multipora f, Reticulofenestra bisecta r, R. dictyoda r, R. small f, R. stavensis r, Sphenolithus cf. conicus r, Thoracosphaera heimii r, Zygrhablithus bijugatus r

Re-deposited Palaeocene /Eocene: Coccolithus cachaoi r, Chiasmolithus sp. r, Ericsonia robusta r, Micula decussata r, Pemma sp. r

Re-deposited Cretaceous: Cribrospaerella ehrenbergii r, Watznaueria barnesae r
Stratigraphic classification: NP24/25?

P 21 – 2636 m, Zupfing Fm.
C, G

Autochtonous Oligocene: Coccolithus pelagicus f, Cyclicargolithus floridanus f, Helicosphaera recta cf. compacta r, Pontosphaera multipora r, Reticulofenestra bisecta f, R. lockeri f, R. stavensis r, R. small f/c, Sphenolithus cf. conicus r, S. cf. dissimilis r, S. moriformis r, Zygrhablithus bijugatus r

Re-deposited Palaeocene /Eocene: Reticulofenestra dictyoda r, Mic. decussata r

Re-deposited Cretaceous: Watznaueria barnesae r
Stratigraphic classification: NP24/25?

P 19 – 2638 m, Zupfing Fm.
C, G

Autochtonous Oligocene: Coccolithus pelagicus r, Coronocyclus sp. r, Cyclicargolithus floridanus f, Pontosphaera multipora r, Reticulofenestra bisecta r, R. small f/c, R. daviesii r, R. lockeri r, R. stavensis f, Sphenolithus moriformis r, Zygrhablithus bijugatus r

Re-deposited Palaeocene /Eocene: Reticulofenestra dictyoda r,
Stratigraphic classification: NP24/25?

P 18 – 2639 m, Zupfing Fm. (Transition zone)
C, G, Cy. fl. bloom

Autochtonous Oligocene: Coccolithus pelagicus f, Cyclicargolithus abisectus r, Cy. floridanus c, Pontosphaera multipora r, Reticulofenestra bisecta r, R. lockerii f, R. small r, R. cf. tokodoensis r, Sphenolithus moriformis r, Thoracosphaera saxea r, Zygrhablithus bijugatus r,

Re-deposited Palaeocene /Eocene: Blackites spinosus r, Coccolithus cachaoi r, Lanternithus mminutus r, Pontosphaera pulchra r, Reticulofenestra hillae 1

Re-deposited Cretaceous: Arkhangelskiella cymbiformis r, Calculithes obscurus r, Eiffellithus turisseifellii r, Watznaueria barnesae r,
Stratigraphic classification: NP24/25?

P 17 – 2640 m, Zupfing Fm. (Transition zone)
C, G

Autochtonous Oligocene: Coccolithus pelagicus r, Cyclicargolithus floridanus f/c, Helicosphaera recta cf. compacta r, Reticulofenestra bisecta r, R. lockerii r, R. scripsae r, R. small c, R. stavensis r, Sphenolithus moriformus r, Zygrhablithus bijugatus r

Re-deposited Palaeocene /Eocene: Lanternithus minutus r, Toweius sp. r

Umgelagert Kreide: Broinsonia parca parca r, Cribrosphorella ehrenbergii r, Eifellithus. gorkae r, Retecapsa crenulata r, Uniplanarius sissinghii r, Watznaueria barnesae r
Stratigraphic classification: NP24/25?

P 16 – 2641 m, Zupfing Fm. (Transition zone)
C, G

Autochtonous Oligocene: Coccolithus pelagicus f, Cyclicargolithus fl. f/c, Helicosphaera recta cf. comp. r, Pontosphaera multipora r, Reticulofenestra bisecta f, R. lockeri c, R. ornata r, R. small r, Sphenolithus moriformis r, Thoracosphaera heimii r, Th. saxea r, Zygrhablithus bijugatus r

Re-deposited Palaeocene /Eocene: Ericsonia formosa r, Ericsonia subdisticha r, Isthmolithus recurvus r, Chiasmolithus altus r, Reticulofenestra dicty. r, R. umbilica r, Sphenolithus radians r, Toweius spp. r

Re-deposited Cretaceous: Arkhangelskiella cymbiformis r, Micula decussata r, Retecapsa crenulata r, Watznaueria barnesae r, Z. ehrenbergii r
Stratigraphic classification: NP24/25?

P 15 – 2642 m, Eggerding Fm.
sterile, calcareous

P 14 – 2643 m, Eggerding Fm.
sterile, calcareous

P 13 – 2644 m, Eggerding Fm.
sterile, lightly calcareous

P 12 – 2645 m, Eggerding Fm.
sterile, calcareous

P 11 – 2646 m, Eggerding Fm.
sterile, calcareous

P 10 – 2647 m, Eggerding Fm.
sterile, calcareous

P 9 – 2648 m, Eggerding Fm.
C, G

Autochtonous Oligocene: Coccolithus pelagicus r, Cyclicargolithus abisectus r, Cy. floridanus c, Pontosphaera multipora r, Reticulofenestra bisecta r, R. lockerii f, R. small r, R. stavensis r, Reticulofenestra sp. r, Sphenolithus moriformis r, Thoracosphaera saxea r, Zygrhablithus bijugatus r

Re-deposited Palaeocene /Eocene: Ericsonia formosa r, Helicosphaera lophota r, Pontosphaera pulchra r, Pontosphara sygmoides r

Re-deposited Cretaceous: Watznaueria barnesae r
Stratigraphic classification: NP24/25?

P 8 – 2649 m, Eggerding Fm.
sterile, calcareous

P 7 – 2650 m, Eggerding Fm.
sterile, calcareous

P 6 – 2651 m, Eggerding Fm.
sterile, calcareous similar to lower Puchkirchen Formation

P 5 – 2652 m, Eggerding Fm.
sterile

P 4 – 2653 m, Eggerding Fm.
sterile, calcareous similar to lower Puchkirchen Formation

P 3 – 2654 m, Eggerding Fm.
sterile

Oberschausberg 1

Osch 60 – 1371.52 m, Eggerding Formation
sterile, no Calcium Carbonate, Pyrite

Osch 61 – 1371.20 m, Eggerding Fm.
F/R, G/M
Autochtonous Oligocene: Coccolithus pelagicus, Cyclicargolithus floridanus, Discoaster sp., Reticulofenestra bisecta, R. lockerii, R. stavensis, Sph. cf. capricornutus
Re-deposited Palaeocene /Eocene: Reticulofenestra cf. dictyoda, Chiasmolithus cf. modestus, Discoaster ornatus, Ericsonia robusta, Micula decussata, Pontosphaera pulchra, Reticulofenestra hillae 1 (gebr.), Toweius sp., Tribrachiatus orthostylus
Re-deposited Cretaceous: Eiffellithus gorkae, Uniplanarius sissinghii, Watznaueria barnesae

Osch 63 – 1370.69 m, Eggerding Formation
sterile, no Calcium Carbonate, Pyrite

Osch 64 – 1370.50 m, Eggerding Fm.
R, G
Autochtonous Oligocene: Braarudosphaera bigelowii small f/c, Coccolithus pelagicus r, Cyclicargolithus floridanus c, Reticulofenestra bisecta r, R. stavensis r, Reticulofenestra sp. r, R. small, Thoracosphaera heimii r
Re-deposited Palaeocene /Eocene: Reticulofenestra hillae r, R. umbilica r, Micula dessueta r, Pontoosphaera exilis r, Reticulofenestra tokodoensis r, Toweius sp. r,
Re-deposited Cretaceous: Watznaueria barnesae r

Osch 66 – 1369.90 m, Eggerding Fm.
calcareous, sterile

Osch 68 – 1369.17 m, Eggerding Fm.
C/F, G
Autochthon Oligozän: Br. bigelowii r, C. pelagicus f, Cy. floridanus r, E. formosa r, R. bisecta f, Reticulofenestra dictyoda r, R. lockeri f, R. minuta r, R. ornata f, R. stavensis r, Sphenolithus cf. capricornutus r, S. moriformis r, Sphenolithus sp. F5x r, Zygrhablithus bijugatus r
Re-deposited Palaeocene /Eocene: Micula decussata f

Re-deposited Cretaceous: Eiffellithus gorkae r, Watznaueria barnesae r, W. brittanica r

Osch 71 - 1368,5m, Eggerding Fm.
sterile, calcareous

Osch 72 – 1368m, Eggerding Fm.
sterile, calcareous, terrestrial plants, Pyrite

Eggerding 2

Egdg 83 – 557.64m, Eggerding Fm.
sterile, no Calcium Carbonate

Egdg 85 – 555.65m, Eggerding Fm.
sterile, no Calcium Carbonate

Egdg 87 – 553.65m, Eggerding Fm.
sterile, no Calcium Carbonate